Universidade de Aveiro

Departamento de Química

2017

José Diogo Resende Cruz

Estudo da influência dos diferentes parâmetros de cultivo e extracção em culturas de microalgas

Study of the influence of different parameters of cultivation and extraction on microalgae cultures

Universidade de Aveiro
2017

**Departamento de Química**

José Diogo Resende Cruz

Estudo da influência dos diferentes parâmetros de cultivo e extracção em culturas de microalgas

Study of the influence of different parameters of cultivation and extraction on microalgae cultures

Dedico este trabalho aos meus pais e aos amigos que todo o apoio me deram.

o júri

**presidente**    **Prof. Doutora Ana Maria Rebelo Barreto Xavier**
**Professora Auxiliar da Universidade de Aveiro**

**Doutor(a) Joana Luísa Lourenço Estevinho Pereira**
**Estagiária de Pós-Doutoramento, CESAM - Centro de Estudos do Ambiente e do Mar**

**Doutora Sónia Patrícia Marques Ventura,**
**Equiparada a Investigadora Auxiliar, Universidade de Aveiro**

agradecimentos

**Agradeço a Rafael García-Cubero pela oportunidade que me deu em integrar o grupo do AlgaePARC, Wageningen University and Research, Holanda. Pela sua supervisão, tempo e apoio que sempre me foi dado ao longo de seis meses de estagio. Agradeço também aos meus colegas de trabalho (Ruut e Rick) que sempre me ajudaram quando alguma adversidade surgia e em especial a Dàmi Rebergen pelo seu companheirismo e cooperação no trabalho aqui apresentado (capitulo I). A sua capacidade de resolução de problemas, característica da cultura holandesa, permitiu que eu próprio me potenciasse.**

**Agradeço imenso a Sónia Ventura, pela sua orientação desde o momento em que parti de Portugal até ao momento em que regressei e me sugeriu uma nova experiencia que não só enriqueceu a minha dissertação como também me pôs à prova. A sua perseverança foi fundamental para finalizar com sucesso esta intensa etapa. Um grande agradecimento à Margarida Martins, que se demonstrou uma pessoa formidável ao me co-orientar no desenvolvimento do presente trabalho (capitulo II).**

**Um agradecimento forte aos meus pais, por tudo que me deram e por serem responsáveis por quem eu sou hoje. Por último e não sem menos importância, aos meus amigos e colegas de casa em Wageningen (Miguel, Laura, Jorge, Manuel e Cristina) e aos meus amigos que já em Aveiro (Simão, Soraia, Catarina, Sara, Félix e Salvatore) foram importantes na execução desta etapa.**

palavras-chave

**Microalgas; cultivo contínuo; fotobiorreactor; extração; líquidos iónicos; ficocianina**

resumo

**As microalgas são uma fonte emergente de alimento, corantes alimentares, combustível e produtos químicos. O estudo dos processos upstream e downstream são de extrema relevância pois de modo a prever a sua exploração industrial. O presente trabalho, está dividido em dois capítulos, um envolvendo o processamento upstream e outro explorando o processamento downstream. A microalga M, está há muito documentada pelo seu potencial como fonte para produção de biopolímeros contudo o cultivo outdoor desta microalga está ainda por otimizar. Desta forma, o estudo do efeito de parâmetros operacionais de cultivo, nomeadamente D, E e F, foram usados para desenvolver três modelos matemáticos em relação a A, B e C para culturas continuas de microalga X em escala de laboratório. Os resultados mostraram ser possível atingir culturas com elevadas A, elevado conteúdo de C ou B com tamanho controlável, através da manipulação das condições de cultivo. Com aplicação do presente estudo é esperado que se aumente a transição de conhecimento de cultivo reduzida para larga escala, de forma a potenciar a aplicação de larga escala.**
**O capitulo de processamento downstream no presente trabalho visa o desenvolvimento de uma metodologia alternativa de extração de ficocianina em culturas de** Anabaena cylindrica**. Os líquidos iónicos são uma classe de solventes que têm atraído muita atenção por parte dos investigadores pelas suas características únicas. O uso de soluções aquosas de líquidos iónicos mostrou-se altamente seletivo para a extração de ficocianina e clorofila. A performance da solução aquosa de [C$_4$mimCl] foi otimizada quando os parâmetros operacionais de extração foram: rácio solido-liquido 0,1 (peso de biomassa fresca/volume de solvente), tempo de extração (43 min.) e concentração do liquido iónico (475 mM). Sob estas condições os rendimentos de ficocianina e grau de pureza alcançados foram $55 \pm 2$ mg$_{ficocianina}$.g$_{biomassa\ fresca}^{-1}$ e 0,54, respetivamente. O uso de soluções aquosas de liquido iónicos resultou num extrato bruto rico em ficocianina com reduzida contaminação de outros pigmentos e outras proteínas. Assim esta metodologia alternativa demonstrou-se mais efetiva do que outras tentativas encontradas na literatura ao passo que tem a capacidade de simplificar os processos de purificação e concentração, comumente reconhecidos por serem dispendiosos e dificilmente escaláveis.**

abstract

Microalgae has been regarded as an emerging source for feed, food colourants, fuel and chemicals. The study of the upstream and downstream processing is of foremost importance in order to foresee its industrial exploitation. Therefore, the present work is divided in two chapters, one comprising the upstream and another the downstream processing. The potential of Microalgae M as a source of biopolymers is already known though its outdoor cultivation is still to optimize. Thus, the effect of relevant environmental parameters, namely D, E and F were studied and used to develop three mathematical models regarding the A, B and C for continuous cultures of Microalgae X at lab scale. The results show that it's possible to achieve increased A, high content of C or B with wieldy size through the manipulation of these culture conditions. The application of the present study is expected to fill the gap between lab and large-scale cultures to enhance and optimize its large-scale performance.

The downstream processing chapter in the present work regards the development of an alternative extraction methodology to recover a natural pigment, the phycocyanin from Anabaena cylindrica cultures. Ionic Liquids are a class of solvents that have been attracting much attention from researchers due to its unique properties. The use of aqueous solutions of ionic liquids has shown highly selective performances for phycocyanin and chlorophyll extraction. The performance of aqueous solutions of an imidazolium-based ionic liquid, namely the [C$_4$mim]Cl was optimized after the operation extraction parameters were set: solid-liquid ratio of 0.1 (weight of fresh biomass/volume of solvent), extraction time (43 min) and ionic liquid concentration (475 mM). Under these conditions phycocyanin yields and purity levels ($A_{615}/A_{280}$) were $55 \pm 2$ mg$_{phycocyanin}$.g$_{fresh\ biomass}^{-1}$ and 0.56, respectively. The use of aqueous solutions of ionic liquids resulted in crude extracts rich in phycocyanin with reduced levels of pigments and proteins contamination, whereas it was shown more effective than other attempts found in literature as well as it can simplify the purification and concentration steps, commonly known for being expensive and hardly-scalable.

**Índex**

## Abbreviations Index

EPA - Eicosapentaenoic acid
DHA - Docosahexaenoic acid
PUFA - Polyunsaturated fatty acids
PE - Polyethylene
PP - Polypropylene
FDCA - 2,5-furandicarboxylic acid
FA – Fatty acid
TAG – Triacylglicerides
EPS – Exopolysaccharide
ECM - Complex extracellular matrix
rRNA – Ribossomal RNA
PBR – Photobiorreactor
PE - Photosynthetic efficiency
PAR - Photosynthetically active radiation
$\mu$ - specific growth rate
$\mu_{MÁX}$ – Maximum specific growth rate
z – reactor light path
I – Photon flux
X – Cell concentration
D – Dilution rate
F – Flow rate
V – Reactor volume
XD – Biomass output rate
-m – Insignificant maintenance energy requirement
+m – Significant maintenance energy requirement
y – Response
$\beta_0$ – Unknown parameters
$x_1$ – Input factors
$\varepsilon$ - Random error
RSM – coded experimental methodology
X004 – coded experimental design
N – Number of experiments
K - Number of factors
$C_p$ – Replicate number of the central point
WTD – coded parameter
ANOVA – Analysis of variance
DW – Durbin-watson
SLR – Solid-liquid ratio
ABS – Aqueous biphasic system
AMTPS – Aqueous micellar two-phase system
A – coded parameter
B – coded parameter
C – coded parameter
D – coded parameter
E – coded parameter
F – coded parameter

# Tables Index

# Figures Index

# 1. GENERAL BACKGROUND

During recent years, the world population growth has led us to the uncontrolled use of non-renewable sources which are now considered exhausted. Fossil fuels have been representing the most relevant and competitive market regarding all the energy sources. Climate change and global warming phenomena are consequences of that fossil fuels use, which should be substituted by the use of clean energy. The bio-based economy concept intends to reduce the fossil fuel dependency through the development of biorefining platforms to convert natural resources into bio-based products and fuels. In fact, the bio-based industries are aiming to replace the oil based chemicals and materials by 30% in 2030, whereas the private sector plays a major role which comprise almost 70% of all the bio-based innovation investments [1]. The renewable biomass has the potential to compete with non-renewable sources, due to its energetic applications. Moreover, technological breakthroughs can provide add-valued products from the conversion processes of biomass, although, considering their need for large scale, these are still in their infancy [2].

Photosynthetic biomass powers carbon dioxide mitigation and the generation of oxygen, and at the same time, it also recycles inorganic nitrogen and phosphorous for growth purposes, making them even more attractive [3]. Microalgae are unicellular organisms that have the potential to produce greater amounts of biomass per hectare than any kind of terrestrial biomass [4]. This ubiquitous feedstock grows fast, does not compete with arable land for food production purposes and also produce a broad range of biomolecules, however, although only a few have reached the market (Astaxanthin, dry *Spirulina,* dry *Chlorella ,* EPA/DHA (omega-3), *β*-carotene, phycocyanin) [5].

Thus, the present dissertation comprises a general background appropriate for the next two chapters, wherein the first chapter regards the optimization of continuous cultivation parameters of one green microalgae species with relevant potential for bioplastics and fuel production, while the second chapter follows an approach of biomass valorisation in which added value compounds, namely pigments, can be extracted. Therefore, it aims to optimize the extraction parameters of the natural blue pigment, phycocyanin, through the use of a more sustainable methodology.

## 1.1 Microalgae

Microalgae and cyanobacteria are the basis for most of the food chain of the aquatic environment. This type of aquatic biomass can use light as the only source of energy and convert inorganic carbon (carbon dioxide, $CO_2$ or bicarbonate, $HCO_3^-$), nitrogen, phosphorous and sulphur into biomass, regularly mentioned as photoautotrophic growth [6,7]. In this process of photosynthesis, algae produce oxygen ($O_2$) which, in a global scale, represents more than 75% of the oxygen required for animal and humans. It is estimated to exist between 200000 and 800000 different microalgae species, however, only a few tens of thousands are described in literature [5]. Currently, the following main groups presented in Table 1.1 are distinguished.

**Table 1.1 -** Description of the microalgae species. Adapted from [8]

| Family | Characteristics |
| --- | --- |
| **Chlorophyceae** | With around 7500 species, this group is composed by uni algae. Contain chlorophyll and a higher content of proteins. These are capable of producing intracellular starch and oil under stress conditions. *Chlorella* is already being commercially explored (2000 tons of dry matter/year). [5] |
| **Rhodophyceae** | With around 5000 species, mostly are multicellular living in the tidal zone of the sea. |
| **Bacillarrophyceae** | Largest group, with 100000 species. These are responsible for most of the Earth biomass. These have a silica-based skeleton, are able to store oil and are considered a vital food source for zooplankton. |
| **Phaeophyceae** | Around 2000 multicellular species exclusively living in the sea. |
| **Chrysophyceae** | Fresh water organisms that possess flagella, which can have a large plethora of colours. |
| **Xanthophyceae** | With around 600 species, this group is in its majority composed of unicellular and fresh water living organisms. *Nannocloropsys* sea water alga is an exception, since it grows fast and produces oil suitable for biodiesel production. |
| **Cyanophyceae** | Some can produce toxins in high concentrations that affect the water quality. Stores starch and more than half out of protein. *Spirulina* represents worldwide this group (5,000 tons of dry matter/year) [5] |

Currently, there are around 200 microalgae species used worldwide in different sectors, namely aquaculture, livestock feed and food colourants.[9]. Microalgae are ubiquitous cells capable of surviving in a broad spectrum of environmental stress conditions and also they possess a huge metabolic plasticity, which makes them a unique reservoir of many added-value compounds[7]. Microalgae are exceptionally fast-growing and productive organisms. In addition, they can be used from the whole cell to the molecular level[9]. The whole cell can be applied as animal feed and as human food, due to the microalgae high nutrition value, in terms of considerable amount of high-quality oils, polyunsaturated fatty acids (PUFA), such as omega-3 and omega-6[5,10]. Intracellular microalgal metabolites such as, proteins, carbohydrates and acyl lipids can together constitute up to 70-90% of the biomass dry weight. Proteins are accumulated under favourable growth conditions while carbohydrates and acyl lipids achieve better yields under limited growth conditions[11–13]. Other intracellular biomass constituents are the pigments; however, their concentration is often too low for commercial exploitation, with the exceptions being the phycocyanin from *Arthrospira platensism*, and the β-carotene and astaxanthin from *Dunaliella* and *Haematococcus pluvialis*[5,14,15]. Meanwhile, the extracellular metabolites production is also under the edge of research, once they can make the downstream processing much easier and enable a continuous product harvesting[16]. The continuous product harvesting could be possible if an effective algal/product separation do not interfere with the algal viability, which would minimize the amounts of required fresh inoculum. Potential examples include, *Porphyridium cruentum* that excretes a sulphured polysaccharide and *Botryococus braunii* that excretes alkane-like structures and also strain-depending exopolysaccharides (EPS)[17]. Recently, Griehl and co-authors[18], have developed an optimized one method of continuous non-destructive extraction of hydrocarbons from *B. braunii* up to six weeks, however better yields are needed.

Notwithstanding, the production of microalgal products can also play a role in the nutrient recirculation due to its capability to grow through the combination of liquid and gaseous waste streams, such as waste water and flue gases, respectively[19]. Domestic and industrial waste water have substantial amounts of inorganic nitrogen and phosphorous, in the same way, power and cementary plants flue gases contains 10-15% of $CO_2$[20,21].

## 1.2 Monitoring and control of PBR

The monitoring of the environmental conditions in the phototrophic growth is an important task for the performance of microalgae cultures. Operational modes used in microbial cultures are adjustable depending on the application, however the monitoring and control of light intensity and cells density [22] is of crucial importance.

There are three main types of operational modes with regard to microalgae cultivation, in liquid media, namely the batch regime, the continuous (D=μ) mode and the semi-continuous culture [23].

### 1.2.1 Batch regime

Batch culture is known to be the simplest and most common operational method for cultivation of microalgae cells. It consists of a single inoculation of cells into a culture vessel of limited amount of culture medium. The culture grows under well controlled conditions without any input or output, except for some samples. In the end of the run, the removal of all the material completes the cycle. During the batch mode, a growing period of several days is defined, in which different operational conditions can be changed, causing the different growth phases of the cells (Figure 1.1).
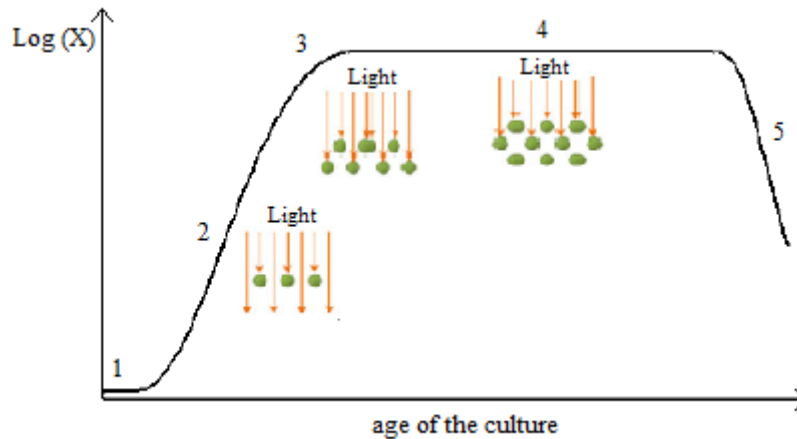


**Figure 1.1 -** Schematic representation of the microalgae cell growth phases for a photobioreactor working in a batch regime. The *yy* axis represents the logarithm function of the number of cells being produced and the *xx* axis represents the culture age (with time), where: 1) represents the Lag or adaptation phase; 2) represents the exponential or log phase; 3) represents the linear growth phase; 4) represents the stationary phase; 5) represents the

death phase. Note that incident light is rate-limiting due to affects the algal growth. Adapted from [24].

Phase 1, represents the lag or adaptation phase, in which there is no increase in cells number. In this phase, the cells are making adaptation in their metabolism to growth, namely by increasing the levels of enzymes and metabolites involved in cell division and carbon fixation. In this case, the inoculum conditions have a strong effect on the duration of the lag phase. Usually, it is transferred when the cells are in their exponential growth, decreasing the time required for up-scaling and cells' adaptation.

Phase 2, represents the exponential or log phase, in which the cell multiplication is quick and the number of cells increases exponentially. The exponential growth of the microalgae cells is defined by the linear differential equation (1.1):

$$\frac{dx}{dt} = \mu X \qquad \textbf{(Equation 1.1)}$$

where X represents the cell concentration (g.L$^{-1}$), t is time (days) and $\mu$ is the specific growth rate (days$^{-1}$). From the integration of the equation (1.1), it is obtained (equation 1.2):

$$X_t = X_0 e^{\mu t} \qquad \textbf{(Equation 1.2)}$$

where $e$ is the exponential function, $X_0$ and $X_t$ are the initial and cell concentration determined after an interval of time t (g. L$^{-1}$), respectively.

During this phase, the nutrients are in excess and the cells are growing at its $\mu_{MÁX}$. The "doubling time", $g$, represents the average time required for all the culture to double in number of cells, which can be calculated by equation (1.3):

$$g = \frac{ln2}{\mu} \qquad \textbf{(Equation 1.3)}$$

Phase 3, is the linear growth phase, where the cells start to experience limitations such as nutrients depletion, pH alterations, light intensity reduction by self-shading or even the auto-inhibition (production of toxic substances by the cells which inhibits its own growth).

Phase 4 corresponds to the stationary phase where the limiting factor and the growth rate are balanced, resulting in the equilibrium between growth and decay.

Phase 5 is the death phase, in which the cells death rate becomes higher than the growth rate, mainly due to nutrients depletion, water quality deterioration and accumulation of toxic compounds [23,24].


### 1.2.2 Continuous regime

The continuous flow culture is a useful tool for studying the growth kinetics, as well as, the physiology and the biochemistry of microalgae. In this regime, the fresh culture medium is supplied to the homogeneously mixed culture, while the culture media (medium and microorganism) is continuously being removed, therefore ensuring the continuous production of new cells (Figure 1.2). This approach is based on the observations that growth-limiting substrates and growth inhibitory products tend to stop the culture growth [24,25]).
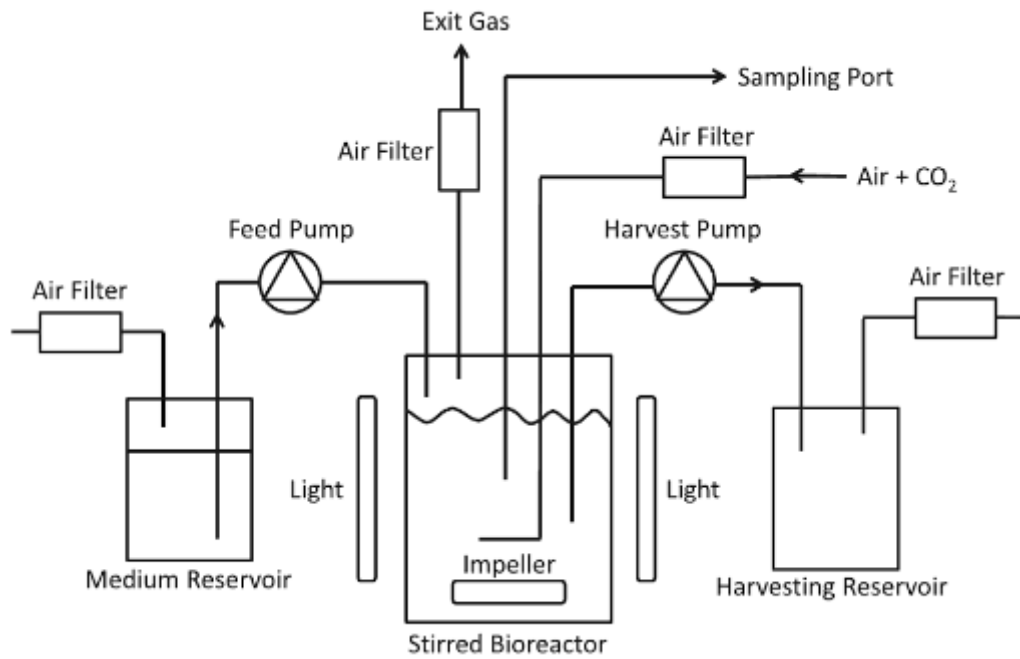
**Figure 1.1 -** Schematic representation of a microalgae continuous culture setup. Adapted from [24].

To establish a constant culture, it is assumed that the medium feed and the rate of culture removal (F) is the same, and the culture volume is constant. Accordingly, the net increase in biomass is equal to the difference between the growth and the biomass removal. At the same time, the culture will reach the steady-state. By definition, a culture is in steady-state when at least after three volumes of reactor have been refreshed and the biomass concentration remains the same for five different and consecutives days.

In that way, the culture experiences constant dilution, where the dilution rate can be defined as (equation 1.4):

$$D = \frac{F}{V} \qquad \text{(Equation 1.4)}$$

where D is the dilution rate (days$^{-1}$), F is the flow rate (L.day$^{-1}$) and V is the reactor volume (L), kept normally constant.

For an infinitely small time interval, *dt*, the balance for the culture could be written as (equation 1.5):

$$\frac{dx}{dt} = (\mu - D)X \qquad \textbf{(Equation 1.5)}$$

In the steady-state the net change of biomass is equal to zero (equation 1.6), where:

$$\mu = D \qquad \textbf{(Equation 1.6)}$$

This relationship imposes that the specific growth rate is determined by the dilution rate, which is an experimental variable. In practice, the monitoring and control of the microalgae growth can be developed through the cells adaptation to an imposed D. If the D is significantly higher, cells remain inside the reactor for shorter periods of time, which will become them unable to adapt and they will eventually experience the wash out. Conversely, a very low D, will allow cells to stay in the reactor for longer periods, thus an adaptation to this environment allow cell division to occur and a high biomass concentration will be reached. For light-limited photosynthetic cultures, a dense culture tends to experience more scattering, while an increased maintenance energy is required, allowing the decrease in the biomass concentration and the biomass output rate, as shown in Figure 1.3 [24,26].
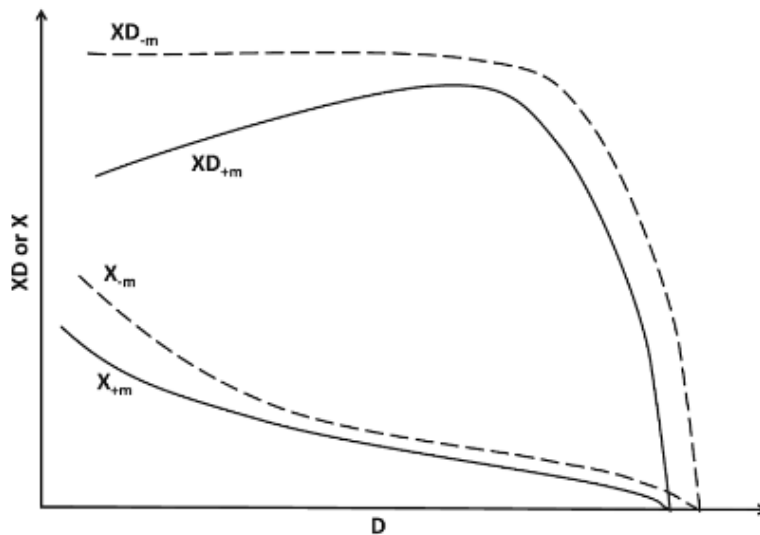


**Figure 1.2 -** Evolution of the steady state biomass concentration ($X$) and biomass output rate ($XD$), along with the dilution rate ($D$) in continuous system, at constant light input. *−m*

represents insignificant maintenance energy requirement and +*m* represents a significant maintenance energy requirement. Adapted from literature [24].


There are three types of continuous cultures, namely the chemostat, the turbidostat and the luminostat. In a chemostat (chemical environment is static) regime, the rate of addition of fresh medium and the rate of culture removal are kept at a steady, predetermined rate. Thus, a rate-limiting vital nutrient (e.g. nitrate) is added at a fixed rate (D), which keeps the growth rate constant and not the cell density [23]. This method is very useful to prevail the culture conditions and to maintain a specific growth rate at pre-determined values [24]. In cases where light/dark cycles are applied, the chemostat principles for nutrient limited algal growth cannot be completely valid, meaning that the instantaneous μ is not equal to the instantaneous D. Instead, only the periodic μ is equal to D. In such cases, it is recommendable to use the theory of the cyclostat growth. This particular case of chemostat is important for cells growing under variable light conditions or (rarely) temperature cycles. It explains the algal culture that exhibit daily rhythms in biosynthetic and reproductive processes, whereas cells are in balanced growth but also in a dynamic equilibrium, thus the growth rate is equivalent to D, over a day. Therefore, it is appropriate to define the culture in terms of quasi-steady state conditions [27].

In turbidostat (being static), the rate of fresh medium and the rate of removal of the culture is varied in order to maintain the cell density constant. The input is controlled by the turbidity of a culture that is set to be steady. If the set threshold exceeds the algal concentration, a dilution in the culture will re-establish to the set point [26]. However, turbidity measurements are not so reliable in cases where the sensitivity of the measurements or the main characteristics of the samples change. In the case of microalgae cells, this could be attributed to the algae changes in size or aggregates formation, but it can be also occurring due to cell adhesion to the surface of the optical cell [25]. Improvements on this methods have led to a modified turbidostat regime, where the dilution rate of the pure water in a concentrated fresh medium stream is used as a manipulated input, instead of the conventional method [28,29].

The luminostat continuous regime changes the control method. Contrarily to the chemostat and turbidostat regimes, that fix, respectively, the dilution rates and dilute by keeping the turbidity constant, the luminostat controls the light transmission through the entire cultivation, in order to avoid the occurrence of dark zones. Light at the back of the reactor

should provide a photosynthetic rate that matches the respiration rate, which is known as the compensation point. This approach could be very useful for environments where light intensity is constantly varying i.e. outdoors. In fact, the luminostat regime should ensure the maximal adsorption of sunlight preventing the occurrence of dark zones in the photobiorreactor and improving the photosynthetic efficiency [30,31].

### 1.2.3 Semi-continuous regime

The semi-continuous regime, also known as fed batch, stands between the batch and the continuous processes, whereas it is a batch culture with feeding of nutrients if the effluent is only removed periodically [24]. This technique is the most widely used among industrial continuous flow culture processes [32]. Such operation is possible either by feeding fresh medium and emptying the bioreactor when the reactor has reached a high biomass concentration, or by feeding dilute fresh medium and emptying the reactor when the tank is filled to its maximum capacity.

The repeated batch process of filling and emptying results in a cyclic variable volume operation (Figure 1.4), however, several authors have claimed that a quasi-steady state can be reached, in which a specific growth rate ($\mu$) virtually is equal to the dilution rate (D) [26,33]. Therefore, it allows continuous reproduction between two specific growth rates [34].
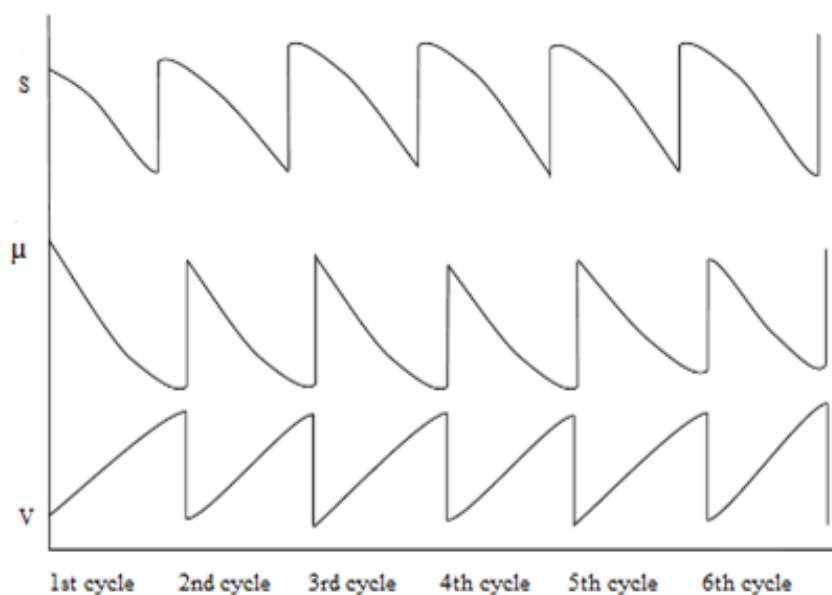
**Figure 1.3** - Schematic representation of the changes in the rate-limiting light input (S), specific growth rate (µ) and culture volume (V) in a cyclic semi-continuous culture. Adapted from literature [24].

## 1.3 Response surface methodology (RSM)

Optimization refers the discovery of the conditions of a system, a process, or a product in order to obtain the maximum benefit from it [35]. The classical methods involve the optimization of just one condition at a time, a method called as single parameter optimization [36]. Formerly, this approach was nothing more than a misconception of the term optimization. It is important that the optimization method takes into account all the interactions and the optimum point of the process under study [37].

Focusing to overcome this limitation, the so-called multivariate statistic analysis is being under development. Among the most relevant techniques used in process optimization, the Response Surface Methodology (RSM) is a collection of experimental strategies, mathematical methods and statistical inference based on the fit of a polynomial equation to the experimental data [38–40]. It's a very economic technique for collecting the maximum amount of complex information by the simultaneous optimization of the levels of variables. In addition, it saves the material used for analyses and personal costs as well (Aslan and Cebeci 2007). The design procedure of RSM follows six basic steps [36], namely:

(i) Selection of the independent variables of major effect on the system through screening experiments and delimitation of the variables levels considering the scope of the study.

(ii) Definition of the experimental design and execution of the experiments according to the experimental matrix.

(iii) Development of a mathematical model of the response in the optimum region through the fit of a polynomial function.

(iv) Estimation of experimental parameters that produce a maximum or minimum value of response.

(v) Verification of the viability of performing a shift towards the optimal region.

(vi) Assessment of the optimal values for each variable in study.

The relationship between the response and the independent variables is usually unknown in a process whereas a linear or square polynomial function can be employed to describe the system studied [41]. The general form for the second-order model (equation 1.7) is expressed as:

$$y = \beta_0 + \sum_{i=1}^{k} \beta_i x_i + \sum_{i=1}^{k} \beta_{ii} x_i^2 + \sum_{i=1}^{k-1} \sum_{j=2}^{k} \beta_{ij} x_i x_j + \varepsilon \qquad \textbf{(Equation 1.7)}$$

where $x_1, x_2, \ldots, x_k$ are the input factors which influence the response $y$; $\beta_0, \beta_{ii} (i = 1,2,\ldots,k)$, $b_{ij} (i = 1,2,\ldots,k; j = 1,2,\ldots,k)$ are the unknown parameters and $\varepsilon$ is a random error. The β coefficients, which should be determined in the second-order model, are obtained by the least square method.

The RSM significance should be properly determined. Depending of the process to be optimized, the RSM design is crucial, as thus the number of variables, levels and experiments need to be carefully selected. The three-level factorial design, the Box-Behnken design, the central composite design and the Doehlert design are some of the most well-known second-order symmetrical design examples [36].

# 2. CHAPTER I – STUDY OF THE INFLUENCE OF DIFFERENT CULTIVATION PARAMETERS ON CULTURES OF *MICROALGAE M*

## 2.1 Overview

After the common fundamentals for the following two chapters were unravelled, the present section covers the upstream processing, which involves the cultivation and harvest steps of a bioprocess. Integrated in the European project SPLASH (Sustainable polymers from algae sugars and hydrocarbons) namely, working package "Process design – production and downstream processing". This research was developed in AlgaePARC facilities of Wageningen and Research University, Netherlands. Due to the confidentiality agreement established, the most relevant information was codified. The aim of this section is to understand which operational factors are determinant on the A and B of continuous cultures of *Microalgae M*. Therefore, a review of the tested microalga and its specific needs for cultivation are firstly presented, while a second part will explore the engineering of photobioreactor used and the theoretical concepts of light scattering inside the broth. Briefly, large-scale application of phototrophic growth is discussed as well as the experimental design used to model the responses of interest. Finally, the three mathematical models obtained here will help to enrich the knowledge of its cultivation and to foresee the largescale applications in the field of commodities for *Microalgae M*.

### 2.1.1 *Microalgae M*

*Microalgae M* is a green pyriform shaped planktonic microalga. It is a member of the Clorophyceae (chlorophyta), and it is widespread in freshwater and brackish water of all continents. The colonies grow in clusters and the individual cells are embedded in an extracellular matrix composed of polymerized and liquid hydrocarbons, constituting a unique colonial organization, also proved by Figure 2.1 [42]. Actually, paleobotanical studies suggest that *Microalgae M* could have had an important contribution on petroleum, coal deposits and oil shales, due to its conspicuously ability to synthetize and accumulate extracellular hydrocarbons. *Microalgae M* has been recognized as a potential source for bioplastics and biofuels production [43,44]. This hydrocarbon content, *i.e.* highly reduced compounds comprising only carbon and hydrogen and a number of specific ether lipids, can be extremely high, up to 80%, however it varies upon culture conditions, species and strains [45,46] ( . On the other hand, it's also prone to produce small quantities of saturated and mono-unsaturated FAs as well as triglycerides (TAGs) [43]. With regard to *Microalgae M* growth rate, it shows a minimum generation time of two days, which can merely be harvested a few times a week [47]. Apart from the synthesized hydrocarbon it also shows EPS production however, as hydrocarbons, the amount of EPS production varies with strains, the race it belongs, the physiological and the culture conditions [48].
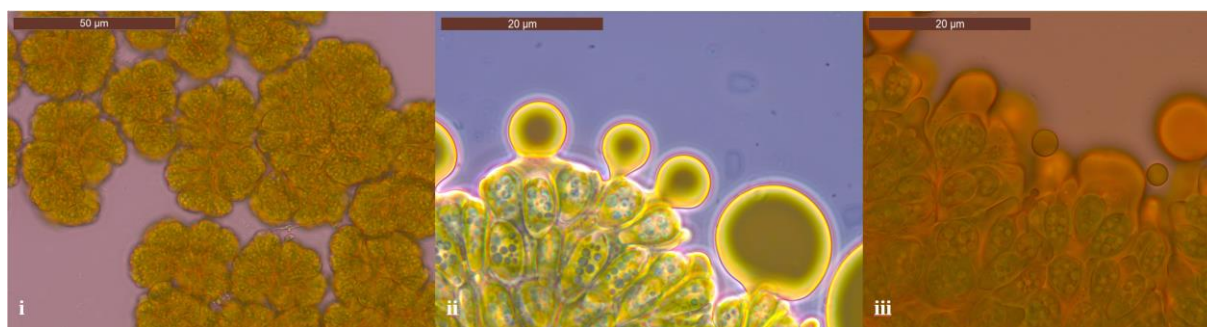


**Figure 2.1-** Magnification of *Microalgae M* cultures with LEICA DM2500: (i) *Microalgae M* colonies magnified 40x; (ii and iii) *Microalgae M* secreting hydrocarbons magnified 100x.

An unusual phenomenon of *Microalgae M* is the hydrocarbon secretion in the extracellular medium, while all known species of microalgae kept them in the cytoplasm [43]. Different studies on the intercellular lipids showed that they are associated with chloroplasts and

endoplasmic reticulum. The cells are associated via a complex extracellular matrix (ECM), comprising three different compartments [42], as shown in Figure 2. Briefly from Figure 2.2:

(i) Each cell is surrounded by a polysaccharide wall.

(ii) A cross-linked hydrocarbon network permeated with liquid hydrocarbons, comprise the intercolonial ECM space.

(iii) The ECM liquid hydrocarbons are sequestered between the colonies enclosed in a retaining wall and a fibrillary sheath, dominated by polysaccharides.

Four chemical races of *Microalgae M* have been documented: A, B, L and S [49]. Differentiation can be made among races due to morphological and physiological features, as presented in Table 2.1, although the hydrocarbons chemical nature constitutes the basis for this classification.
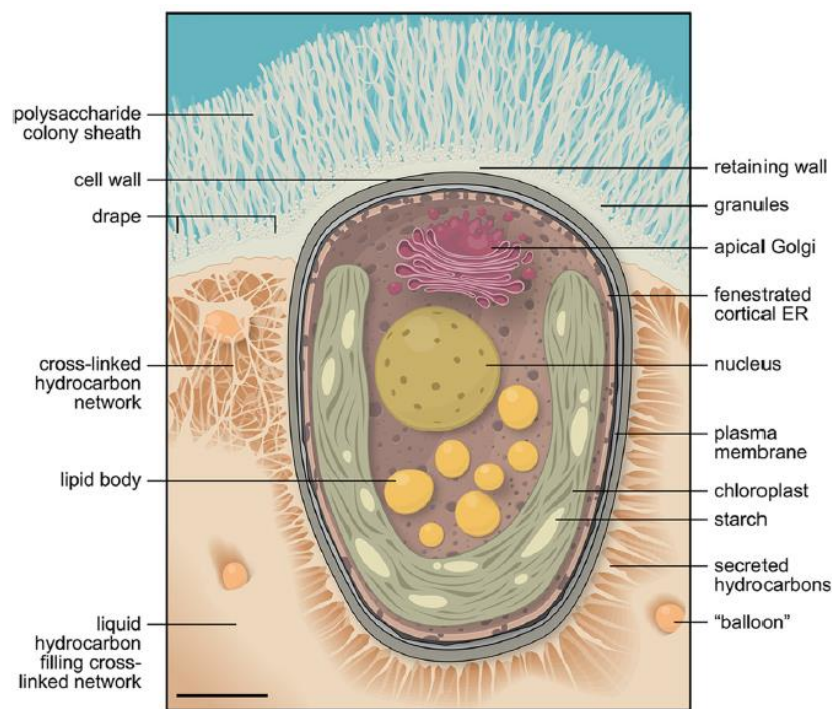


**Figure 2.2** - Model of a *Microalgae M* cell and its surrounding extracellular matrices. For simplification, only relevant organelles are presented. Adapted from literature [42].

**Table 2.1 -** Description and comparison of the different features of the *Microalgae M* races A, B and L. Adapted from literature [50].

| | *Microalgae M* | | |
|---|---|---|---|
| **Features** | **Race A** | **Race B** | **Race L** |
| **Colony Size** | 13 µm × 7-9 µm | | 8-9 µm × 5 µm |
| **Colony colour in steady-state** | Pale yellow or green | Orange reddish or orange brownish due to accumulation of carotenoids | |
| **Long chain alkenyl phenols** | Present | Absent, terpenoids instead | |
| **Biopolymers nature** | Very long aliphatic chains cross-linked by ether bridges and bearing fatty esters | Tetraterpenoid cross-linked ether bridges | |

Briefly, race A produces essentially $C_{21}$-$C_{31}$, odd-numbered hydrocarbons n-alkadienes and trienes, whereas an active-state can constitute 61% of the dry cell mass. Race B produces polymethilated unsaturated triterpenes, known as botryococcenes, $C_{30}$–$C_{37}$, which can constitute up to 27 to 86% of the dry cell mass. Race L only produces a single hydrocarbon, $C_{40}H_{78}$, a tetraterpene, called lycopadiene, accounting for 2 to 8% of the dry biomass [50,51]. Race S produces epoxy-n-alkane and saturated n-alkane chains with carbon $C_{18}$ and $C_{20}$, respectively. The chemical structure of the main hydrocarbons *per* race is shown in Figure 2.3, with race S being the exception due to its recent classification.
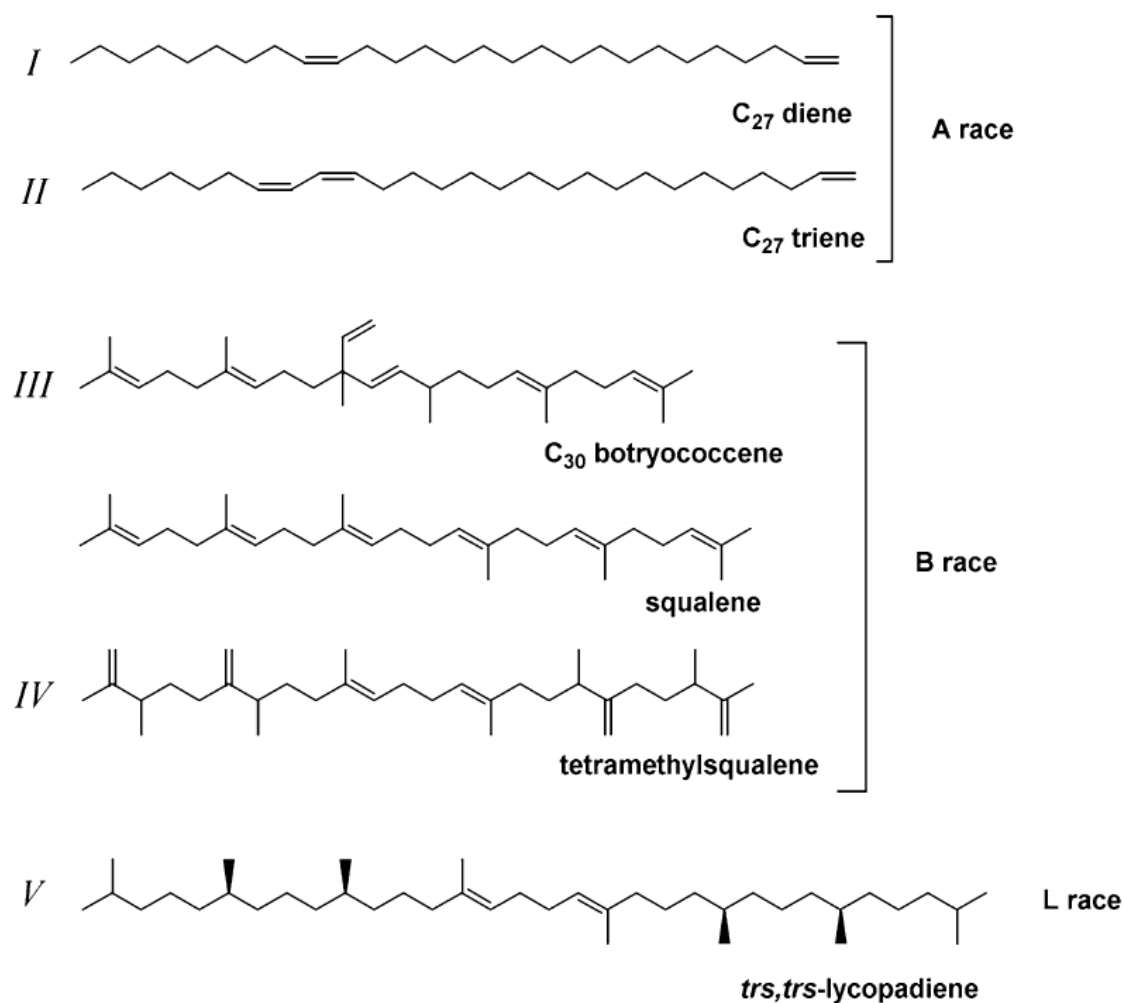
**Figure 2.3 -** Types of hydrocarbons produced by the three chemical races of *Microalgae M*. Adapted from literature [48].

For all *Microalgae M* races, the hydrocarbon and ether lipids productivity is optimal during the exponential phase of growth, decreasing considerably as the cells enter the early growth phase [45].

The hydrocarbon oil produced by race B (mainly *Botryococcenes*) can be used in the oil refineries of nowadays. Oil, kerosene and diesel could be obtained by the hydrocracking and distillation of *Botryococcenes* in an extension of 97% of yield, as shown in Figure 2.4 [25]. In addition, the kerosene could be applied in jet fuels [46].
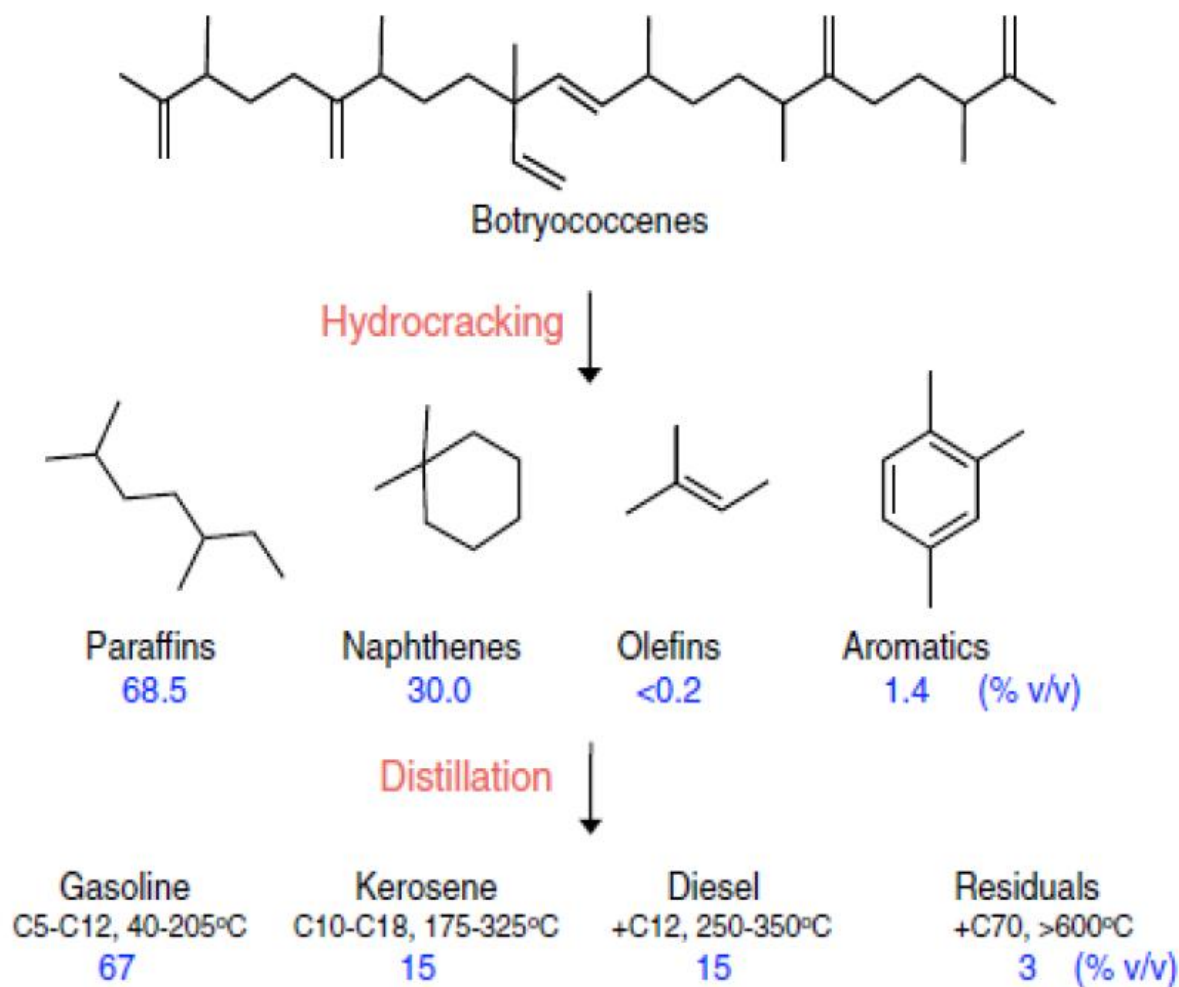
**Figure 2.4** - Hydrocracking/Distillation of Botryococcene catalyses different types of fuels. Botryococcenes Hydrocracking produces Paraffins (68% v/v), Naphthenes (30% v/v), Olefins (<0.2% v/v), Aromatics (1.4% v/v); Distillation of these compounds produces Gasoline (67% v/v), Kerosene (15% v/v), Diesel (15% v/v) and some residues (3% v/v) [25]

## 2.1.2 Cultivation of *Microalgae M*

Due to the increased interest in the *B. braunii* bioactive composition, its proper cultivation is a crucial demand. The phototrophic *Microalgae M* growth requires $CO_2$, light, temperature, inorganic nutrients and water to grow. To increase the biomass and hydrocarbon's yields, the cultivation parameters need a careful optimization to understand which factors are the most significant. It has been shown that a modified Chu medium is suitable for the *Microalgae M* growth [52–54]. Yoshimura and collaborators [55] have shown that the cultivation of *Microalgae M* with sparge air in $CO_2$ (0.3%) had a threefold increase in the specific growth rate, however optimal $CO_2$ concentrations for the growth are strain specific [56]. Jin and co-authors [21], shown that the hydrocarbon productivity is affected by the pH, being determined the optimal pH in the range of 5.5 and 8.0. Moreover, the *Microalgae M* growth can be optimal between 25–30 °C and have a maximum growth temperature of 32 °C [57]. A wide range of irradiance is accepted by *Microalgae M* cells, since they can increase or decrease the capability of capturing the light [58].

Micronutrients, such as vitamins, have been considered as a potential limiting factor for microalgae growth since they are unable to synthesize them [59]. In fact, bacterial presence in *Microalgae M* cultivation cannot be avoided, whereas studies on a possible symbiotic interaction have been carried out [60,61]. Some reports have proposed that the occurrence of bacteria do not have impact on the hydrocarbon profiles of *Microalgae M,* while others have suggested that some algal-bacterial symbiotic consortia may have a potential to improve the productivity of hydrocarbons [21,62]. Some of these bacteria have been identified as *Pseudomonas* sp. and *Rizhobium* sp. [60]. Recently, a draft bacterial genome sequence of a long-term consortium with *B. braunii* strain Guadeloupe (race B) was screened for new bacterial species from analysis of 16S rRNA gene sequence. Genes encoding for thiamine, cobalamin and biotin synthesis were found among their genomes, which seem to be essential micronutrients for auxotrophic algae like *Microalgae M* [63].

### 2.1.3 Photobiorreactors, PBR

Bioreactor is defined as an apparatus or system capable of supporting any kind of biological active environment [64]. Bioreactors can be distinguished based on the reactant or product that has the strongest effect on the reaction rate and the way this rate-limiting component is supplied or removed from the reactor.

Photobiorreactors (PBR) are also a type of reactor limited by the input rate of light, such as sugar-limited or oxygen-limited reactors [65]. They have been designed and experimented as the basic tool to improve the biological conversion of photosynthetic organisms since the 1940s. There are laboratory and large scale PBR, ranging from closed controlled to open less predictable systems, which can be set indoors or outdoors. Nowadays, the open raceway ponds have been the most used large-scale production system, mainly because they are easily build [66]. Limitations on the species and biomass productivity that can be used and achieved, respectively, are reasons to develop these closed systems (Janssen and Lamers 2014).

In general, closed systems are more expensive and productive however, they are less prone to evaporation and contamination than open raceway ponds. In addition, they provide a much more accurate control of the culture parameters, being thus considered as reliable systems for the development of mathematical models, through its application in outdoor systems. Common closed PBR that are used for growing algae include flat panels, vertical and horizontal tubular, stirred tank, helical type and the hybrid type which has the purpose of combine the closed and open designs in order to overcome the disadvantages of the other [67–69]. Despite several research efforts developed to date, the most suitable system is situation-dependent, by the simple fact that, even the algal species and the intended final product will play a role [67].

To develop the knowledge considering the outdoor production, a closed PBR in the laboratory scale should guarantee a reliable control to monitor the operational parameters, as well as, be time saving through an easy and fast cleaning/sterilization.

2.1.3.1 Algaemist – A flat panel tool

For controlled algae growth experiments, the Algaemist Photobiorreactores developed by the *Ontwikkelwerkplaats of* Wageningen University, shown in Figures 2.5 and 2.6, is a very wise choice regarding its tailor made details. First of all, these have a flat vessel instead of a circular one, which enables to facilitate the entrance of the light, making the light measurement a much easier task. The Algaemist Photobiorreactores have a sparger on the bottom instead of a stirrer, which enables a higher contact between the cells and the nutrients and $CO_2$, allowing the effective mass and gas transfer. This flat panel photobiorreactor has a working volume of $\pm400$ mL with a total gas flow of $\pm400$ mL min$^{-1}$. It is a closed system with a light path of 14mm and the mixing of the culture is done by sparging air/$CO_2$ at 30 mm height from the bottom of the reactor. The pH is constantly measured through an electrode on the top of the reactor and controlled by the $CO_2$ addition. This Algaemist Photobiorreactor can work in a pH range of 2-12. Due to the consumption of $CO_2$ by the microalgae, the culture becomes more alkaline as the bicarbonate equilibrium (equation 2.1) will shift to the right. Generally, microalgae grow within the pH range of 6-9, therefore this equilibrium is dominant and once the pH becomes higher than the set point, $CO_2$ is injected.

$$HCO_3^- \rightleftharpoons CO_2 + OH^- \qquad \textbf{(Equation 2.1)}$$
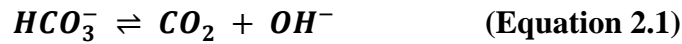
Regarding the photobiorreactor temperature, a water jacket provides the heating or cooling. The light is supplied by six Bridgelux LED lamps, controlled continuously with two light sensors putted before and after the algae compartment. Algaemist photobiorreactors provide a chemostat or turbidostat control, with regard to light and flow rate. Further specifications of the Algaemist photobioreactor can be found in the *Algaemist manual* from Mooij 2012 [70].
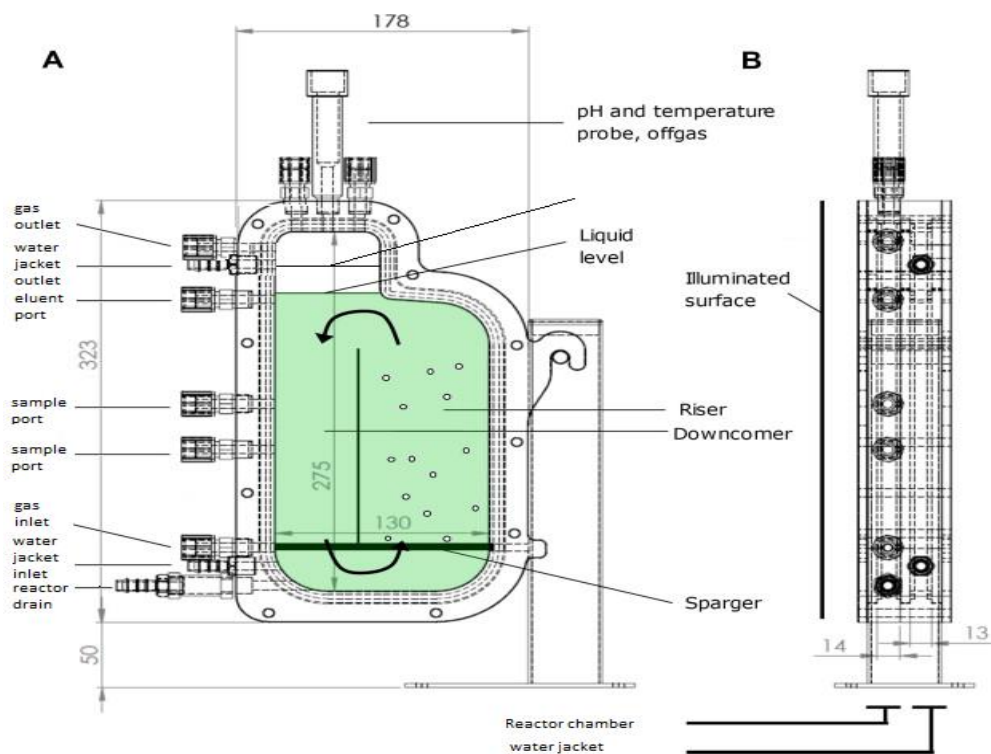
**Figure 2.5** - Algaemist-S flat panel bioreactor. Adapted from literature [70].
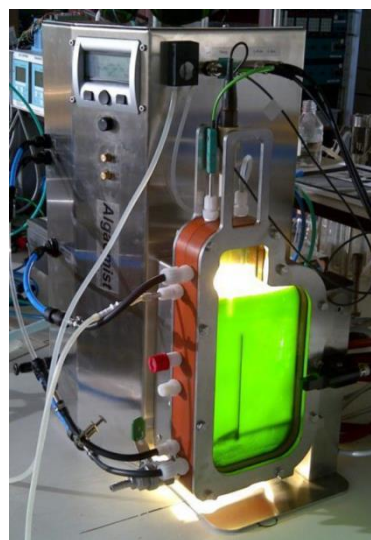


**Figure 2.6 -** Algaemist-S photobiorreactor dimensions, front and side view with the respective components. Adapted from literature [70].

2.1.3.2 Light-limited cultures

The photosynthetic efficiency (PE) is defined as the efficiency with which the energy of light is converted into the chemical energy. Actually, the PE of microalgae cultures is not higher than the PE of plants (C3 and C4), mainly due to photosaturation and photoinhibition energy losses representing the carbohydrate production. Inside the microalgae culture, photons (light unit) are absorbed by the pigments of the photosystems located in the thylakoid membranes of chloroplasts, in which the absorbed photons are only comprehended in the visible zone (400 to 700 nm). This range is called photosynthetically active radiation (PAR) and it is measured in µmol PAR $m^{-2}$ $s^{-1}$. Once algal cells are in the presence of light, they have a limited capability of increasing or decreasing their size and pigmentation regarding the available light, in a mechanism known as photoacclimation [71].

In order to minimize variations in the light regimen in time and space, in this work, the short light path inside a flat panel was preferred, as represented in Figure 2.7 [72]. Considering the closest place to the illumination window, the cells are saturated (0 to $L_1$), capturing as much light as they can and the synthesis machinery is working linearly at is maximum. This is translated in the algal maximum specific growth rate ($\mu_{MÁX}$) but, at the same time, in a waste of surplus energy as heat, due to refraction and reflection (Figure 2.8). In cases where high light intensities are applied, the culture surfaces may cause photoinhibition, which decreases the PE [22]. When the incident light becomes lower than $L_1$, cells are considered to be in the light-limiting zone ($L_1$ to L). The growth rate is no longer equal to $\mu_{MÁX}$ and tends to decrease along with the reactor light path (z) while, at this moment, the light is used with the maximum efficiency. For farthest zones of incidence of light, the cells may experience the decay zone where light is no longer sufficient to maintain the growth rate [65].
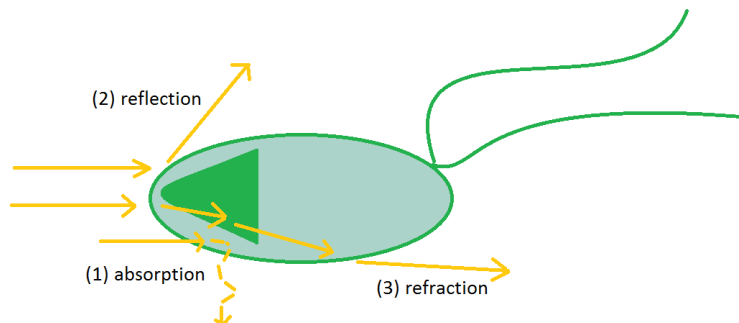


**Figure 2.7** - Photon flux profile (I) in the top graph and specific growth rate profile (µ) in the bottom graphic along the flat-panel reactor depth (z). Adapted from literature [65].
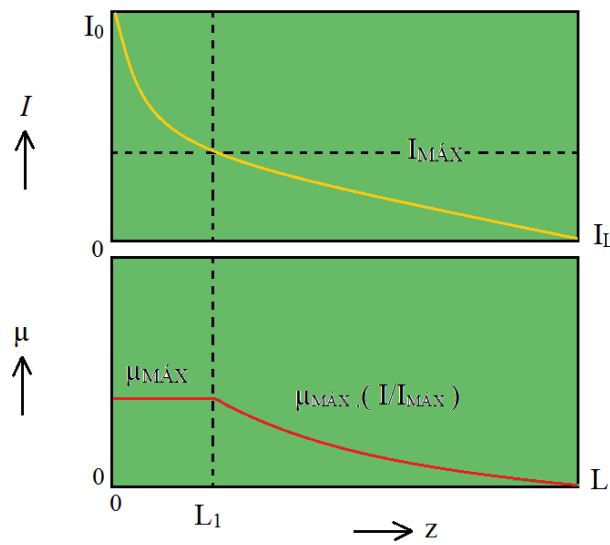
**Figure 2.8 -** Light absorption and scattering by microalgae cells. Scattering comprises both reflection and refraction of light of the surrounding water. Adapted from literature [16].

### 2.1.4 Modelling for scale-up

In recent years, many attempts have been made to envision the scale-up of the microalgae production for a large-scale production. Unfortunately, the productivities have been based on crude extrapolations from the lab scale, when the conditions differ drastically from those of the outdoors production systems. Moreover, the scale-up brings other issues that indirectly affect the algae culture such as, the liquid circulation time, the hydrodynamic stress and the mass transfer [73]. Moreover, and if in the one hand, the microalgae energy harvest strategy strongly depends of light, on the other hand, as they grow, the incident light will have different absorption rates. Therefore, modelling the microalgae production is much more difficult when compared with classical microorganisms (bacteria, yeast or fungi). This additional complexity stems from a wide range of mechanisms used by microalgae to respond to, or protect themselves from, light and other local environmental factors. In this sense, different strategies have been studied, being the mathematical modelling the example of an essential tool to understand and to fulfil the gap between lab-scale and the industrial scale reality [74].

2.1.4.1 X004 design

The experimental design is widely used for controlling the effects of different parameters in many processes. The number of experiments is proportional to the time and resources consummation [37]. Through efficient experimental design and statically application methods, these numbers can be reduced and the experimental errors can be minimized. Therefore, X004 appears as a class of rotatable second-order design based on a three-level incomplete factorial design - Figure 2.9a [75]. X004 design is described in Figure 2.9b.
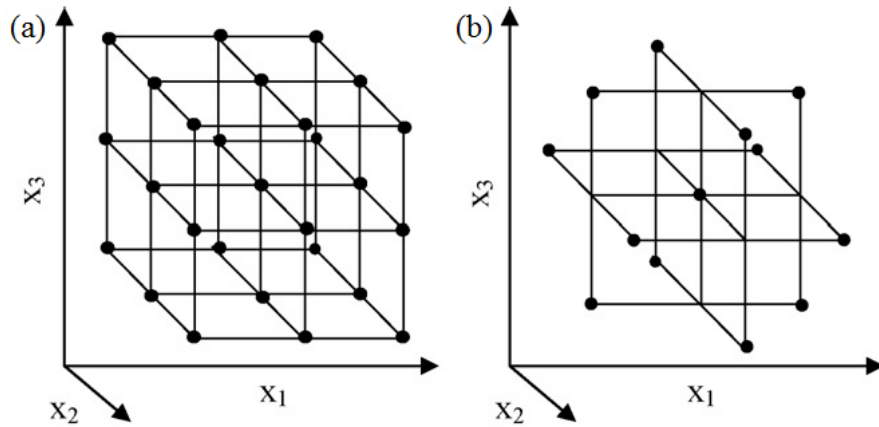


**Figure 2.9 -** Experimental design based on the study of three variables in three levels: (a) complete three-level factorial design and (b) X004 design as an incomplete three-level factorial design. Adapted from literature [36].

Regarded as a cube, the experimental points of the X004 are located on a hypersphere equidistant from the central point [75]. The requirements for its development concern that:
(i) all the factor levels have to be adjusted only at three levels ($-1, 0, +1$) with equally spaced intervals between these levels.
(ii) The number of experiments (N) is defined (equation 2.2) as:

$$N = k^2 + k + c_p \qquad \text{(Equation 2.2)}$$

where $k$ is number of factors and $C_p$ is the replicate number of the central point.
The experimental matrix for the X004 design for three variables containing the coded values of the factor levels is represented in Table 2.2.

**Table 2.2 -** Coded factor levels for a X004 design of a three-variable system. Adapted from literature [76].

| Experiment | $X_1$ | $X_2$ | $X_3$ |
|:---:|:---:|:---:|:---:|
| 1 | -1 | -1 | 0 |
| 2 | 1 | -1 | 0 |
| 3 | -1 | 1 | 0 |
| 4 | 1 | 1 | 0 |
| 5 | -1 | 0 | -1 |
| 6 | 1 | 0 | -1 |
| 7 | -1 | 0 | 1 |
| 8 | 1 | 0 | 1 |
| 9 | 0 | -1 | -1 |
| 10 | 0 | 1 | -1 |
| 11 | 0 | -1 | 1 |
| 12 | 0 | 1 | 1 |
| C | 0 | 0 | 0 |
| C | 0 | 0 | 0 |
| C | 0 | 0 | 0 |

In summary, the X004 design is useful to avoid experiments under extreme factors, since it is not comprising all factors combinations. Furthermore, the comparison on efficiency of the X004 and other response surface methods (central composite, Doehlert matrix, complete three-level factorial design) has demonstrated the X004 as slightly better than the central composite but much better than the three level full-factorial design, mainly due to its large number of experiments [76].

Regarding the microalgae cultivation optimization for biofuels production several attempts have been carried out, with relevant significance between the model and the experimental data, however the focus has remained on medium optimization [19,77,78].

## 2.2 Materials and Methods

### 2.2.1 Organism, medium and cultivation

The green *Microalgae M*, was obtained from (University of Bielefeld, Germany) and batch-grown in shake flasks inside an illuminated shake cabinet (120 rpm, 2.2 $CO_2$ (v/v) at 25ºC) until the stationary phase was achieved. The culture was grown in a modified Chu13 Medium (12mM nitrate): 0.32 µM $CuSO_4 \cdot 5H_2O$, 0.76 µM $ZnSO_4 \cdot 7H_2O$, 0.32 µM $CoSO_4 \cdot 7H2O$, 7.93 µM $MnSO_4 \cdot H2O$, 0.25 µM $Na_2MoO_4 \cdot 2H2O$, 46.26 µM $H_3BO_3$, 734 µM $CaCl_2 \cdot 2H2O$, 811 µM $MgSO_4 \cdot 7H2O$, 602 µM $K_2HPO_4$, 11.87 mM $KNO_3$, 55 µM FeNaEDTA, 50 µM HEPES, 0.1 µM Vitamin $B_{12}$, 3.26 µM Thiamine, 0.11 µM Biotin. Medium pH was adjusted to 7.2 with KOH. Six calibrated Bridgelux LED lamps (BXRA W1200, Bridgelux, Livermore, USA) were controlled on 12 hours *per* day. Prior to use, lights were calibrated with a PAR light meter (LI-COR LI-250A), a pattern of ten points was repeated for five different light intensities. The microcontroller calibration was done at five different speeds to assess the flow rate, meaning the dilution rate. A water jacket controlled the temperature in the reactor. A pH probe (Q-I-S QP150X) monitored the pH which was kept at 7.2 (±0.1), the process control was done by $CO_2$ injection on demand in the airstream. Aeration was done with humidified air at a flowrate of 0.5 (v/v) which was also used for the airlift loop. Furthermore, Algaemist photobioreactor and control systems can be observed in Figure 2.10. All the experiments were performed in timed cyclostat operated, aseptic, heat-sterilized, airlift, loop flat panel photobioreactors (Algaemist-S, further specifications 2.1.3.1). Batch-grown cells were inoculated and five days after inoculation, the photobioreactor (PBR) was switched to continuous mode, F4, F5 and F6 regarding the experiment under test, with withdrawal of culture at the same rate. Once steady state was achieved, analytical procedures were performed. It was assumed that cultures achieved a steady state ($\mu = D$) after harvesting

3 times the volume of the reactor (400 mL) followed by 5-15 constant determinations of dry weight.
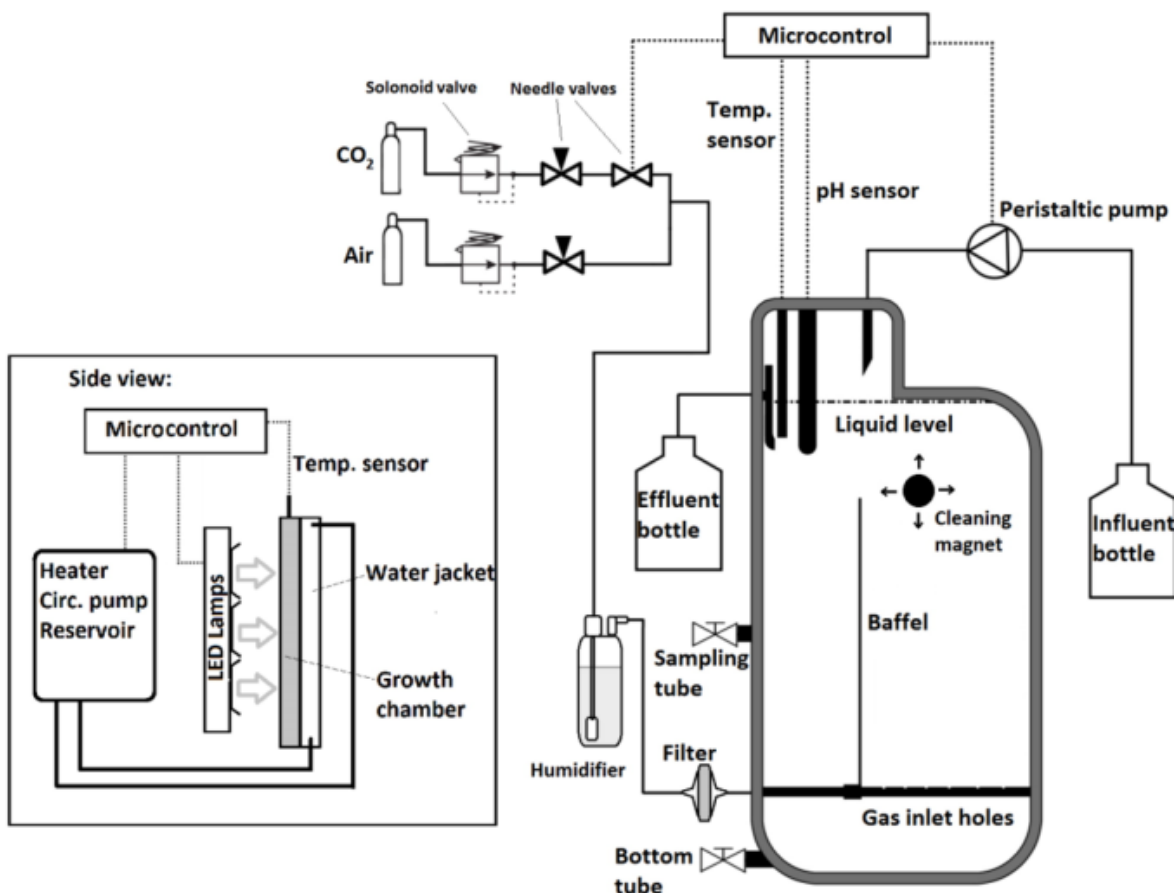


**Figure 2.10** - Algaemist photobioreactor and control systems for biomass concentration, pH and gas supply (A). Side view of photobioreactor and the temperature control mechanism (B). Adapted from literature [70].

### 2.2.2 Analytical Procedures

Dry cell weight was determined according to Kliphuis and collaborators [79]. Cells were filtrated under mild vacuum and washed with ammonium formate (0.5M) upon pre-weighed 0.7 μm GF/F glass microfibre filters (Whatman). All used filters were dehydrated (oven at 100ºC for 24 hours and proceeded by silica chambers for 1 hour) before (W1) and after (W2) biomass retention. The dry biomass composition comprised all the insoluble material which includes living, non-living algae, as well as, hydrocarbon content. It was weighted under highly precise scale, and the WTD was obtained in g/L and calculated according to equation

2.3. The colony size, was determined using a multisizer (Malvern Hydro SM coupled to a Malvern Mastersizer 2000). The Malvern Hydro SM was set to 1200 rpm and was filled to 1 cm below the top with milliQ water. Sample from the reactor was added until obscuration reached 2%. Five replicates were obtained for each sample. Results were expressed in $\mu m^3$. Three times a week, culture is checked regarding contaminations microscopically, namely protozoa (LEICA Laborlux S). Also, all samples were maintained for 20 min at room temperature (21ºC), for hydrocarbon droplets observation. Extraction and quantification of hydrocarbons content was analysed once the cultures achieved and proved a steady-state. A solid-liquid extraction of the cultures with n-hexane (5:1 v/v) was performed to extract the target hydrocarbons. The cultures were heated at 85 °C for 10 min. Afterward 2 mL of n-hexane were added and the sample was shaken for 10 min, which was proceeded by a centrifugation at 1200 rpm for 10 min. The upper layer was transferred to GC-FID vials and stored at 4°C. The hydrocarbon content was analysed in a GC-FID *via* a standard curve of squalene and expressed in mg L$^{-1}$ day$^{-1}$ according to equation 2.5.

### 2.2.3 Numerical methods:

Biomass concentration was calculated by equation 2.3.

$$\boldsymbol{WTD} \ = \ \frac{\boldsymbol{W2\ (g) - W1\ (g)}}{\boldsymbol{V\ (mL)}} \times \boldsymbol{1000} \qquad \textbf{(Equation 2.3)}$$

The parameter A, was determined once the reactor achieve the steady-state by equation 2.4

$$\boldsymbol{A = WTD \times F} \qquad \textbf{(Equation 2.4)}$$

The parameter C, was determined once the reactor achieve the steady-state by equation 2.5.

$$\boldsymbol{C = MD \times F} \quad \textbf{(Equation 2.5)}$$

### 2.2.4 Experimental Design for M4S201

With regard to generate mathematical models that express A, B and C of the green Microalgae *M* the combined effect of D, F and L was assessed through a M4S201. An experimental design was used to identify the relationship existing between the response functions and the process variables, as it shown in Table 2.3. Thus, the grid of experiments

based on three different levels is presented in Table 2.4. The selection and range of these three factors was based on preliminary experimental data found in outdoors (data not shown). The middle level is meant to be the cornerstone of all the experiments.

**Table 2.3 -** Chosen levels for each cultivation factor (D, F and E).

| Factor | Level 1 | Level 2 | Level 3 |
|--------|---------|---------|---------|
| D | D1 | D2 | D3 |
| F | F1 | F2 | F3 |
| E | E1 | E2 | E3 |

**Table 2.4 -** Resume of all fifteen experiments according to the X004 experimental design with experimental values for the independent variables.

| Experiment | D | E | F |
|------------|-----|-----|-----|
| 1 | D1 | E2 | F1 |
| 2 | D3 | E2 | F1 |
| 3 | D1 | E2 | F3 |
| 4 | D3 | E2 | F3 |
| 5 | D1 | E1 | F2 |
| 6 | D3 | E1 | F2 |
| 7 | D1 | E3 | F2 |
| 8 | D3 | E3 | F2 |
| 9 | D2 | E1 | F1 |
| 10 | D2 | E1 | F3 |
| 11 | D2 | E3 | F1 |
| 12 | D2 | E3 | F3 |
| 13* | D2 | E2 | F2 |
| 14* | D2 | E2 | F2 |
| 15* | D2 | E2 | F2 |

*middle level reinforced with three replicates.

## 2.2.5 Statistical Analysis

The STATGRAPHICS Centurion XVI software was used to conduct the experimental design and the statistical analysis. A response surface methodology and analysis of variance (ANOVA) were employed to determine the regression coefficients, statistical significance of the model terms and to fit the mathematical models of the experimental data that aimed to optimise the overall region for both response variables. Based on the experimental data, regression analysis was performed and was fitted into the following second order polynomial model (equation 2.6):

$$\alpha = \theta_0 + \sum_{\psi=1}^{\lambda} \theta_{\psi}\Omega_{\psi} + \sum_{\psi=1}^{\lambda} \theta_{\psi\psi}\Omega_{\psi}^2 + \sum_{\psi=1}^{\lambda-1} \sum_{\psi=2}^{\lambda} \theta_{\psi@}\Omega_{\psi}\Omega_{@} + \acute{\eta} \qquad \textbf{(Equation 2.6)}$$

where $\Omega_{\lambda}$, $\Omega_{\lambda}$, ..., $\Omega_{\lambda}$ are the input factors which influence the response $\alpha$; $\theta_0$, $\theta_{\psi\psi}$ ($\psi = 1,2,$ ... $\lambda$, ), $\theta_{\psi@}$ ($\psi = 1,2,$ ..., $\lambda$; $@ = 1,2,$ ..., $\lambda$) are the unknown parameters and $\acute{\eta}$ is a random error. The $\theta$ coefficients, which should be determined in the second-order model, are obtained by the least square method. The adequacy of the model was predicted through the regression analysis ($R^2$), $F$-ratio value and Durbin-Watson obtained from the analysis of variance (ANOVA). Therefore, the relationship between the independent variables ($D$, $E$ and $F$) and the response variables ($A$, $C$ and B) was demonstrated by the response surface plots.

## 2.3 Results

### 2.3.1 M4S201

Instead of optimizing by a one-factor-at-a-time approach, the statistical M4S201 design provides the opportunity to determine the optimal conditions in any given parameters by establishing the relationship between factors and predicted responses. Values of independent variables were considered, as well as measured and predicted values for both responses, A, B and C, given by Table 2.5. In supporting information, Tables S1.1 and S1.2 include the conversion of A and C responses previously obtained from equations 2.4 and 2.5, respectively.

**Table 2.5 – X004 experimental design for the three culture parameters with three levels (coded values are also present).**

| Run | $X_1$ | $X_2$ | $X_3$ | Response 1 (D) | | Response 2 (E) | | Response 3 (F) | |
|-----|-----|-----|-----|-----|-----|-----|-----|-----|-----|
| | D | F | E | Experimental | Predicted | Experimental | Predicted | Experimental | Predicted |
| 1 | -1 | -1 | 0 | 0.00 | 0.23 | 0.00 | -6.78 | 0.00 | 9.4 |
| 2 | 1 | -1 | 0 | 1.03 | 1.01 | 119.36 | 128.17 | 0.74 | 16.3 |
| 3 | -1 | 1 | 0 | 0.00 | 0.02 | 105.43 | 96.62 | 0.00 | -8.9 |
| 4 | 1 | 1 | 0 | 0.50 | 0.27 | 232.50 | 239.28 | 5.87 | 10.2 |
| 5 | -1 | 0 | -1 | 0.00 | -0.17 | 0.00 | 14.62 | 0.00 | 7.9 |
| 6 | 1 | 0 | -1 | 0.04 | 0.12 | 126.17 | 125.20 | 3.19 | 24.3 |
| 7 | -1 | 0 | 1 | 0.01 | -0.08 | 48.32 | 50.97 | 0.00 | -8.4 |
| 8 | 1 | 0 | 1 | 0.49 | 0.66 | 232.64 | 218.02 | 1.80 | 1.1 |
| 9 | 0 | -1 | -1 | 0.42 | 0.36 | 127.05 | 119.21 | 10.00 | 82.7 |
| 10 | 0 | 1 | -1 | 0.09 | 0.24 | 0.00 | 151.66 | 3.20 | 11.7 |
| 11 | 0 | -1 | 1 | 1.18 | 1.03 | 103.19 | 109.00 | 0.51 | 4.1 |
| 12 | 0 | 1 | 1 | 0.13 | 0.19 | 283.21 | 291.05 | 10.07 | 50.8 |
| 13* | 0 | 0 | 0 | 0.38 | 0.40 | 235.19 | 138.01 | 20.04 | 91.2 |
| 14* | 0 | 0 | 0 | 0.09 | 0.40 | 152.22 | 138.01 | 16.54 | 91.2 |
| 15* | 0 | 0 | 0 | 0.49 | 0.40 | 81.82 | 138.01 | 18.11 | 91.2 |

*middle level reinforced with three replicates.

## 2.3.2 Model for A

By applying multiple regression analysis on the data experimentally determined by equation 2.4, the regression coefficients were estimated and the following second-order polynomial equations was obtained, given by equation 2.7.

$$A = \text{'}\Omega + \text{''}\Omega + \text{'}\Omega - \text{''}\Omega \qquad \textbf{(Equation 2.7)}$$

The quality of the model fit is evaluated by the coefficient of determination ($R^2$) which the model gives an $R^2$ of (0.874) indicating good relation between the experimental and predicted values. ANOVA of this quadratic model is presented in Table 2.6. The *p-values* are used as a tool to check the significance of each term. The smaller the magnitude of $p$, the more significant the corresponding coefficient was. Though the F-ratio among the model terms indicates suggestive effects in the response, only model terms ($p < 0.05$) are found to be statistically significant. Thus, the regression analysis of the experimental design demonstrated that the linear model terms (*D, F*) were significant ($p < 0.05$). Nevertheless, linear model term (E) has a marginally significant ($p < 0.1$) effect on A. The autocorrelation between errors in the model and linear association between determination coefficient residuals was evaluated by Durbin–Watson (DW) static method. The range of DW statistic varies between 0 and 4. The DW value below 2 indicates positive correlation whereas above 2 indicates a negative correlation [80]. In this study, DW value was 2.31 close to 2, wherein for a level of significance of 5%, our model shows no evidence of autocorrelation.

**Table 2.6 -** ANOVA results for response surface quadratic model of A.

| Term | Sum of Squares Error | Degrees of Freedom | Mean Squares Error | F ratio | *p*-value |
|---|---|---|---|---|---|
| D | 0,53045 | 1 | 0,53 | 10,93 | **0,0213** |
| F | 0,456013 | 1 | 0,46 | 9,39 | **0,0279** |
| E | 0,195313 | 1 | 0,20 | 4,02 | 0,1012 |
| $D^2$ | 0,10881 | 1 | 0,11 | 2,24 | 0,1946 |
| DF | 0,070225 | 1 | 0,07 | 1,45 | 0,2829 |
| DE | 0,050625 | 1 | 0,05 | 1,04 | 0,3540 |
| $F^2$ | 0,0840026 | 1 | 0,08 | 1,73 | 0,2454 |
| FE | 0,1296 | 1 | 0,13 | 2,67 | 0,1632 |
| $E^2$ | 0,0363103 | 1 | 0,04 | 0,75 | 0,4266 |
| Total Error | 0,242692 | 5 | 0,05 | | |
| Total (corr.) | 1,91929 | 14 | | | |
| Durbin-Watson | 2,31 (*p*=0,675) | | | | |

Based on the ANOVA table, the standardized effects of model terms were studied for the A response. The data reveal a significant positive and negative correlation for D and F, respectively. In the one hand, higher D would significantly benefit A, on the other hand higher F would have a significant negative effect on A. For the range of E tested there is no significant effect ($p < 0.05$) on A, though through its marginally significant ($p < 0.1$) effect, all the terms were considered in the model to minimize the error.

The mathematical model for A estimated a maximum of A0, which can be achieved with the optimum conditions as shown in Table 2.7. This shows that the A under the continuous regime becomes greater when D and E are at the highest tested level while the F is optimum at the minimum tested. As an example, a three-dimensional plot at fixed E, namely at E2, was generated since this factor has the least significant effect among the others. Note that for similar reasons the following models are fixed at the same E. Through this analysis, namely Figure 2.11, we can observe the positive effect of increasing the D, as well as, the negative effect of increasing the F, on the A. Furthermore, it should be stressed that the

optimal conditions attained could be slightly different by means of a study where parameters D and F were increased and decreased, respectively.

**Table 2.7 -** Range of tested values and optimal conditions for A.

| Term | Level 1 | Level 3 | Optimal |
|:---:|:---:|:---:|:---:|
| **D** | D1 | D3 | **D3** |
| **E** | E1 | E3 | **E1** |
| **F** | F1 | F3 | **F3** |
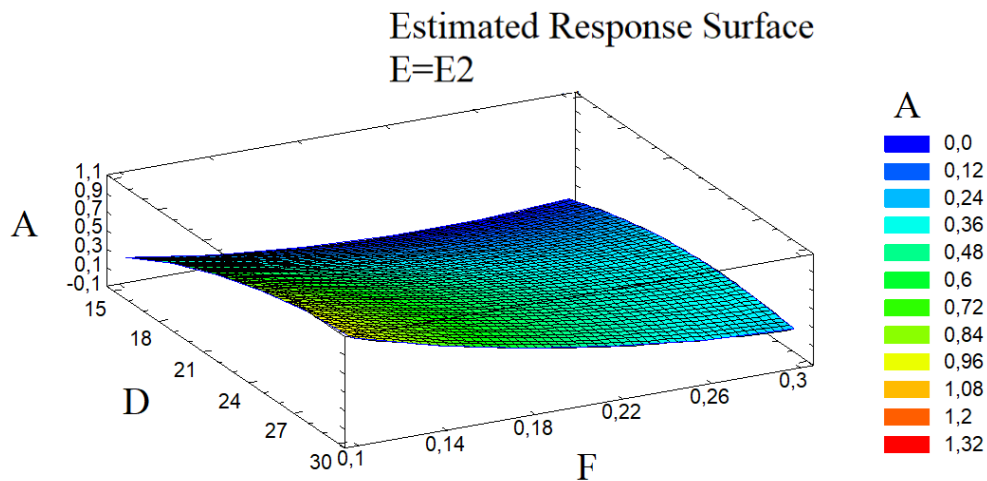


**Figure 2.11** - Response surface of A by *Microalgae X* continuous culture as a function of D and E, when E = E2.

### 2.3.3 Model for B

For this response, we did not need previous conversion since the experimental data was already in the desired form. Thus, applying multiple regression analysis on the experimentally determined data the predicted coefficients were determined, as is shown in equation 2.8. The $R^2$ value of this regression related to significant effects was 0.946.

$$B = \text{'}\Upsilon + \text{''}\Upsilon + \text{'}\Upsilon - \tilde{\Upsilon} \qquad \textbf{(Equation 2.8)}$$

Model summary ANOVA in Table 2.8 indicated the adequacy of this model. Most of the model terms F-ratio were found to be high, although the $p$-value determine their significance, namely for linear model term ($D$) ($p < 0.01$), linear model term ($F$) and quadratic linear term ($D^2$) ($p < 0.05$). A marginally effect of significance ($p < 0.1$) for the linear ($E$) and quadratic ($E^2$) model terms are also reported. The DW statistic, gives 1.53 value, approaching to 2, wherein for a level of confidence of 5%, results indicated this model might be autocorrelative.

**Table 2.8 -** ANOVA results for response surface quadratic model of CS.

| Term | Sum of Squares Error | Degrees of Freedom | Mean Squares Error | F ratio | $p$-value |
|---|---|---|---|---|---|
| D | 63131,5 | 1 | 63131,5 | 49,99 | **0,0009** |
| F | 13088,0 | 1 | 13088,0 | 10,36 | **0,0235** |
| E | 5426,22 | 1 | 5426,22 | 4,30 | 0,0929 |
| $D^2$ | 15141,6 | 1 | 15141,6 | 11,99 | **0,0180** |
| DF | 3200,16 | 1 | 3200,16 | 2,53 | 0,1723 |
| DE | 2833,97 | 1 | 2833,97 | 2,24 | 0,1944 |
| $F^2$ | 722,616 | 1 | 722,616 | 0,57 | 0,4835 |
| FE | 5595,04 | 1 | 5595,04 | 4,43 | 0,0892 |
| $E^2$ | 913,26 | 1 | 913,26 | 0,72 | 0,4339 |
| Total Error | 6314,48 | 5 | 1262,9 | | |
| Total (corr.) | 117451, | 14 | | | |
| Durbin-Watson | 1,53 ($p$=0,0404) | | | | |

Model predicts colony size to reach B0 under optimal conditions, as it shown in Table 2.9. A three-dimensional plot shows how D and F influence the B at a fixed E - Figure 2.12. Most influential parameters for B response were found to be D and F, whereas an increased input

would positively affect B. The reverse is in the same way concordant. Analogous to A model, the highest levels of D also positively affect this response, while F has an opposite effect. In addition, the response B might be improved through a second test where D and F are both increased, as the yellow/orange in Figure 2.12 suggests.

**Table 2.9 -** Range of tested values and optimal conditions for B.

| Term | Level 1 | Level 3 | Optimal |
|---|---|---|---|
| **D** | D1 | D3 | D3,5 |
| **E** | E1 | E3 | E3 |
| **F** | F1 | F3 | F3 |
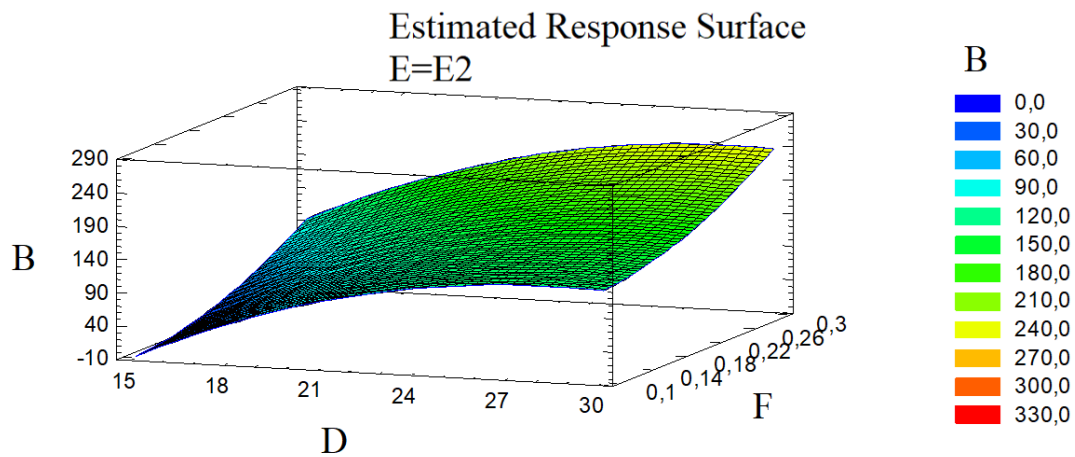


**Figure 2.12 -** Response surface of B by *Microalga M* continuous culture as a function of D and F, when E = E2.

## 2.3.4 Model for C

This model was generated based on the hydrocarbon content of those reactors who achieved the steady-state. At this stage pictures taken, as it shown in figure 2.13, *Microalga M* excretes oil droplets from intracolonial space. Thus, applying multiple regression analysis on the experimentally determined data, the predicted coefficients were determined, as it is shown in equation 2.9. The value of the determination coefficient $R^2 = 0.939$ indicates that the model cannot explain only 6.11% of the total variations, thus the model fits quite well.

$$C = p + p + p - p \quad \textbf{(Equation 2.9)}$$

The ANOVA results described in Table 2.10, clearly demonstrate that interactive and quadratic model terms ($FE$, $D^2$, $F^2$, $E^2$) have significant effect on C. The DW value points for serial autocorrelation on the residuals for the first order model shows to be non-autocorrelative for a level of significance of 5%.
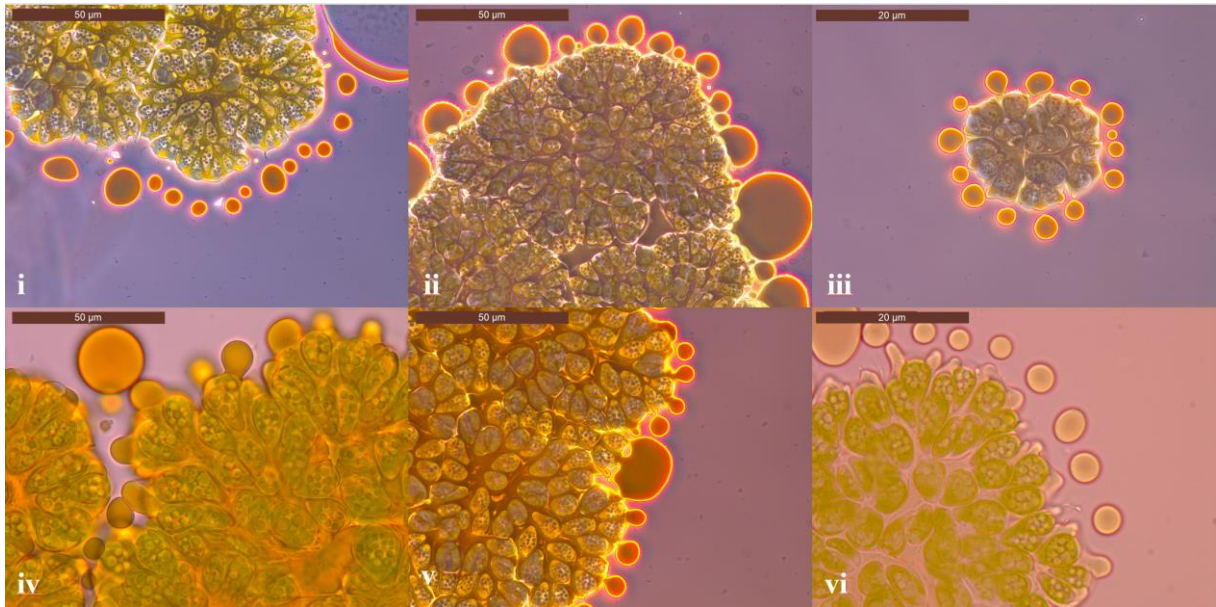


**Figure 2.13** - Magnification of *Microalga M* cultures with LEICA DM2500: *Microalga M* secreting hydrocarbons magnified 40x (i, ii, iv and v) and 10x (iii and vi).

**Table 2.10 -** ANOVA results for response surface quadratic model of C.

| Term | Sum of Squares Error | Degrees of Freedom | Mean Squares Error | F ratio | *p*-value |
|---|---|---|---|---|---|
| D | 337,1 | 1 | 337,1 | 1,25 | 0,3144 |
| F | 296,1 | 1 | 296,1 | 1,10 | 0,3428 |
| E | 779,3 | 1 | 779,3 | 2,89 | 0,1499 |
| $D^2$ | 12315 | 1 | 12315 | 45,65 | **0,0011** |
| DF | 36,91 | 1 | 36,9 | 0,14 | 0,7266 |
| DE | 12,04 | 1 | 12,0 | 0,04 | 0,8410 |
| $F^2$ | 2626 | 1 | 2626 | 9,73 | **0,0263** |
| FE | 3471 | 1 | 3471 | 12,87 | **0,0158** |
| $E^2$ | 2723 | 1 | 2723 | 10,10 | **0,0246** |
| Total Error | 1348 | 5 | 269,7 | | |
| Total (corr.) | 22099 | 14 | | | |
| Durbin-Watson | 2,31 (*p*=0,675) | | | | |

The most influential cultivation parameters are represented by the combination of F and E, whereas it results in positive effect on C. The model predicts *Microalga M* can reach a maximum C of C0, when the optimal conditions, namely those presented in Table 2.11, are imposed to this microalga. The tested conditions for this model specifies a decrease in D and E, regarding A and B models, while optimal F slightly fits its analogous, A model. As an example, a three-dimensional surface plot was generated, namely figure 18. The response surface of D and F indicate optimal C (C0) can be achieved close to the middle conditions.

**Table 2.11** - Range of tested values and optimal conditions for C.

| Term | Level 1 | Level 3 | Optimal |
|:---:|:---:|:---:|:---:|
| **D** | D1 | D3 | D2,5 |
| **E** | E1 | E3 | E1,5 |
| **F** | F1 | F3 | F1,5 |
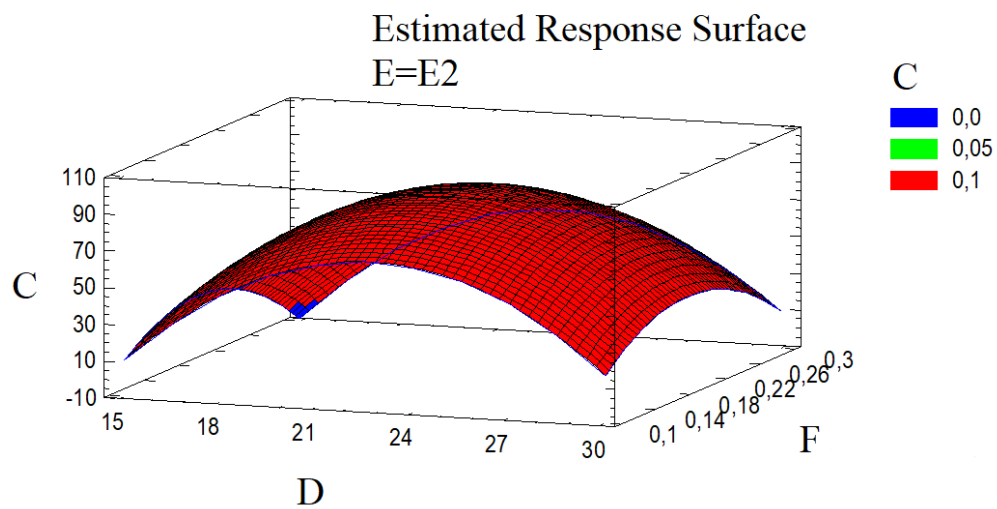


**Figure 2.14** - Response surface of A by *Microalga M* continuous culture as a function of D and F, when E = E2.

## 2.4 Discussion

Modelling is an interesting tool to develop the finest methodologies for large scale production. The present study determined mathematical models regarding the combined effect of different culture parameters (i.e. D, F and E) on A, B and C of *Microalga M* cultures. So far, few studies have been performed under continuous regime [25,51,81,82]. Simone Zenobi work [25] was conducted in continuous regime, namely considering the cyclostat mode (photoperiod of 12-12h) as in the present work. Compared to chemostat mode, cyclostat was found to be more productive. Unfortunately, steady-state was never attained, for the imposed dilution rate (0.05 day^{-1}) the operation time should be 60 days instead of 10 days, therefore these results are not suitable for comparison purposes. Thus, the models proposed will be discussed to provide reliable information to foresee outdoor PBR flat panel production. In continuous cultures at proven steady state, it is assumed D equals the growth rate ($\mu$) [83] . Low F increase the retention time inside PBR, thus higher A can be expected. Depending on how fast the organism is capable to replicate the optimal F is not necessarily low [84]. In addition, *Microalgae M* is a slow growing organism, which takes around 2 days to duplicate [85] . Therefore, highest A can be achieved at F (F1), according to present work. When faster F (F2 and F3) were applied, the cultures remained for shorter periods inside PBR, leading to lower A. One important factor that was not yet discussed is the D of the broth, which was found as the most relevant culture parameter for A model. Enzymatic activity is highly related with D, wherein above a certain threshold, enzymes responsible for photosynthesis, carbohydrate and hydrocarbon synthesis work at maximum rate [86]. Previous reports indicate *Microalgae X* to grow under a wide range of D (D1-D3) [87,88,89]. Yoshimura and collaborators [55] found highest growth rate of *Microalgae M* occurs at D3. The A model has indicated the optimal D for *Microalgae M* growth as A0, being concordant to literature. *Microalgae M* could grow at D1, merely expressing very low  A (A1). The combined effect of culture parameters operation (F = F2 and E = E3) at this D, makes *Microalgae M* capable to attain steady-state in cold environments.

Though it may seem counterintuitive for phototrophic organism as *Microalgae M*, E was found as the culture parameter with less effect on A model. However, for the first time a model combining the effect of these culture parameters has been performed on *Microalgae M*. Formerly, the effect of E on *Microalgae M* growth was found to be significant although they were performed under batch regime [55,57,88,90,91,92]. Batch to continuous regime

comparisons have large errors associated, since batch only describes instantaneous volumetric productivity [51]. Those reports have indicated *Microalgae M* can grow well in a wide range of light from 60 to 1900 μmol PAR $m^{-2}$ $s^{-1}$. Similar to the present results *Microalgae M* did not show photo-inhibition despite the high irradiance (máx. E3). Overall, the model predicts optimal conditions for A as follows: D = D3; F = F1; E = E3. In these conditions, cultures are expected to render A0.

For B model, D was found as the most influential culture parameter. Similar to A model, optimal D was found at D1,5, though optimal B was found at higher F (F3). Analogous to this study, the size of *Microalgae M* colonies were highly affected by dilution rate, wherein colonies quadrupled size through increased dilution rate (0.075 $day^{-1}$) [51]. Operating at F (F2 and F3) led to more diluted cultures, meaning more light available. Though more light, thus more energy for photosynthetic machinery operation, algae under these conditions were not found to increase A but rather increase their own size. Therefore, under continuous regime, F (F1) promote biomass growth, thus higher A. At F (F2 and F3) low biomass concentrations are likely to attain the steady-state, whereas colonies grow and experience limited colony breakup due to imposed F or either by pigment production as protection due to increased irradiance. In addition, it is also proved that the B is dependent on more factors such as dissolved $CO_2$ and $O_2$ [6] B model predicts optimal conditions for B as follows: D = D1.5; F = F3; E = E3. In these conditions, cultures are expected to achieve a maximum volume of B0. From a process engineering perspective, the major factor for economic feasibility, in hydrocarbon production, is the volumetric productivity. Despite, reports have indicated hydrocarbon production is highly associated with cellular division, wherein highest quantities are obtained during exponential growth phase [50,81,90,93] . At continuous regime in trickle-film PBR, *Microalgae M* hydrocarbon productivity reached maximum (340 mg $L^{-1}$ $day^{-1}$) for operational dilution rate (0.075 $day^{-1}$), wherein dilution rate (> 0.15 $day^{-1}$) led to washout of the cultures [51]. In comparison, the present study was conducted in flat panel PBR, found an F of F1.5 which in combination with optimal E (E1.5) C is favoured. With this, reactor design and culture conditions are crucial to provide reliable comparative information, wherein from the present study C seems dependent on this operational combination, namely light dilution. Optimal D for C was considered as the same for growth, since the C has been shown highly associated with growth rate [55,89,91]. Kalacheva and collaborators [94], while studying different cultivation D on C production did not found significant differences.

Similar to this study, statistical analysis did not found significant effect of D for C model, plus the optimal D given by the C model do not correspond with the optimal D from A model. Overall, the C model predicts optimal conditions for C as follows: D = D1.5; F = F1.5; E = E1.5. In these conditions, cultures are expected to render C0. Compared with Kathri and collaborators [51] work it is expected lower optimal C0, however their work was done at lower E. The present work is intended to use sunlight, therefore we started with 600 µmol PAR m$^{-2}$ s$^{-1}$ since at Wageningen, between April and September, averages 770 µmol PAR m$^{-2}$ s$^{-1}$ [95]. In addition, reactor design, F range and C extraction method highly contributed for differences in C.

## 2.5 Conclusion

In this work three models have been developed with a high grade of accuracy for A, B and C for continuous cultures of *Microalga M*. Since one of the major limitations of outdoor algae production is the lack of knowledge regarding to the optimal conditions for growing this microalga, D, F and E were tested. The results show that it's possible to achieve dense cultures, high content of liquid hydrocarbons or colonies with wieldy size through the manipulation of these culture conditions. Contrary to what has been reported, we found the optimal conditions for A are not the same for C under the continuous regime. Therefore, by the use of these theoretical models, equation 2.7, 2.8 and 2.9, the shift of culture conditions is expected to fill the gap between lab and large-scale cultures in order to enhance and optimize its large-scale performance.

$$A = {}^{\backprime}\Omega + {}^{\prime\prime}\Omega + {}^{\backprime\backprime}\Omega - {}^{\prime\prime}\Omega \qquad \textbf{Equation 2.7}$$

$$B = {}^{\backprime}\Upsilon + {}^{\prime\prime}\Upsilon + {}^{\backprime\backprime}\Upsilon - {}^{\sim}\Upsilon \qquad \textbf{Equation 2.8}$$

$$C = \mathrm{p} + \mathrm{p} + \mathrm{p} - \mathrm{p} \qquad \textbf{Equation 2.9}$$

# 3. CHAPTER II – ALTERNATIVE METHODOLOGY FOR PHYCOCYANIN EXTRACTION FROM *ANABAENA CYLINDRICA* BATCH CULTURES

## 3.1 Overview

Following the same approach as before, this chapter involves the study on the downstream processing of a bioprocess, namely from the harvesting until the biomass extraction of product of interest. It was developed in cooperation between Path-CICECO (Process and Product Applied Thermodynamics - Centre for Research in Ceramics and Composite Materials) and CESAM (Centre for Environmental and Marine Studies) both are associate laboratories of Aveiro University, Portugal. This chapter intends to study the use of alternative solvents, namely ionic liquids and surfactants, in extracting phycocyanin from previously grown *Anabaena cylindrica* cultures. This review and work follows an approach of biomass valorisation, since the organism selected is potentially recognized as harmful to other organisms. Thus, *A. cylindrica* features are discussed as well as the existing market of phycocyanin. In addition, its conventional extraction methodologies are explored, with the aim to augment the interest for more sustainable and efficient solvents, namely ionic liquids. This experimental work intends to develop a rapid and environmentally friendly extraction methodology of phycocyanin from an unexplored cyanobacteria, through solid-liquid extraction using aqueous solutions of alternative solvents.

### 3.1.2 *Anabaena cylindrica*

*Anabaena cylindrica (A. cylindrica)* is a filamentous cyanobacteria, depicted in figure 3.1, commonly found in fresh waters, wherein its genus was firstly described by Lothar Geitler [96]. The genus *Anabaena* is documented as an ecological relevant organism, since it can persist on freshwater as well thrive under eutrophication conditions [97,98]. These filamentous cyanobacteria are composed of vegetative cells, which due to environmental conditions or cell to cell interaction can evolve to resistence structures known as heterocysts and akinetes. Akinetes or spores are its survival form, while heterocysts have an advantageous feature to survive under nutrient depleted conditions, though the intake atmospheric nitrogen [99–102]. A comparative study on nutritional composition of the walls of vegetative cells, heterocyst's, akinetes and sheath material (present in the outer layer of the cell wall) found that aminoacid composition is mainly present in the walls of vegetative cells, while carbohydrates are often found in the walls of heterocysts, akinetes and the sheath material [103]. So far, there are no industrial applications for *A. cylindrica*, whereas its main fundamental interest has been regarded on its nitrogenarse activity, capable to fix atmospheric nitrogen and produce hydrogen [102]. Besides that, from a set of 30 *Anabaena* strains, from 3 different continents, it was found phycobiliproteins accessory pigments in photosynthesis in their composition, and namely phycocyanin. In addition, its content can be up to 30% of phycobiliproteins while on average 15% of phycobiliproteins is total protein [104]. Therefore, due the presence of these phycobiliproteins in abundance, it seems interesting to study the potential of these natural pigments, namely phycocyanin for the pigments market and to establish new products.
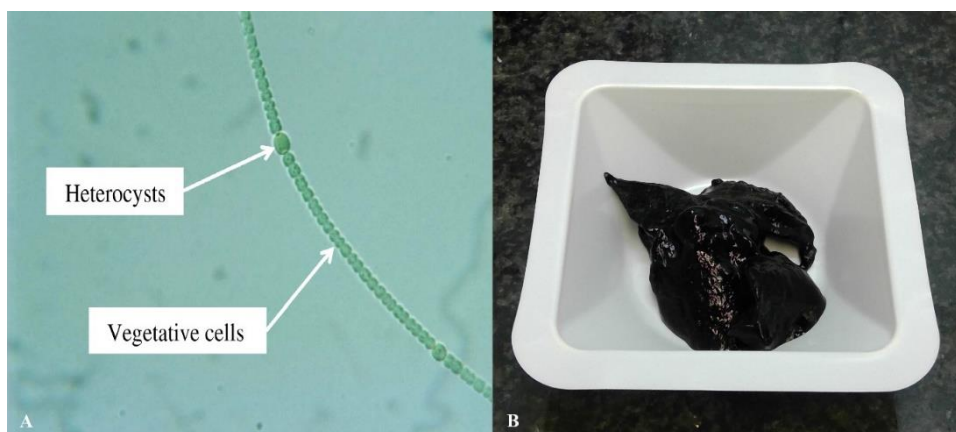
**Figure 3.1 –** *A. cylindrica*: (A) Magnification of vegetative cells and heterocysts 2.5–3 μm in diameter, adapted from literature [105]; (B) concentration of biomass after 13 days of batch cultivation.

### 3.1.3 Phycocyanin

Phycobiliproteins, carotenoids and chlorophyll families comprise the most important metabolic group of pigments in cyanobacterias [106]. Phycobiliproteins are the highest fraction of the foregoing group and it is covalently bond to accessory structures, namely chromophore groups, wherein it is organized in a supramolecular structure called phycobilissomes, located on the stroma [107]. Commonly found in cyanobacteria, these accessory photosynthetic pigments are composed by complexes of pigment-protein that act as very effective energy transducers to chlorophylls which only capture light in a limited region of solar spectrum [108]. Phycobiliproteins can be divided in three classes, namely phycocyanin, phycoerythrin and allophycocyanin [109]. Cyanobacterial phycocyanin also known as C-phycocyanin is characterized by blue colouring with a molecular mass of 140–210 kDa structured by two polypeptide subunits, α and β, repeated for six times [110,111]. Regarding visible absorption properties, phycocyanin has its maximum absorption between 615 and 640 nm [112]. This protein is also known by its high solubility in water and fluorescence, and is relatively stable to pH (pH 5-7.5), and temperature (-4 to 45 ºC), though colour may be affected [106]. Recent studies have announced promising bioactivity properties, namely anti-inflammatory, hepatoprotective and antitumoral [111,113,114,115,116]. The increased demand for the use of natural compounds over their synthetic counterparts allied to C-phycocyanin versatile properties has gained significant interest in many different sectors, namely food, pharmaceutical, and cosmetic industry. For instance, the commercial value of

phycocyanin for food degree costs around US$ 0.13 mg$^{-1}$, for reactive degree costs from US$1 to 5 mg$^{-1}$, while the one with analytical grade can cost more than US$15 mg$^{-1}$ [117]. In addition, phycocyanin market value was reported to be US$ 10-50 millions *per* year [118]. A common approach to assess the purity level of phycocyanin is based on the ratio of absorbance's of phycocyanin peak with total proteins peak ($Abs_{615}/Abs_{280}$), whereas a ratio above 0.7, 3.9 and 4.0 corresponds to food, reactive and analytical degree, respectively [119]. Usually, phycocyanin undergoes an isolation process, whereas chemical and physical methods are useful for cell breakage. The extraction step has been reported with Na-phosphate buffer [120]. Conventional biomass pre-treatments have not been shown very useful, though alternative treatments, namely osmotic cell disruption, lysozyme treatment, sonication, high pressure and freeze-thaw cycles were shown as most efficient. Regarding the purification procedures, phycocyanin has been usually obtained by a combination of different sulphate precipitation, ion-exchange chromatography, and gel filtration chromatography [121]. A novel phycocyanin extraction (24 hours) and purification (8 hours) with ammonium chloride and ammonium phosphate as precipitation agents has attained a purity level of 2.81 [117]. Silveira and collaborators [122] optimized the extraction of phycocyanin from *Spirulina platensis* and studied the influence of different solvents, wherein water was found the most suitable solvent, after 4 hours of extraction resulting in a purity level of 0.46. Extremely pure phycocyanin (6.69) was attained from a two-phase aqueous solution followed by ion-exchange chromatography, although organic solvents, long extraction time and high energy input still limit this novel approaches to reach industrial exploitation [123]. Briefly, the purity ratio of the present work will follow the same approach as the one followed by the previously announced reports, *i.e.* spectrophotometric ratio of phycocyanin and total protein absorption peak, though phycocyanin selected peak might slightly differ (615 - 620 nm) between studies. Nonetheless, the need of novel production approaches for algal derived products must be regarded from cultivation under controlled conditions to low-cost downstream processing, to softer the economic and political barriers [121].

### 3.1.3 Alternatives for Conventional Solid-Liquid Extraction

Solid-liquid extraction is defined by the contact of a liquid, normally designated as solvent (e.g., hydrophobic, hydrophilic, acid, basic, among other's features) with a solid matrix wherein a compound of interest is extracted to the liquid phase [64]. Throughout the years, this

approach has suffered many improvements regarding the type of solvent and strategy used. However, costly drawbacks have resisted, namely low extraction efficiencies, poor selectivity, long extraction times, high energetic inputs, unsustainable nature of solvents and many others [124]. Consequently, market needs and environmental policies have been frequently becoming more exigent, making researchers to struggle for the development of ground-breaking downstream processes with more sustainable credentials. From the development of new strategies, a new class of solvents has emerged, the ionic liquids. Generally described as "designer solvents", these salts are liquids at low temperatures and composed by two opposite charged species of ions resulting in very different possible interactions with solute [124–126]. Thus, a tailor-made extraction can be found through the test of the existing ionic liquids combinations as well as through their synthesis with desired features, namely biodegradable and lower toxicity [127]. The main advantages of ionic liquids over the conventional solvents are negligible volatility and non-flammability [125]. Moreover, unique solvation ability, high selectivity, thermophysical properties, biodegradability and high ionic conductivity, rank it as potential solvents for industrial application, although due to recent research its exploitation is still in its infancy [128,129]. In addition, the complexity and content of the matrix to extract usually represents another associated problem. For a solid matrix, as fresh biomass, a high water content is often found, wherein it might hurdle effectiveness of solvent and compound of interest interaction. Strategies to reduce the water content to reach easily the compound have been highly used, namely drying, freeze-drying, etc., [118]. However, these strategies are nothing more than a step back, carrying additional steps and increased costs to the final product. Envisioning an integrated bioprocess where cultivation, extraction and purification can be done in the same place, the use of fresh biomass is a requirement to conduct the experiments. Therefore, to avoid energy costly steps like dehydration, lyophilisation, *A. cylindrica* in the form of fresh biomass was intended to be studied in the present work, with aqueous solutions of alternative solvents, namely ionic liquids [128] being tested as task-specific solvents to extract phycocyanin.


3.1.3.1 Aqueous Solutions of Ionic Liquids

To conjugate ionic liquids with other co-solvents increases the complexity of interaction between ions, though water, due to its abundance, non-toxicity, and biological importance is the most frequently used co-solvent [126]. Even in water the ionic liquid is capable to modify

the properties of water, for instance, more hydrophobic compounds can become more soluble in aqueous media due to the hydrotropic effect [130]. In addition, hydrophilic ionic liquids generally with short alkyl chains are capable to create a water network of hydrogen bonds, though the network has to be sufficiently strong to promote the formation of structures like micelles. The increase of the length of cationic alkyl chain reflects a stronger tensioactive nature, which in the case of proteins may affect its stability and activity [126]. Thus, the use of aqueous solutions of ionic liquids in extraction processes gives an outstanding advantage over the use of organic solvents due to its tunability to hit the compound of interest. Briefly, the study of the extraction of added-value compounds from biomass lead to unravel determinant features here stated: capability to destroy the cell wall; and the capacity to solvate selectively a large range of compounds. In addition, recent reports have used the solid-liquid extraction to couple with microwave or ultrasound treatments which increased the extraction yields [124]. So far, regarding the use of aqueous solutions of ionic liquids, the extraction process has shown to be successfully for alkaloids, flavonoids, terpernoids, aromatic compounds, phenolic acids, lipids, and natural mixtures such as essential oils, suberin and saponins [128]. More recently, a set of various aqueous solutions of ionic liquids was successfully used to extract phycobiliproteins from fresh biomass of the macroalga *Gracilaria sp.*, in which 46% yield increase over the conventional methodology was attained [129]. Therefore, it seems promising to develop an alternative extraction methodology for phycocyanin, based on the work previously announced.

## 3.2 Materials and Methods

### 3.2.1 Organism, medium and cultivation

The strain of *A. cylindrica* was obtained from culture collection produced in the Biology Department from Aveiro University regarding its batch-growth in Erlenmeyer flasks (50 mL) in a photo incubator chamber at $20\pm2$ °C under 16:8 light/dark cycles with light intensity of 130 μmol PAR $m^{-2}$ $s^{-1}$, provided by cool white fluorescent tubes. The culture was grown in Woods Hole MBL culture medium: 36.76 mg $L^{-1}$ $CaCl_2 \cdot 2H_2O$, 36.97 mg $L^{-1}$ $MgSO_4 \cdot 7H_2O$, 12.60 mg $L^{-1}$ $NaHCO_3$, 8.71 mg $L^{-1}$ $K_2HPO_4$, 85.01 mg $L^{-1}$ $NaNO_3$, 28.42 mg $L^{-1}$ $Na_2SiO_3 \cdot 9H_2O$, 4.36 g $L^{-1}$ $Na_2 \cdot EDTA$, 3.15 g $L^{-1}$ $FeCl_3 \cdot 6H_2O$, 0.01 g $L^{-1}$ $CuSO_4 \cdot 5H_2O$, 0.022 g $L^{-1}$ $ZnSO_4 \cdot 7H_2O$, 0.01 g $L^{-1}$ $CoCl_2 \cdot 6H_2O$, 0.18 g $L^{-1}$ $MnCl_2 \cdot 4H_2O$, 0.006 g $L^{-1}$ $Na_2MoO_4 \cdot 2H_2O$, 250 g $L^{-1}$ Tris (hydroxymethyl)-aminomethane [131]. Medium pH was adjusted to 7.2 with HCl. The culture media components were sterilized together with the cultivation apparatus (60-90 min, 120ºC, 1atm), except for vitamins, which were added posteriorly. For culture production, the 15-day inoculum was used to inoculate 4 L of liquid MBL culture medium into 5 L glass vessels (Schott Duran) and incubated under the same conditions as the inoculum for a batch period of 13 days. Agitation was provided by aeration in bottom of the glass vessels. After cultivation period, the cells were harvested by self-sedimentation and soft centrifugation at 4000×g for 7 min at 4 °C, and then supernatant was removed. The fresh biomass was stored at −20 °C in dark for further processing.

### 3.2.2 Chemicals

The solvents used in the conventional extraction method were methanol (purity 100%, Chem-Lab) and Na-phosphate buffer ($Na_2HPO_4/NaH_2PO_4$). The components of the sodium phosphate buffer, sodium phosphate dibasic, $Na_2HPO_4$ ($\geq$ 98 wt%), and sodium phosphate monobasic, $NaH_2PO_4$ ($\geq$ 99 wt%) were purchased from Merck and Panreac, respectively. A commercial standard of phycocyanin ($\geq$ 10.0 mg $mL^{-1}$) and chlorophyll-*a* was acquired from Sigma-Aldrich. The series of 1-alkyl-3-methylimidazolium chloride ionic liquids [$C_n$mim]Cl, including the 1-ethyl-3-methylimidazolium chloride, [$C_2$mim]Cl (98 wt%), 1-butyl-3-methylimidazolium chloride, [$C_4$mim]Cl (99 wt%), 1-hexyl-3-methylimidazolium chloride, [$C_6$mim]Cl (98 wt%), 1-octyl-3-methylimidazolium chloride, [$C_8$mim]Cl (98 wt%), 1-decyl-3-methylimidazolium chloride, [$C_{10}$mim]Cl (98 wt%), 1-dodecyl-3-methylimidazolium chloride, [$C_{12}$mim]Cl (>98 wt%), 1-tetradecyl-3-methylimidazolium chloride, [$C_{14}$mim]Cl (98 wt%), 1-

hexadecyl-3-methylimidazolium chloride, [C$_{16}$mim]Cl (98 wt%), 1-butyl-3-methylimidazolium dicyanamide, [C$_4$mim][N(CN)$_2$] (98 wt%), 1-butyl-3-methylimidazolium trifluoromethanesulfonate, [C$_4$mim][CF$_3$SO$_3$] (99 wt%), 1-butyl-3-methylimidazolium acetate, [C$_4$mim][CH$_3$CO$_2$] (98 wt%), 1-butyl-3-methylimidazolium methanosulfonate, [C$_4$mim][CH$_3$SO$_3$] (99 wt%), 1-butyl-3-methylimidazolium thiocyanate, [C$_4$mim][SCN] (98 wt%), 1-butyl-1-methylpiperidinium chloride, [C$_4$mpip]Cl (99 wt%), and 1-butyl-1-methylpyrrolidinium chloride, [C$_4$mpyrr]Cl (99 wt%), 1-butyl-3-methylpyridinium chloride, [C$_4$mpyr]Cl (98 wt%), and choline acetate, [Ch]Ac (>99 wt%) were acquired from IoLiTec (Ionic Liquids Technologies, Germany). The cholinium chloride, [Ch]Cl (99 wt)% and Tween 20 were purchased from Sigma-Aldrich. Tetrabutylphosphonium chloride, [P$_{4,4,4,4}$]Cl and tributyltetradecylphosphonium chloride, [P$_{4,4,4,14}$]Cl was supplied by Cytec. Surface-active ionic liquids tested were tetradecyltrimethylammonium bromide, [N$_{1,1,1,14}$]Br (99% wt%), acquired at Acros Organic, 1-hexadecylpyridinium chloride, [C16pyr]Cl (99% wt%) and dodecyltrimethylammonium bromide, [N$_{1,1,1,12}$]Br (99% wt%) purchased from Alfa Aesar. The anionic surfactants tested was sodium dodecyl sulfate, SDS (99% wt%) acquired at Acros Organics. The non-ionic surfactant tested was Tween 20 purchased from Sigma-Aldrich. The acronyms, chemical formula, molecular weight, critical micelle concentration (CMC) and chemical structures of these surface-active compounds as well as for ionic liquids (when possible) are provided in Table S2.1 (Supporting Information).

### 3.2.3 Conventional Solvent Extraction

The collected cells were called "fresh biomass". The methodology used by [106] and [132] was adapted and applied in this work for the extraction of phycocyanin and chlorophyll *a*, respectively, and used as a control. Fresh biomass was thawed and homogenized in Na-phosphate buffer aqueous solutions at 20 mM, pH 7.0 for phycocyanin extraction and in pure methanol for chlorophyll extraction. Both extractions were performed at room temperature and in an orbital shaker at 50 rpm (Grant-bio PTR-30) protected from light exposure. After the solid-liquid extraction, the solution was centrifuged in a Thermo Scientific Heraeus Megafuge 16 R centrifuge at 12000 rpm for 10 minutes. The pellet was discarded and the phycocyanin and the chlorophyll based supernatants were collected and further analyzed in a UV-Vis microplate reader (Synergy HT microplate reader – BioTek). The absorption spectra were analyzed between 300 and 700 nm to identify and better characterize the typical region of both pigments.

Phycocyanin and chlorophyll content were quantified at 615 and 670 nm, which are the maximum peaks of absorbance in each spectrum in the visible region, respectively, by using proper calibration curves previously calculated. The yields of extraction of phycocyanin and chlorophyll were expressed in $mg_{phycocyanin}.g_{fresh\ biomass}^{-1}$ and $mg_{chlorophyll}.g_{fresh\ biomass}^{-1}$, respectively. The tested conditions were done in duplicate. Optimization of operational conditions were performed, namely time of extraction ($t$) and solid-liquid ratio (SLR).

### 3.2.4 Screening of various aqueous solutions of ionic liquids and surfactants on the chlorophyll and phycocyanin extraction

Twenty-four aqueous solutions of ionic liquids and surfactants were used to evaluate their extractive performance in recovering phycocyanin and chlorophyll. The output of conventional solvent extraction optimization was defined as the starting conditions for the screening step using the ionic liquids and surfactants aqueous solutions to extract as much phycocyanin and chlorophyll content as possible. All the ionic liquids and surfactants aqueous solutions tested were prepared at 500 mM, whereas (m/m) approach was used due to hygroscopic effect of certain ionic liquids. Based on different structural features, thus chemical affinity of these aqueous solutions, their effect on the extraction of phycocyanin and chlorophyll was evaluated from previously grown fresh samples of *A. cylindrica*.

### 3.2.5 Optimization of the extraction conditions for phycocyanin: Response Surface Methodology (RSM)

The screening step of phycocyanin sorted thirteen aqueous solutions as most promising, based on spectrum analysis and accuracy of maximum peak (615 nm). From this step on, chlorophyll was considered as contaminant element since screening phase found four aqueous solutions with extractive performance better than conventional extraction. Therefore, optimization of extraction parameters, namely time of extraction ($t$) and concentration of ionic liquid and surfactant, was carried out for phycocyanin. A Response Surface Methodology (RSM) was applied since it can simultaneous gather complex information and clearly describe the relationship of the most significant parameters in the extraction process. In addition, this economic technique also contributed for assessing the extractive performance of phycocyanin from the fresh biomass. For that purpose, a $2^k$ factorial design was carried, comprising a total of 11 extractions, including 3 replicates of the central point which is meant to be the building block of this modeling, plus

various processing conditions were repeated to guarantee the accuracy of the data. The experimental planning is provided in Supporting Information (Table S2.3), wherein the central point (zero level), factorial points (1 and −1, level one) and axial points (level α) were defined. The axial points are encoded at a distance α (Eq. 3.1) from the central point [133], defined as:

$$\alpha = (2^k)\frac{1}{4} \quad \textbf{(Equation 3.1)}$$

The experimental data was fitted according to the second order polynomial equation (equation 3.2) described as follows:

$$y = \beta_0 + \sum_{i=1}^{k}\beta_i x_i + \sum_{i=1}^{k}\beta_{ii} x_i^2 + \sum_{i=1}^{k-1}\sum_{j=2}^{k}\beta_{ij} x_i x_j + \varepsilon \qquad \textbf{(Equation 3.2)}$$

where $x_1, x_2, \ldots, x_k$ are time of extraction and SLR which influence content of phycocyanin extracted $y$; $\beta_0, \beta_{ii} (i = 1,2,\ldots,k)$, $b_{ij} (i = 1,2,\ldots,k; j = 1,2,\ldots,k)$ are the unknown parameters and $\varepsilon$ is a random error. The β coefficients, which should be determined in the second-order model, are obtained by the least square method. The STATISTICA software was used to conduct the experimental design, the statistical analysis and the response surface plots. Results obtained with a confidence level of 95% were considered statistically significant, though 90% confidence was designated as marginally significant, when necessary. The predicted phycocyanin content, the relative deviations considering the amount of phycocyanin predicted and experimentally determined, the regression coefficients and the standard deviations of $2^{2(1/4)}$ factorial design were also determined in the same software. The attained model was validated, through the extraction under the given optimal operational conditions in triplicate.

### 3.2.6 pH effect on the optimized ionic liquid aqueous solution

The aim of the experiments was to understand the interaction of ionic liquid in aqueous solutions in contact with biomass without the presence of additive salts to extract phycocyanin. Therefore, a pH screening was carried in order to determine if the extractive performance of the best alternative solvent or the contamination level of chlorophyll is affected along the pH stability range of phycocyanin. From the previous step, solid-liquid

ratio, time of extraction and ionic liquid concentration best conditions were adopted for a pH range comprising pH 5, 6 and 7. For this step, the solutions were prepared in the McIlvaine buffer, due to its wider range of pH values than the Na-phosphate buffer [134].


## 3.3 Results and Discussion

The aim of this work was to develop an effective extraction process based on aqueous solutions of ionic liquids to extract phycocyanin with higher selectivity from the fresh biomass of *Anaebena cylindrica*. Thus, the present work is divided in two parts: the first regards the optimization results of operational parameters for conventional methodology, wherein phycocyanin and chlorophyll were extracted with sodium phosphate buffer and methanol, respectively; the second addresses the optimization of an alternative methodology for phycocyanin extraction using aqueous solutions of ionic liquids. Therefore, the use of this alternative approach emerges as more sustainable and environmentally friendly whereas in one single-step the typical drawbacks of conventional methodology, namely long extraction times, complexity and limited selectivity, become groundless.


### 3.3.1 Conventional methodology

The use of a conventional extraction methodology in this work was to guarantee a reliable comparison standard as control for aqueous solutions of ionic liquids and surfactants. Adapted from literature [106,132], phycocyanin and chlorophyll extractions were performed with Na-phosphate buffer and pure methanol, respectively. Therefore, the optimization of extraction time and solid-liquid ratio (SLR) was conducted.


3.3.1.1 Time of extraction

A kinetic study of 45 min for phycocyanin was carried considering a solid-liquid ratio of 0.1 (mass of fresh biomass/volume of solvent). Results are expressed in figure 3.2. Phycocyanin extraction (blue squares) with Na-phosphate buffer approaches the edge from 15 until 45 minutes, wherein the maximum yield (73 $mg_{phycocyanin}.g_{fresh\ biomass}^{-1}$) is attained at 30 minutes. For chlorophyll, the initial conditions were the same as for phycocyanin, though the period tested was significantly higher, considering phycocyanin localization at the external part of phycobilissomes

[129]. The results (green circles) show the chlorophyll extraction with pure methanol come near a limit after 30 minutes, whereas the maximum yield of chlorophyll (0.75 $mg_{chlorophyll} \cdot g_{fresh\ biomass}^{-1}$) occurs at 60 minutes. However, with a yield of 0.74 $mg_{chlorophyll} \cdot g_{fresh\ biomass}^{-1}$ at 45 minutes seems reasonable to fix the extraction time of chlorophyll to 45 minutes. Attempting to conduct both extractions at the same time, phycocyanin and chlorophyll time of extractions were fixed at 45 minutes.
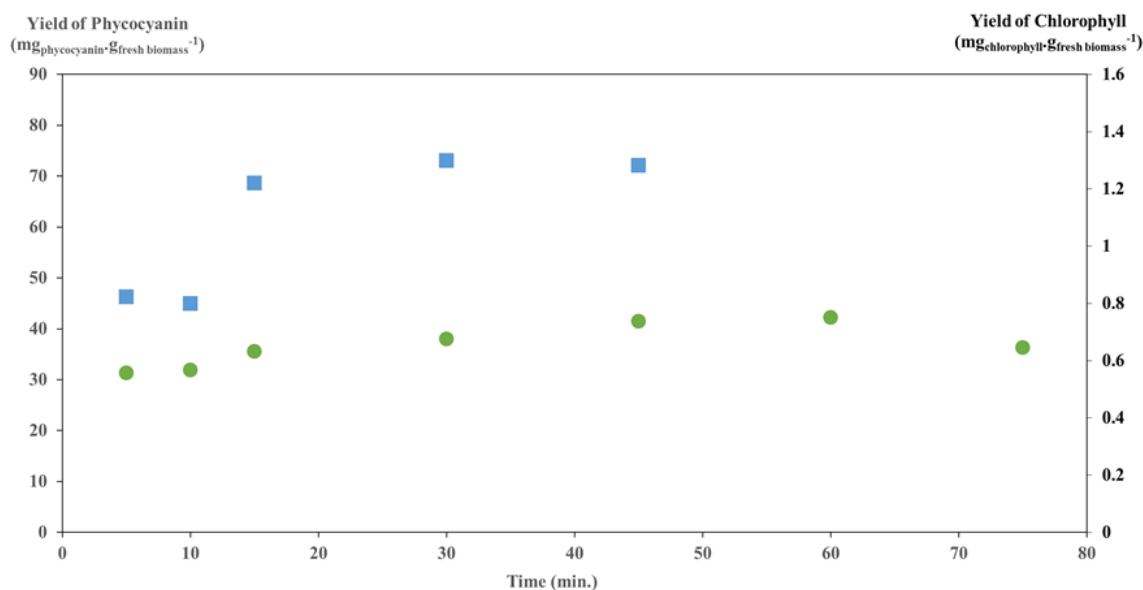


**Figure 3.2 –** Evolution of yield of extraction trough the time from *Anaebena cylindrica*: of phycocyanin (blue circles) during 45 min and chlorophyll (green circles) during 75 min. Maximum variation coefficient for phycocyanin and chlorophyll of 1% and 11%, respectively.

3.3.1.2 Solid-Liquid Ratio (SLR)

One of the most relevant parameters in the extraction step is the biomass/solvent ratio, which can determine the efficiency of extraction [122]. For this study, the extraction time (45 minutes) obtained previously, was considered. The results depicted in figure 3.3, show that extraction efficiency is highly affected by the solid-liquid ratio, whereas the phycocyanin (73 $mg_{phycocyanin} \cdot g_{fresh\ biomass}^{-1}$) and chlorophyll (1.1 $mg_{chlorophyll} \cdot g_{fresh\ biomass}^{-1}$) yields are greatest when the tested solid-liquid ratio is 0.02. These results are concordant, once the efficiency of extraction is increased when there is enough solvent to contact with all the biomass. However, for industrial purposes this means high volumes of solvent per low masses of biomass, thus increasing the costs and the

83

sometimes imposing experimental restrictions. Therefore, there must be a moderate consideration, and thus in the present study, it was assumed the most suitable solid-liquid ratio as 0.1.
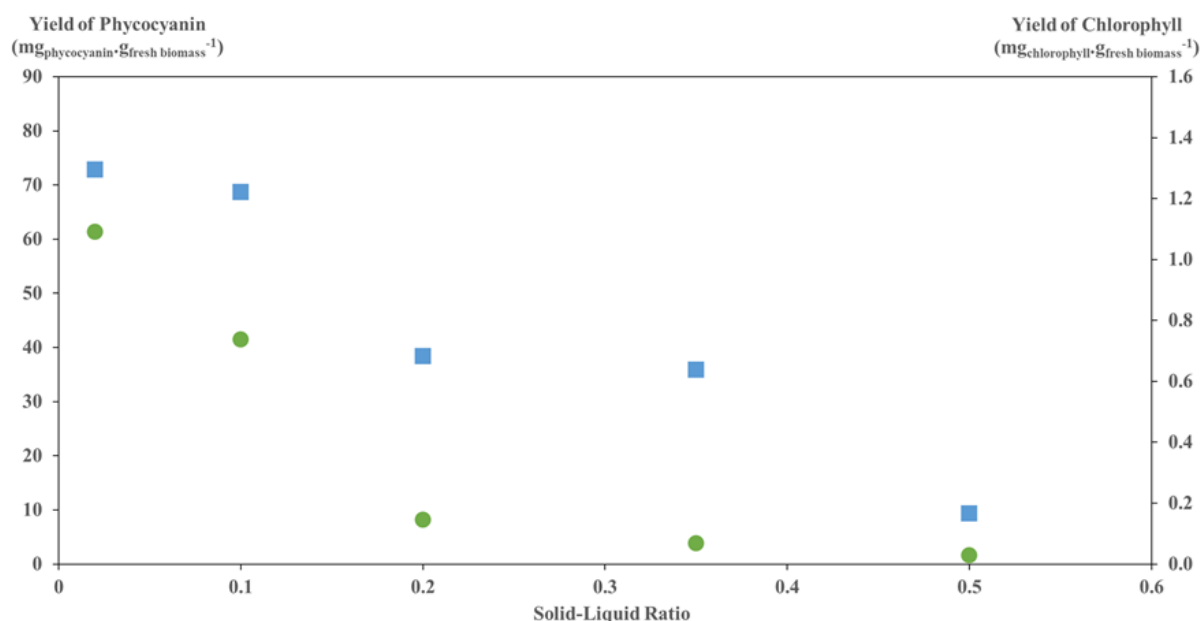


**Figure 3.3 -** Yield of extraction from the *Anaebena cylindrica*, regarding the effect of different solid-liquid ratio: of chlorophyll (●) with maximal variation coefficient of 24%; of phycocyanin (■) with maximal variation coefficient of 44%.

### 3.3.2 Aqueous solutions of ionic liquids and surfactants on the chlorophyll and phycocyanin extraction: screening of solvents

Several aqueous solutions of ionic liquids and surfactants were used to assess its extractive performance on the phycocyanin and chlorophyll under the optimized operational conditions from conventional methodology: solid-liquid ratio of 0.1 (mass of fresh biomass/volume of solvent) and extraction time of 45 minutes in the absence of light. The aqueous solutions of ionic liquids were fixed at 500 mM. The chemical structure and respective additional information of the ionic liquids and surfactants considered are shown in Supporting Information (Table S2.1). The distance between the maximum peak of absorbance of phycocyanin and chlorophyll (615 and 670 nm) allowed to track the extractive performance for each pigment. Therefore, within this section, the yields of phycocyanin and chlorophyll extraction

are estimated over the effect of the alkyl chain length and the cation, the anion and the surfactant type. These results are detailed below. Although it was screened 24 aqueous solutions of ionic liquids and surfactants, the results presented here were chosen based on accuracy of the respective maximum absorption peak and the contamination level of the spectrum baseline.

### 3.3.2.1 Alkyl chain length effect

To study the effect of the alkyl chain length of aqueous solutions of ionic liquids on the extraction of phycocyanin, the imidazolium family was selected. This family was chosen to start the screening since it has been widely used in the extraction of added-value compounds from biomass [128]. Therefore, a series of 1-alkyl-3-methylimidazolium chloride compounds was carried, namely [C$_2$mim]Cl, [C$_4$mim]Cl, [C$_6$mim]Cl, [C$_{10}$mim]Cl, [C$_{12}$mim]Cl, [C$_{14}$mim]Cl and [C$_{16}$mim]Cl. The absorbance spectra from 400 to 700 nm, the yields of phycocyanin and chlorophyll extracted are depicted in figure 3.4. The increase of alkyl chain length ([C$_{10}$mim]Cl, [C$_{12}$mim]Cl, [C$_{14}$mim]Cl, [C$_{16}$mim]Cl) in the extraction of phycocyanin was shown to be highly affected, whereas it is favoured when alkyl chain lengths are shorter ([C$_2$mim]Cl, [C$_4$mim]Cl, [C$_6$mim]Cl). Phycocyanin is a water-soluble protein which is likely to share affinity with hydrophilic compounds, namely shorter alkyl chain ionic liquids, being concordant with the present results. The yields of extraction achieved with the use of ionic liquids were not higher than the conventional methodology with Na-phosphate buffer (73 mg$_{phycocyanin}$.g$_{fresh\ biomass}$$^{-1}$ $\pm$ 4), whereas [C$_4$mim]Cl attained the highest phycocyanin yield (61 mg$_{phycocyanin}$.g$_{fresh\ biomass}$$^{-1}$ $\pm$ 0.4) and reduced amounts of chlorophyll contamination, within the imidazolium based ionic liquids, resulting in a more selective extraction. A similar study on the extraction of a protein from phycobiliprotein family found the identical relation between the length of ionic liquid alkyl chain [129]. With the aim to develop a more selective and efficient phycocyanin extraction methodology, [C$_4$mim]Cl was selected to conduct the study over the cation effect for shorter alkyl chain.

In the case of chlorophyll being the pigment of interest, longer alkyl chains attain better yields, which is shown by the absorption spectra of figure 3.4B and further by the yields attained in figure 3.4C. By this screening, [C$_{14}$mim]Cl was shown the extract more chlorophyll (1.0 $\pm$ 0.05 mg$_{chlorophyll}$.g$_{fresh\ biomass}$$^{-1}$) than conventional methodology with methanol (0.74 $\pm$ 0.01 mg$_{chlorophyll}$.g$_{fresh\ biomass}$$^{-1}$). Furthermore, by the analysis of figure 3.4C,

its intuitive to see a distinct nature of these pigments under alkyl chain length effect of imidazolium family. Huddlestone and collaborators [135] showed that increasing the length of alkyl chain, increases the hydrophobicity of the ionic liquid, which is concordant with the present results. In cases where both pigments were present, another salt/polymer could be used to form an aqueous biphasic system (ABS) or for cases where alkyl chain is long an aqueous micellar two-phase system (AMTPS) can be performed, in which only by the increase of temperature, the formation of two phases can promote the partitioning of these two different (in properties) molecules.
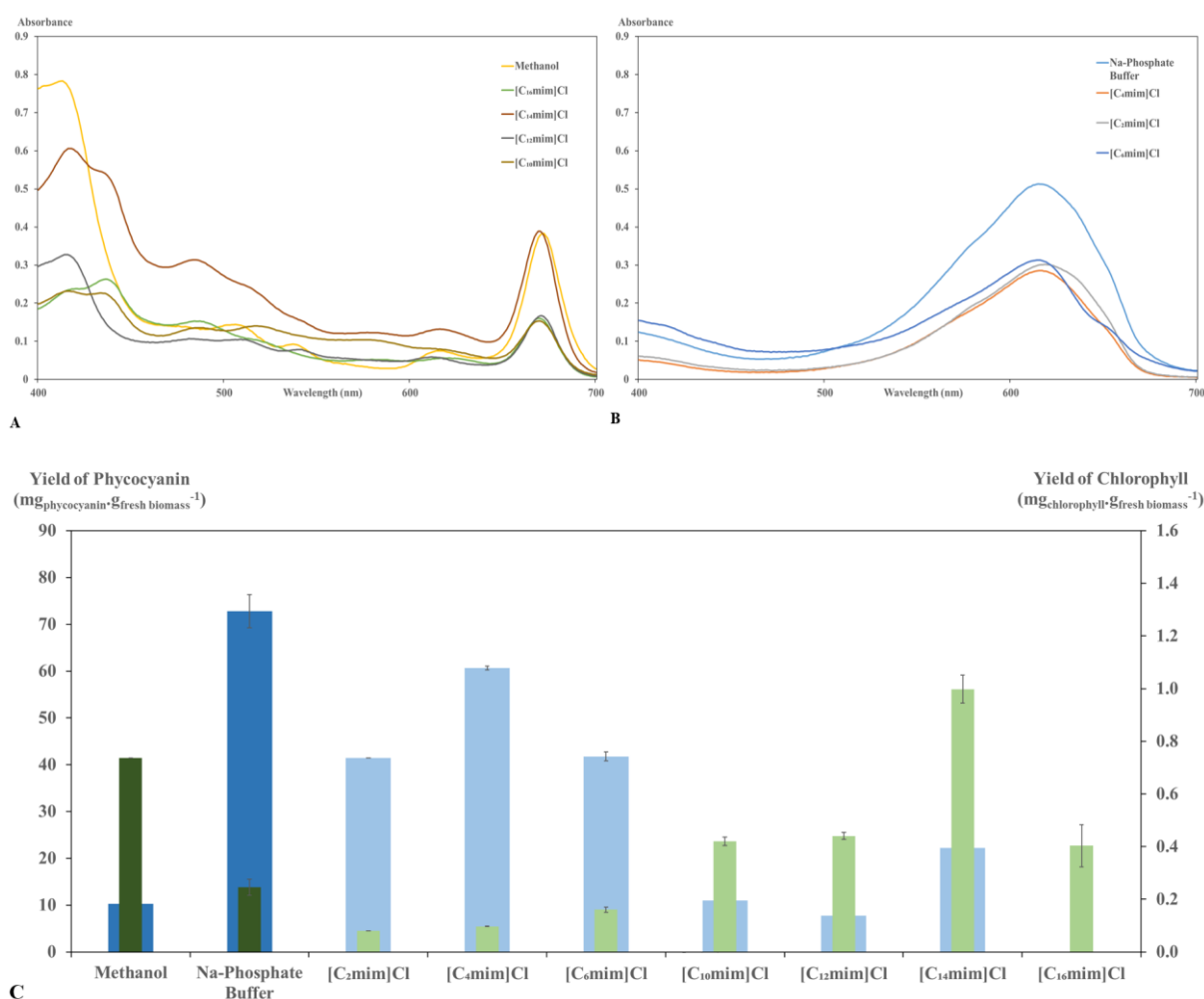


**Figure 3.4 –** Results obtained for different [C$_n$mim]Cl-based ionic liquids, showing: (A) absorption spectra of the crude extracts obtained by the use of the short alkyl chain-based [C$_n$mim]Cl ionic liquids; (B) absorption spectra of crude extracts obtained by the use of the long alkyl chain-based [C$_n$mim]Cl ionic liquids; (C) yields of extraction of phycocyanin ( ) and chlorophyll ( ) using the different ionic liquids' aqueous solutions (lighter colour) are

compared against the yields attained by conventional methodology (dark colour) for each pigment.


3.3.2.2 Cation effect

After the selection of hydrophilic ionic liquids, namely with an alkyl side chain of 4 carbons, as the most promising alternative solvent for the extraction of phycocyanin, different cations with short alkyl chains were studied. The cation effect is known to influence the hydrophobicity or hydrogen accepting ability of the ionic liquids [135]. The set of ionic liquids chosen included the [C$_4$mim]Cl, [Ch]Cl, [C$_4$mpip]Cl, [C$_4$mpyrr]Cl and [C$_4$mpyr]Cl. Results are displayed in Figure 3.5.
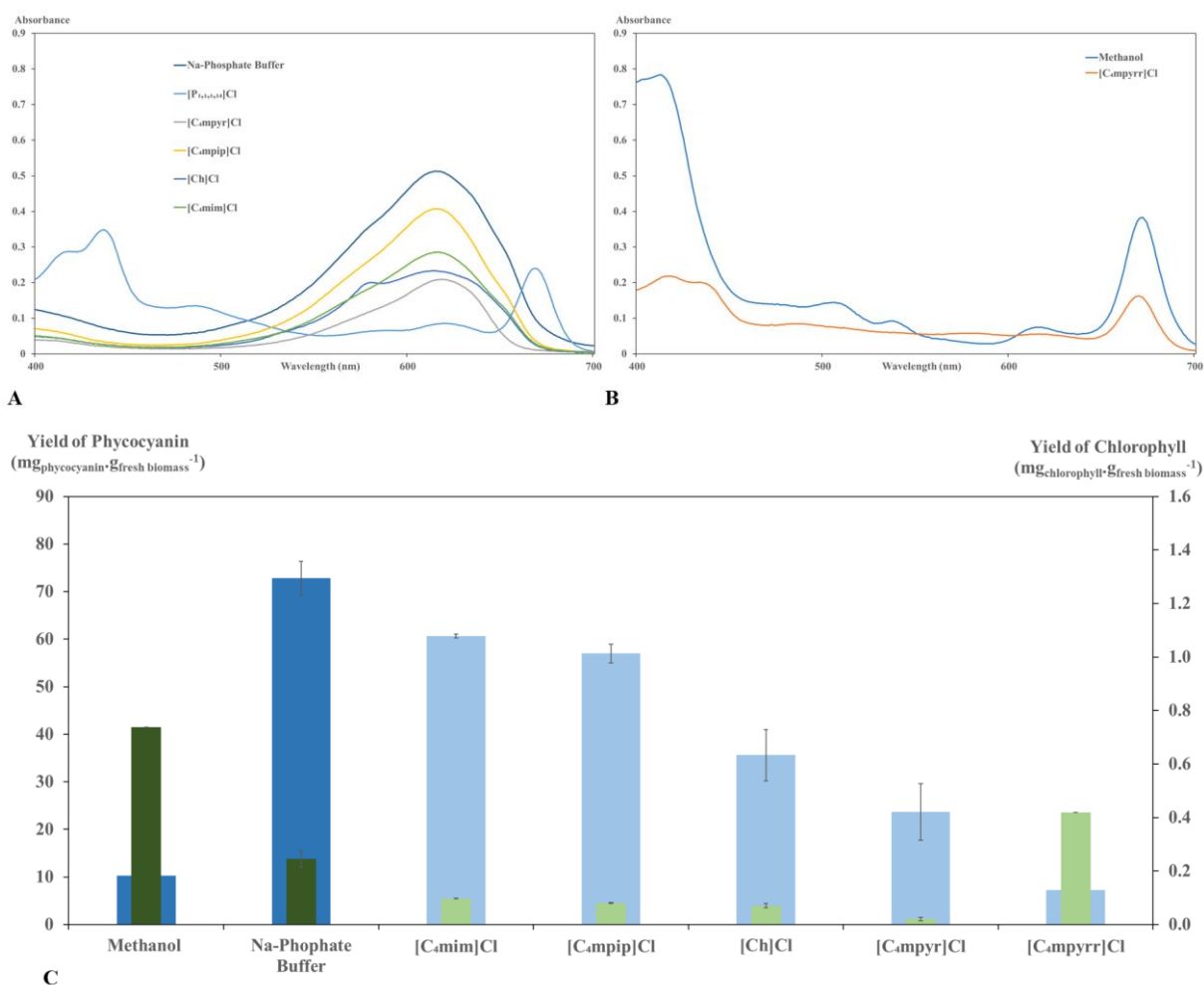


**Figure 3.5** - Results obtained using ionic liquids with different cations, showing: (A) absorption spectra of the crude extracts with maximum absorption peak for phycocyanin

(615 nm); (B) absorption spectra of crude extracts obtained with maximum absorption peak for chlorophyll (670 nm); (C) the yields of extraction of phycocyanin ( $\blacksquare$ ) and chlorophyll ( $\blacksquare$ ) using the different ionic liquids' aqueous solutions (lighter bars colour) are compared against the yields attained by conventional methodology (dark bars colour) for each pigment.

The screening output resulted with increased selectivity for phycocyanin than for chlorophyll, which is concordant with the set chosen, based on shorter alkyl chains. The yields of phycocyanin extraction from aqueous solutions of ionic liquids did not overcome the one from Na-phosphate buffer. Though, some remarks for phycocyanin extraction can be done: i) [C$_4$mim]Cl still have the highest yield for aqueous solutions of ionic liquids; ii) sorted by decreasing order [C$_4$mim]Cl > [C$_4$mpip]Cl > [Ch]Cl > [C$_4$mpyr]Cl shown to be capable of capturing phycocyanin.

Regarding the absorption spectra of methanol, [C$_4$mpyrr]Cl was found to be selective for chlorophyll. Martins and collaborators [129] when using the same aqueous solutions of ionic liquids to extract phycobiliproteins, namely R-Phycoerythrin from the macroalgae *Gracilaria sp.* found similar results, whereby the [C$_4$mpyrr]Cl also showed a significant absorption peak for chlorophyll (670 nm). In the same work, the highest extractive performance was attained with [Ch]Cl aqueous solution while in the present study [Ch]Cl was found as not significant. On the other hand, [C$_4$mim]Cl and [C$_4$mpip]Cl attained better extraction yields on both works for these two pigments from phycobiliproteins family. From the foregoing ionic liquids studied, [C$_4$mim]Cl was slightly better than [C$_4$mpip]Cl, therefore it was selected to conduct the anion study effect.

### 3.3.2.3 Anion effect

A set of chloride, dicyanamide, thiocyanate and trifluoromethanesulfonate anion's was chosen to combine with the previously selected imidazolium based ionic liquid, namely [C$_4$mim]$^+$. The extractive performance through the anion effect and the maximum absorption peaks for phycocyanin are depicted in Figure 3.6. Supporting information contains the list of $\beta$ values *for* 1-butyl-3-methylimidazolium ionic liquids family, namely S2.2.
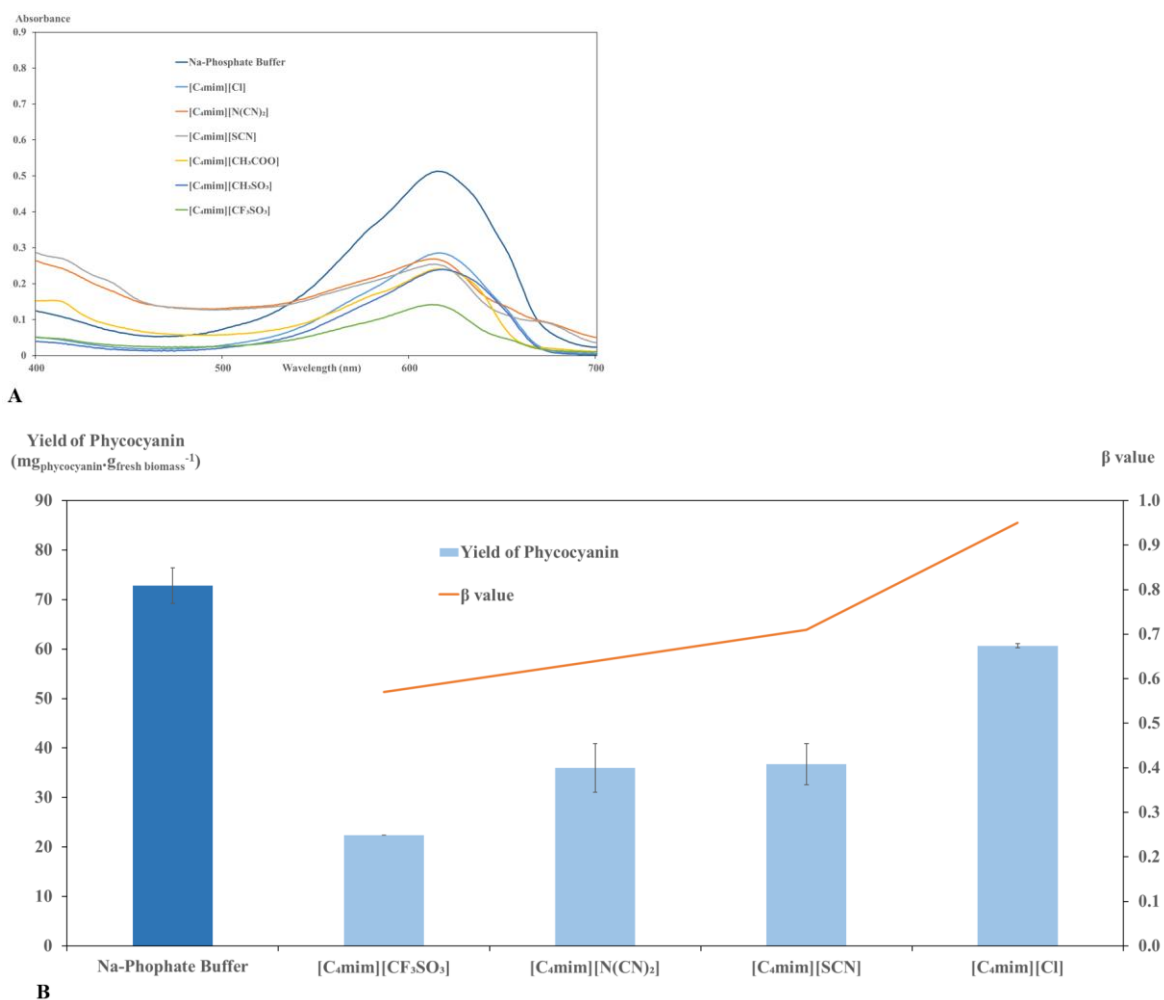
**Figure 3.6 –** Main results obtained for different anion-based ionic liquids (light blue bars) and conventional approach (dark blue bar), showing: (A) the absorption spectra of the crude extracts with maximum absorption peak for phycocyanin (615 nm); and (B) the yield of extraction of phycocyanin present in the crude aqueous extracts obtained and depicted by increasing the $\beta$ values of different [C$_4$mim]X-based ionic liquids (orange line).

The results from the spectra analysis indicate [CF$_3$SO$_3$]$^-$ as the anion with less competence to extract phycocyanin, though the [Cl]$^-$ achieved the highest yields on phycocyanin extraction. Thereby, the following order indicate the decreasing strength of the anion Cl$^-$ > [SCN]$^-$ > [N(CN)$_2$]$^-$ > [CF$_3$SO$_3$]$^-$ when combined with [C$_4$mim]X-based ionic liquids. These results are supported in the same way with a decreasing degree of the hydrogen bond accepting ability, also known as $\beta$ value [136–138]. Therefore, the augment of the yields of

phycocyanin extraction are linked with the increase of the β values, as shown in Figure 3.6B, which means that the increase in the hydrophilicity or polarity of the ionic liquid is favourable to the extraction increase. Once again no other anion combination of ionic liquid was capable to overcome the yield of [C$_4$mim]Cl, as well as the yield obtained by the conventional methodology. In order to develop an alternative methodology for the extraction of phycocyanin, the most promising aqueous solution of ionic liquid so far, namely [C$_4$mim]Cl, was used for further optimization of the operational extraction parameters.

### 3.3.2.4 Surfactant effect

Despite the fact that chlorophylls here were considered as contaminants, actually their applications are also of high interest. In this case, the optimization of the chlorophyll was also attested in this work. As mentioned before, the present screening serves as additional research, to understand whether besides aqueous solutions of ionic liquid promoting the extraction, another class show extractive performance for chlorophyll, namely surfactants. These tensioactive compounds are amphiphilic molecules which have been reported to extract hydrophobic biomolecules such as, carotenoids and chlorophylls [124,139]. Conventional extraction of chlorophylls is commonly performed with organic solvents such as, methanol and ethanol [140]. Therefore, a set of three cationic ([N$_{1,1,1,14}$]Br, [N$_{1,1,1,12}$]Br and ([C$_{16}$pyr]Cl), one anionic (SDS) and three non-ionic (Tween 20, Brij L4, and Triton X-114) surfactants were chosen.
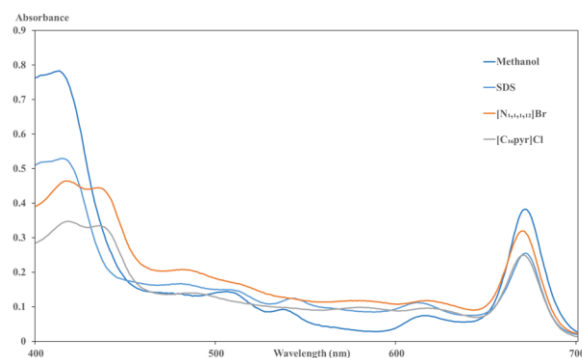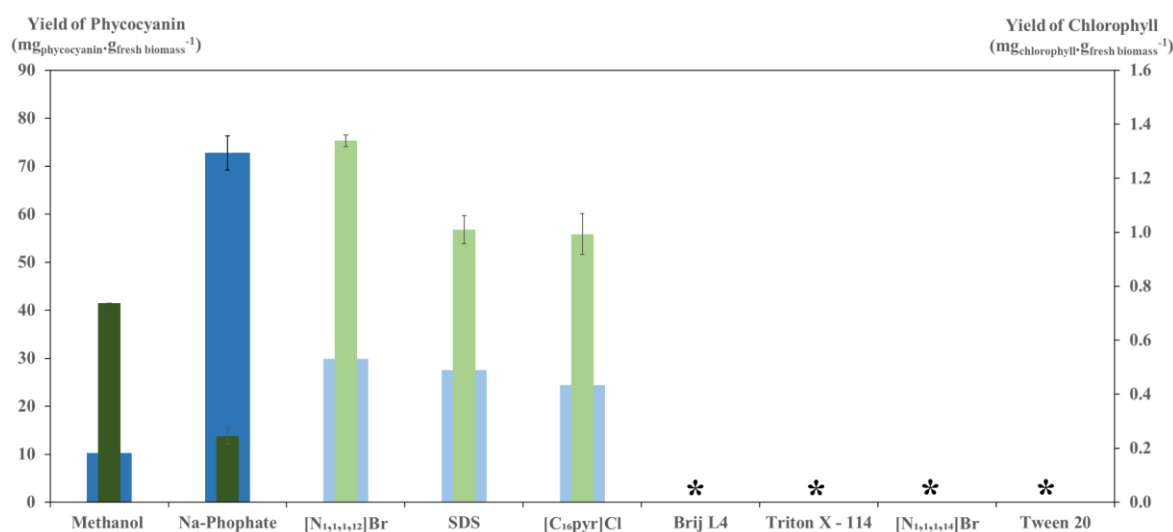
**Figure 3.7 –** Results obtained from the use of different surfactants: (A) the absorption spectra of the crude extracts with maximum absorption peak for phycocyanin (615 nm) and chlorophyll (670 nm); (B) representing the yields of chlorophyll (▮) and phycocyanin (▮) extraction obtained with conventional (dark colour) and alternative methodology (lighter colour); the (*) represents an ineffective performance of the correspondent surfactants.

The extractive performance on chlorophyll of the tested surfactants was successful, whereas all yields where higher than conventional methodology (methanol), shown in figure 3.7. However not all the surfactants reached the end of extraction, thus they were depicted by (*) on figure 3.7B. Aqueous solution of $[N_{1,1,1,12}]Br$ showed the best chlorophyll extraction yield (1,34 $mg_{chlorophyll} \cdot g_{fresh\ biomass}^{-1}$), which is 50% superior than conventional methodology. The present results also demonstrate the expected lower yields of phycocyanin extraction, whereas a possible explanation might be on the previous results for phycocyanin chemical

affinity to shorter alkyl chains, since surfactants are commonly constituted by long hydrophobic tails.

### 3.3.3 Optimization of the extraction conditions for phycocyanin: Response Surface Methodology (RSM)

From the previous screening step, [C$_4$mim]Cl was selected as the most promising alternative solvent to extract phycocyanin. Therefore, with view to improve the extractive yields of the blue natural pigment, the present work focused on the optimization of operational extraction parameters by applying a Response Surface Methodology (RSM). The RSM allows to conduct in one single experimental design the optimization of several extraction parameters, whereas in the present case, the complex input of information retrieves simple information as the optimal conditions for a maximum phycocyanin extraction yield. The extraction time optimization on conventional methodology, outputted similar phycocyanin yields between 30 to 45 minutes of extraction. Thereby, it is suggested that an optimum extraction time for the alternative methodology might also be found. Moreover, the ionic liquid concentration throughout the screening study was fixed at 500 mM. Therefore, it seems reasonable to carry an optimization study on the effect of: extraction time (7 - 46 minutes) and ionic liquid concentration (77 – 923 mM). Through a $2^{2(1/4)}$ factorial experimental design, eleven experiments with three replicates in the cornerstone of the model were carried considering a solid-liquid ratio of 0.1 (in fresh weight of biomass/volume of solvent). The analysis of variance (ANOVA), the Pareto chart and the plot of real against predicted values were developed and are presented in Supporting information (Table S2.4 and Figures S2.1 and S2.2). The extracts pictures of the eleven experiments are shown in Figure 3.8A.
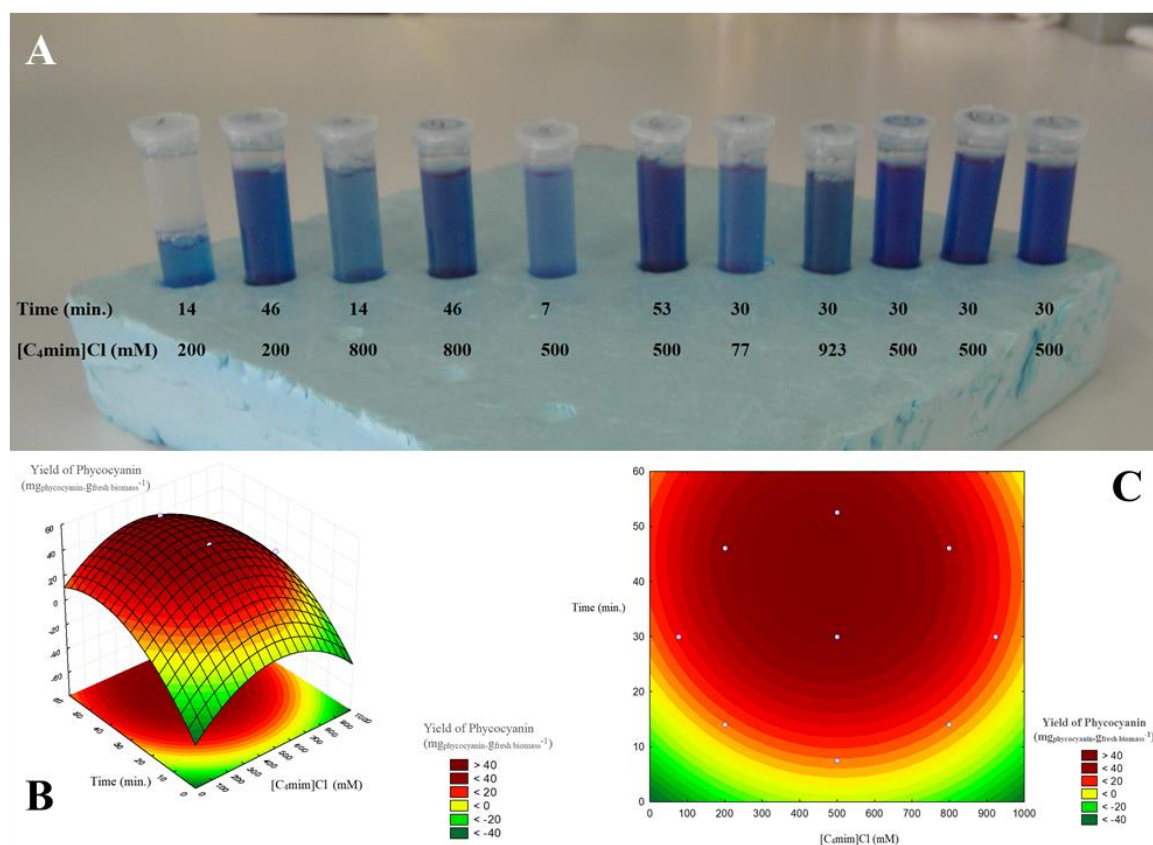
**Figure 3.8 –** Main results from the optimization study: (A) a photography of the eleven runs with depicted test conditions; (B) response surface plot and contour plot; (C) showing the yield of extraction of phycocyanin ($mg_{phycocyanin}.g_{fresh\ biomass}^{-1}$) with the combined effect of extraction time and ionic liquid concentration.

No significant differences ($p$-value = 0.05) were observed from the plot of experimental values with the predicted mathematical equation. The accuracy and precision of the model was confirmed by the coefficient of determination (0.95). The response surface and the contour plot are represented in figure 3.8B and 2.8C, respectively. The main results presented are a reflection of the interaction of extraction time and ionic liquid's concentration, which behaves almost like a parabola, whereas a maximum yield of phycocyanin can be attained. This evidence is also supported by the Pareto chart analysis, depicted in support information (Figure S2.18). This means that phycocyanin yield increases with time, though attains a maximum after 40 minutes and decreases after 50 minutes. On the other way, the concentration of the ionic liquid has a more defined parabola, whereas

depending on time it can reach more than 40 $mg_{phycocyanin} \cdot g_{fresh\ biomass}^{-1}$ between 400 to 600 mM of [C$_4$mim]Cl. Wherein the model suggested a theoretical maximum yield (52 $mg_{phycocyanin} \cdot g_{fresh\ biomass}^{-1}$). The optimum extraction time was 43 min while the optimal ionic liquid concentration was 475 mM. In order to validate the model, a three-replicate extraction under the theoretical optimum conditions was carried. The validation yield of phycocyanin (55 ± 2 $mg_{phycocyanin} \cdot g_{fresh\ biomass}^{-1}$) was slightly higher than the theoretical yield (52 $mg_{phycocyanin} \cdot g_{fresh\ biomass}^{-1}$), thereby it is still reasonable to consider the model as reproducible. Moreover, it should be stressed that the biomass used in the present work was batch grown. In order to generate enough biomass for the extraction process, two different batches were considered, namely one for the screening and other for the optimization studies. In Figure 3.9A, it can be observed the extraction yields of phycocyanin and chlorophyll from the conventional methodology with Na-Phosphate Buffer and the optimized alternative methodology with aqueous solution of [C$_4$mim]Cl, whereas pictures of extracts are also presented, namely in figure 27B.



**A**
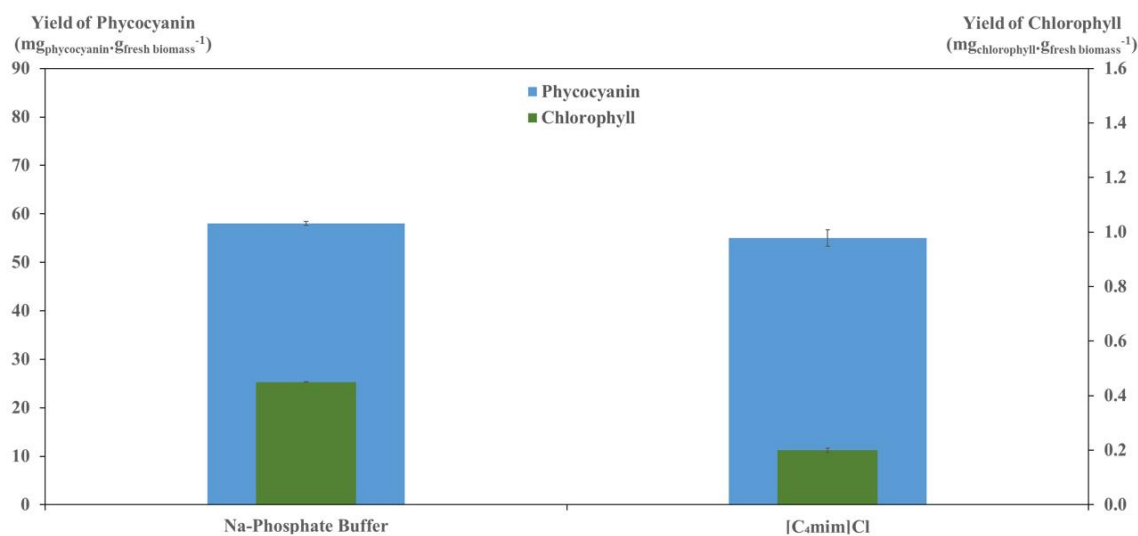


**B**

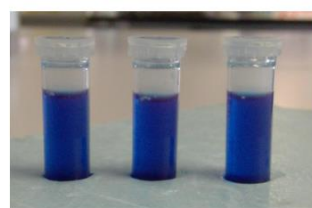Na-Phosphate Buffer extracts    [C$_4$mim]Cl-based aqueous extract

**Figure 3.9** – Results obtained from optimization study: (A) different [C$_4$mim]Cl-based aqueous extracts , showing: (A) the yields of extraction of phycocyanin (▯) and chlorophyll (▯) using the [C$_4$mim]Cl aqueous solutions (lighter colour) are compared against the yields attained by conventional methodology (dark colour) for each pigment; (B) pictures of the crude extracts from the conventional and alternative optimized methodology using an aqueous solutions of [C$_4$mim]Cl.

From the analysis of Figure 3.9A, phycocyanin extraction yields attained after the alternative methodology optimization ($55 \pm 1.7$ mg$_{phycocyanin}$·g$_{fresh\ biomass}^{-1}$) were slightly lower than the ones attained by the conventional methodology ($58 \pm 0.4$ mg$_{phycocyanin}$·g$_{fresh\ biomass}^{-1}$). The contamination with chlorophyll in phycocyanin extracts obtained using the optimized process conditions, the **[C$_4$mim]Cl**-based aqueous solution and a Na-phosphate buffer were determined. The chlorophyll contamination was reduced up to 3 times, which can be observed by comparing the colour of the Na-Phosphate extracts with the one from the ionic liquid aqueous extract, depicted in Figure 3.9B. Actually, the cost and application of phycocyanin are highly dependent on its purity index [119,121]. Therefore, purity of the crude extracts was evaluated. The purity relates the amount of phycocyanin and total proteins, being the ratio between the maximum absorption peak of phycocyanin (615 nm) and the maximal absorption peak (280 nm) of aminoacids with aromatic rings (total proteins) [141]. The extraction with the optimized [C$_4$mim]Cl-based aqueous solution resulted in a phycocyanin purer extract (0.56) compared to the purity achieved by the conventional extraction methodology (0.38). Though are far from the higher-grade markets (ratio $\geq 3.9$), it should be noted that the purity level attained in the present work is respective to a crude extract, which has still to undergo further purification and concentration steps. Furthermore, comparing the results obtained in the current work with the recently reported literature, a compilation of alternative approaches to increase purity index of crude phycocyanin extracts is presented in Table 3.1.

**Table 3.1** – Comparisons on the methodology, time of extraction and purity level [ratio of maximum absorption peak of phycocyanin and the maximum absorption peak of total proteins (280 nm)] between the published approaches and the alternative extraction suggested in this work used to attain a crude extract rich in phycocyanin from fresh biomass.

| Solvent | Methodology of extraction | Time (hours) | Crude extract purity | Organism | Reference |
|---|---|---|---|---|---|
| Na-Phosphate Buffer | **Under agitation** | **0.75** | **0.38** | *A. cylindrica* | **Present Study** |
| | Lysozyme assisted extraction | 24 | 0.4 | *Calothrix* sp. | [111] |
| Ionic Liquid | **Under agitation** | **0.72** | **0.56** | *A. cylindrica* | **Present study** |
| Water | Under agitation | 4 | 0.46 | *Spirulina platensis* | [122] |
| Tris-HCl Buffer | Liquid nitrogen freezing by mortar and pestle | - | 0.42 | *Phormidium fragile* | [142] |
| Ammonium Chloride | Repeated freezing and thawing cycles | 25 | 0.85 | *Arthrospira platensis* FACHB-314 | [117] |

From the foregoing analysis, many attempts have been carried to improve the extraction yields of phycocyanin with increased purity, however or the impairment of extraction time or the unsustainability of the solvent still weaken its suitability for industry. Therefore, in comparison, the present study proves to be more balanced due to its fast extraction time, water-based solvent composition and convenient purity index.

## 3.4 Conclusions

The present work brought conclusive insights on the development of an added value extractive platform of the unrated cyanobacteria *A. cylindrica*, through an alternative methodology based on alternative solvents use. Phycocyanin is one of the major constituents of phycobiliproteins family in cyanobacteria, which its exploitation remains as a potential source for this blue natural pigment. The cultivation of *A. cylindrica* was not in the aim of the study whereas to meet the needs of downstream process, the increase of biomass productivity is mandatory. A conventional methodology was used since it was important to compare and also to understand that despite the possible higher yields, the contamination with undesired compounds is also high, whereby it is a burden for purification processing. With regards to the alternative methodology based on aqueous solutions of ionic liquids it turned out to be highly selective whereas it was possible to almost like refine the composition of the most suitable solvent, through a selective screening. Not only it was proven for phycocyanin but also for chlorophyll, once only in the screening study it surpassed the conventional chlorophyll extraction yields up to 50%. Despite its optimization has been excluded since it was out aimed, these results open new possibilities of valorisation. Thereby, it can be highlighted the affinity of phycocyanin for shorter alkyl chains, whilst for chlorophyll, surfactants or ionic liquids with longer alkyl chains achieved better extractive performance. The optimization process of [C$_4$mim]Cl lead to understand the combined effect of ionic liquid concentration and extraction time as important parameters to extract phycocyanin from cultures of *A. cylindrica*. The optimal extraction conditions attained for higher phycocyanin yields are a solid-liquid ratio of 0.1 in fresh weight of biomass/volume of solvent, extraction time of 43 min and ionic liquid concentration of 475 mM. Under these conditions, the validation of the model lead to similar extraction yields. Although the extraction yields were lower, the crude ionic liquid's extracts attained a purer phycocyanin index, than those attained by conventional methodology. In terms of other pigments namely, chlorophylls, the contamination was reduced up to 3 times, while the contamination of other proteins was also reduced by 1.5 times. In addition, the use of ionic liquids might be expensive than buffer like salt solutions, although in the present case the ionic liquid only represents 8% of the total solvent composition (m/v). Thus, its feasibility is justified when coupled to its promising extractive capability to achieve purer phycocyanin yields in only 43 minutes of extraction. Even the cost of the process can be decreased, if an integrated process using aqueous biphasic systems is considered, due to the presence of salts in the extract itself. Finally, the present study developed a fast, sustainable, economic and

selective extraction methodology which is water based. In conclusion, the use of aqueous ionic liquid solutions with increased purity levels of phycocyanin is of high relevance since it can simplify the purification and concentration steps, commonly known for being expensive and hardly-scalable.

# 5. FINAL REMARKS

## 5.1 Conclusions

Microalgae are a ubiquitous natural resource with the potential volumetric productivity that no other organism can attain. The environmental plasticity of these organisms give rise to a unique reservoir of many added-value compounds. Therefore, the present work endorsed the knowledge on the upstream and the downstream processing of microalgae.

The upstream processing evaluated in the present work, was integrated on the working package 3 – production and downstream processing of the European project Sustainable Polymers from Algae Sugars and Hydrocarbons (SPLASH). The most relevant cultivation parameters, namely C, D, E from outdoor production were simulated in an indoor flat panel PBR at lab scale. Whereby, three mathematical models were developed, namely A, B and C models, for continuous cultures of *Microalgae X*. The output resulted in a tuned tool which is ready to be used as a starting condition to fine the outdoor production of this microalgae foreseeing the bulk scale. Therefore, the comprehension of the optimal environmental conditions for outdoor production of a certain product like the present work, might work towards a bio-based economy transition.

The second part of the present work was focused on the downstream processing, namely extraction step. Envisioning the valorisation of unexplored freshwater biomass, the cyanobacteria *A. cylindrica* was used to conduct the development of an alternative extraction methodology of added value compounds namely, phycocyanin. The use of aqueous solutions of ionic liquids and surfactants revealed to be highly selective for pigments as for proteins while extraction time was shown as a valuable factor. The hydrophilic ionic liquid family was shown to have more affinity for phycocyanin, whereas [$C_4$mim]Cl demonstrated the best yields as well as reduced pigment and protein content contamination after RSM optimization. The obtained crude extract of phycocyanin in the present work is purer and faster to be attained than other published work. Moreover, the sustainability of this recently developed alternative method is supported by the solvent composition, wherein a water-based solution where only 8% of ionic liquid.

## 5.2 Future Work

The upstream processing on *Microalgae X* could be integrated with downstream processing, in order to decrease the renewal of biomass and to reduce the allocation of needed machinery. The study on the feasibility of growth and extraction (milking) of the product in the same compartment is a task that should be addressed. In addition, understand whether it exits some sort of stimulus which can induce algae to excrete the product or some stress that can increase the amount of product formed are important questions to unravel. Nonetheless innovative PBR designs should not be discarded since the volumetric productivity potential of microalgae is still far to reach.

The alternative extraction methodology developed could be improved by the application of aqueous biphasic systems to purify the crude extracts. Alternative ways, could try to increase the potential of biomass towards a biorefinery approach. Successive extractions using different solvents could led to extract multiple classes of compounds (phycocyanin, chlorophyll, carotenoids, etc.,) from the same biomass.

# S. SUPPORTING INFORMATION

## S1 - Chapter I - Study of the influence of different cultivation parameters on cultures of *Microalgae M*

**Table S1.1 –** X004 design used for M4S201 with experimental and predicted values for the A model.
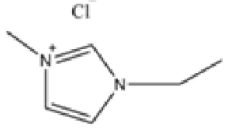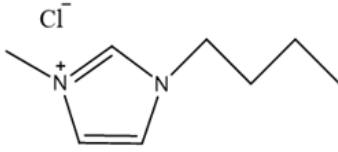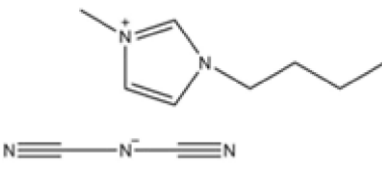
| Experiment | Average WTD | Experimental A | Predicted A |
|:---:|:---:|:---:|:---:|
| 1 | 0.00 | 0.00 | 0.23 |
| 2 | 10.34 | 1.03 | 1.01 |
| 3 | 0.00 | 0.00 | 0.02 |
| 4 | 1.65 | 0.50 | 0.27 |
| 5 | 0.00 | 0.00 | -0.17 |
| 6 | 0.20 | 0.04 | 0.12 |
| 7 | 0.06 | 0.01 | -0.08 |
| 8 | 2.45 | 0.49 | 0.66 |
| 9 | 4.21 | 0.42 | 0.36 |
| 10 | 0.00 | 0.00 | 0.24 |
| 11 | 11.8 | 1.18 | 1.03 |
| 12 | 0.42 | 0.13 | 0.19 |
| 13 | 1.90 | 0.38 | 0.40 |
| 14 | 0.45 | 0.09 | 0.40 |
| 15 | 2.45 | 0.49 | 0.40 |
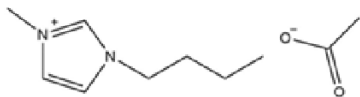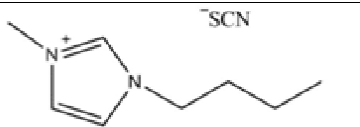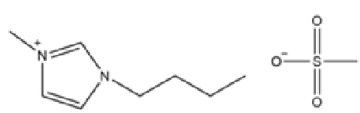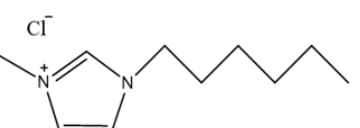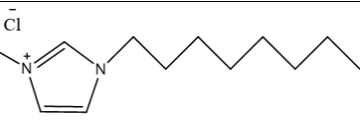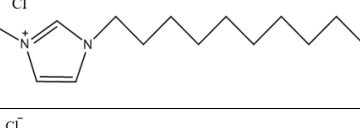
**Table S1.2 –** X004 design used for M4S201 with experimental and predicted values for the C model.

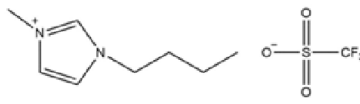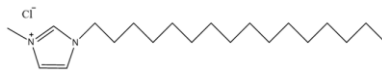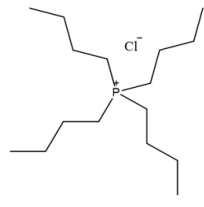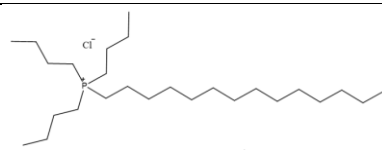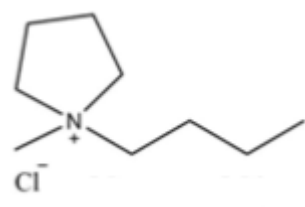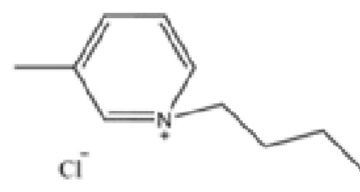| Experiment | Average MD | Experimental C | Predicted C |
|:---:|:---:|:---:|:---:|
| 1 | 0.00 | 0.00 | 0.23 |
| 2 | 7.40 | 0.74 | 1.01 |
| 3 | 0.00 | 0.00 | 0.02 |
| 4 | 19.6 | 5.87 | 0.27 |
| 5 | 0.00 | 0.00 | -0.17 |
| 6 | 15.9 | 3.19 | 0.12 |
| 7 | 0.00 | 0.00 | -0.08 |
| 8 | 9.00 | 1.80 | 0.66 |
| 9 | 100 | 10.0 | 0.36 |
| 10 | 10.7 | 3.20 | 0.24 |
| 11 | 5.10 | 0.51 | 1.03 |
| 12 | 33.6 | 10.1 | 0.19 |
| 13 | 100.2 | 20.0 | 0.40 |
| 14 | 82.7 | 16.5 | 0.40 |
| 15 | 90.56 | 18.1 | 0.40 |
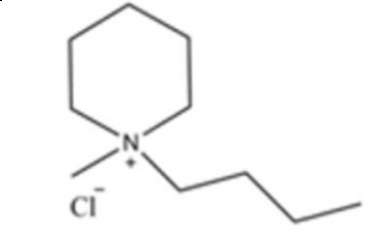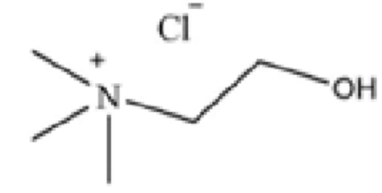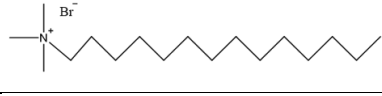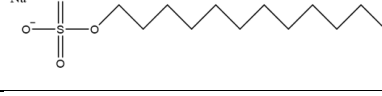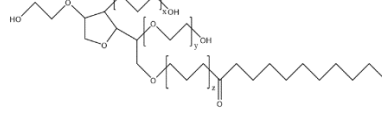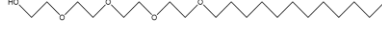
# S2 - Chapter II - Alternative methodology for phycocyanin extraction from *Anabaena cylindrica* batch cultures

**Table S2.1 -** Ionic liquids and surfactants information: full name, acronyms, chemical formula, molecular mass, CMC and chemical structures.

| Type | | Name (acronym) | Chemical formula | Molecular weight (g mol$^{-1}$) | CMC in water (mM) | Chemical structure |
|---|---|---|---|---|---|---|
| Ionic Liquids | Imidazolium | 1-ethyl-3-methylimidazolium chloride, [C$_2$mim]Cl | C$_6$H$_{11}$ClN$_2$ | 146.6 | - |  |
| | | 1-butyl-3-methylimidazolium chloride, [C$_4$mim]Cl | C$_8$H$_{15}$ClN$_2$ | 174.7 | - |  |
| | | 1-butyl-3-methylimidazolium dicyanamide, [C$_4$mim][N(CN)$_2$] | C$_{10}$H$_{15}$N$_5$ | 205.7 | - |  |
| | | 1-butyl-3-methylimidazolium trifluoromethanesulfonate, [C$_4$mim][CF$_3$SO$_3$] | C$_9$H$_{15}$F$_3$N$_2$O$_3$S | 288.3 | - |  |

| | | Name | Formula | MW | | Structure |
|---|---|---|---|---|---|---|
| | | 1-butyl-3-methylimidazolium acetate, [C$_4$mim][CH$_3$COO] | C$_{10}$H$_{18}$N$_2$O$_2$ | 198.3 | - | |
| | | 1-butyl-3-methylimidazolium thiocyanate, [C$_4$mim][SCN] | C$_9$H$_{15}$N$_3$S | 197.3 | - | |
| | | 1-butyl-3-methylimidazolium methanosulfonate, [C$_4$mim][CH$_3$SO$_3$] | C$_9$H$_{18}$N$_2$O$_3$S | 234.3 | - | |
| | | 1-hexyl-3-methylimidazolium chloride, [C$_6$mim]Cl | C$_{10}$H$_{19}$ClN$_2$ | 202.7 | - | |
| | | 1-octyl-3-methylimidazolium chloride, [C$_8$mim]Cl | C$_{12}$H$_{23}$ClN$_2$ | 230.8 | 227 | |
| | | 1-decyl-3-methylimidazolium chloride, [C$_{10}$mim]Cl | C$_{14}$H$_{27}$ClN$_2$ | 258.8 | 58.7 | |
| | | 1-dodecyl-3-methylimidazolium chloride, [C$_{12}$mim]Cl | C$_{16}$H$_{31}$ClN$_2$ | 286.9 | 15.2 | |
| | | 1-tetradecyl-3-methylimidazolium chloride, [C$_{14}$mim]Cl | C$_{18}$H$_{35}$ClN$_2$ | 314.9 | 3.90 | |

| | | 1-hexadecyl-3-methylimidazolium chloride, [C$_{16}$mim]Cl | C$_{20}$H$_{39}$ClN$_2$ | 343.0 | 0.950 |  |
|---|---|---|---|---|---|---|
| Phosphonium | | tetrabutylphosphonium chloride, [P$_{4,4,4,4}$]Cl | C$_{16}$H$_{36}$ClP | 294.9 | |  |
| | | tributyltetradecylphosphonium chloride, [P$_{4,4,4,14}$]Cl | C$_{26}$H$_{56}$ClP | 563.8 | 260 |  |
| Pyrrolidinium | | 1-butyl-1-methylpyrrolidinium chloride, [C$_4$mpyrr]Cl | C$_9$H$_{20}$ClN | 177.7 | - |  |
| | | 1-butyl-3-methylpyridinium chloride, [C$_4$mpyr]Cl | C$_{10}$H$_{16}$ClN | 185.7 | - |  |

| | | | | | |
|---|---|---|---|---|---|
| Piperidinium | 1-butyl-1-methylpiperidinium chloride, [C$_4$mpip]Cl | C$_{10}$H$_{22}$ClN | 191.7 | - |  |
| Colina | cholinium chloride, [Ch]Cl | C$_5$H$_{14}$ClNO | 139.6 | - |  |

| Surfactants | | | | | | |
|---|---|---|---|---|---|---|
| | Cationic | dodecylTrimethylammonium Bromide ([N$_{1,1,1,12}$]Br) | C$_{15}$H$_{34}$BrN | 308.4 | 14.6 |  |
| | | tetradecyltrimethylammonium bromide ([N$_{1,1,1,14}$]Br) | C$_{17}$H$_{38}$BrN | 336.4 | 1.50 |  |
| | | 1-hexadecylpyridinium chloride ([C$_{16}$pyr]Cl) | C$_{21}$H$_{38}$ClN | 399.9 | 0.960 |  |
| | Anionic | sodium dodecyl sulfate (SDS) | C$_{12}$H$_{25}$NaO$_4$S | 288.4 | 8.00 |  |
| | Non-anionic | Tween 20 | C$_{58}$H$_{114}$O$_{26}$ | 1228 | 0.00694 |  |
| | | Brij L4 | C$_{20}$H$_{42}$O$_5$ | 362.0 | 0.0600 |  |

| | | Triton X-114 | $C_{14}H_{22}O(C_2H_4O)$ 7-8 | 537.0 | 0.210 |  |
| --- | --- | --- | --- | --- | --- | --- |
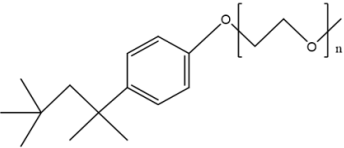
**Table S2.2** − β value of 1-butyl-3-methylimidazolium ionic liquids family. Adapted from literature [136].

| Anion | β value |
|---|---|
| **Cl$^-$** | 0.95 |
| **Br$^-$** | 0.87 |
| **CH$_3$COO$^-$** | 0.85 |
| **CH$_3$SO$_3$$^-$** | 0.85 |
| **NO$_2$$^-$** | 0.81 |
| **CH$_3$OSO$_3$$^-$** | 0.75 |
| **NO$_3$$^-$** | 0.74 |
| **OctOSO$_3$$^-$** | 0.77 |
| **I$^-$** | 0.75 |
| **CF$_3$COO$^-$** | 0.74 |
| **SCN$^-$** | 0.71 |
| **N(CN)$_2$$^-$** | 0.64 |
| **CF$_3$SO$_3$$^-$** | 0.57 |
| **BF$_4$$^-$** | 0.55 |
| **PF$_6$$^-$** | 0.44 |
| **Ntf$_2$$^-$** | 0.42 |

**Table S2.3 -** Factor levels for the surface response design for a $2^{2(1/4)}$ factorial planning.

| Run | Time (min) | [C₄mim]Cl (mM) |
|---|---|---|
| 1 | 14 | 200 |
| 2 | 46 | 200 |
| 3 | 14 | 800 |
| 4 | 46 | 800 |
| 5 | 7 | 500 |
| 6 | 53 | 500 |
| 7 | 30 | 77.0 |
| 8 | 30 | 923 |
| 9* | 30 | 500 |
| 10* | 30 | 500 |
| 11* | 30 | 500 |

* middle level reinforced with three replicates.

**Table S2.4** –Regression coefficient of the predicted polynomial model of second-order for the yield of extraction of phycocyanin obtained from the RSM design, whereas for 95% of confidence the $p$-value is bold.

| Term | Sum of Squares | Degrees of freedom | Mean Squares | F-ratio | *p*-value |
|---|---|---|---|---|---|
| [C₄mim]Cl | 12.32 | 1.000 | 12.32 | 0.5527 | 0.4906 |
| ([C₄mim]Cl)² | 923.4 | 1.000 | 923.4 | 41.42 | **0.001346** |
| Time (min.) | 1270 | 1.000 | 1271 | 56.99 | **0.000646** |
| (Time)² (min.) | 370.9 | 1.000 | 370.9 | 16.64 | **0.009552** |
| 1L by 2L | 5.726 | 1.000 | 5.726 | 0.2568 | 0.6339 |
| Error | 111.5 | 5.000 | 22.30 | | |
| Total Sum of Squares | 2442 | 10.00 | | | |
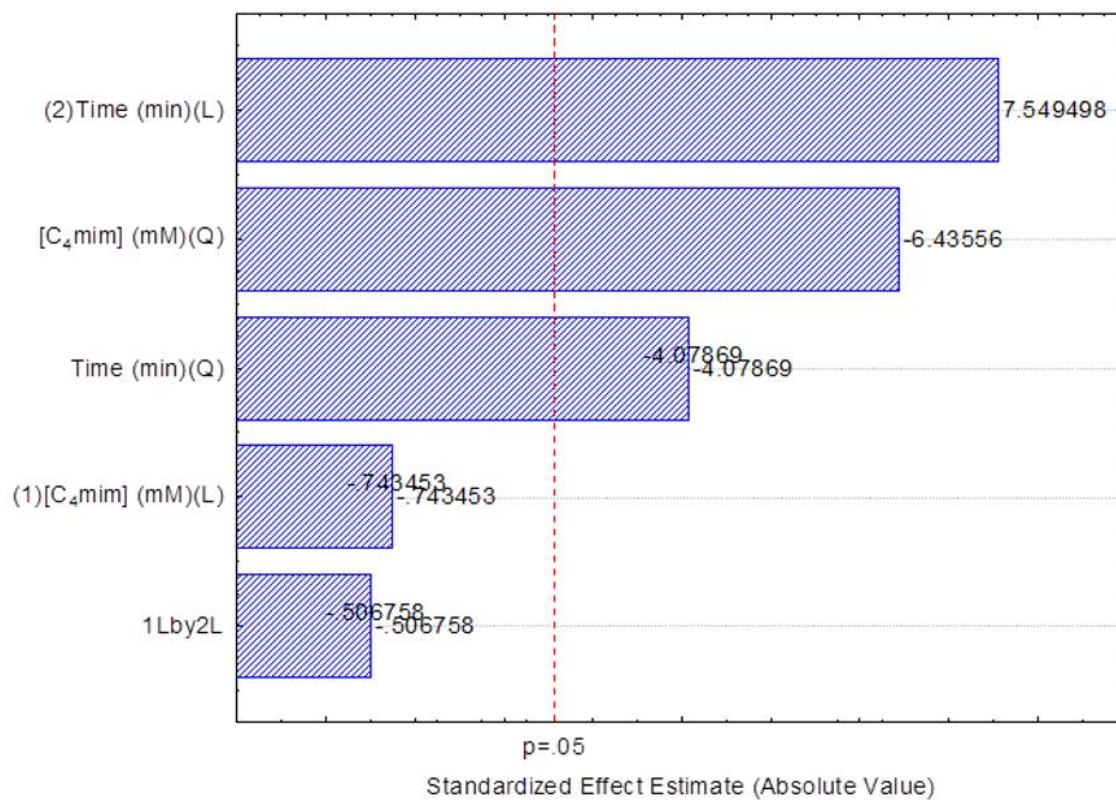
**Figure S2.1** - Pareto chart of the standardized effects using a $2^{2(1/4)}$ factorial design, for the variable extraction yield of phycocyanin ($mg_{phycocyanin} \cdot g_{fresh\ biomass}^{-1}$).
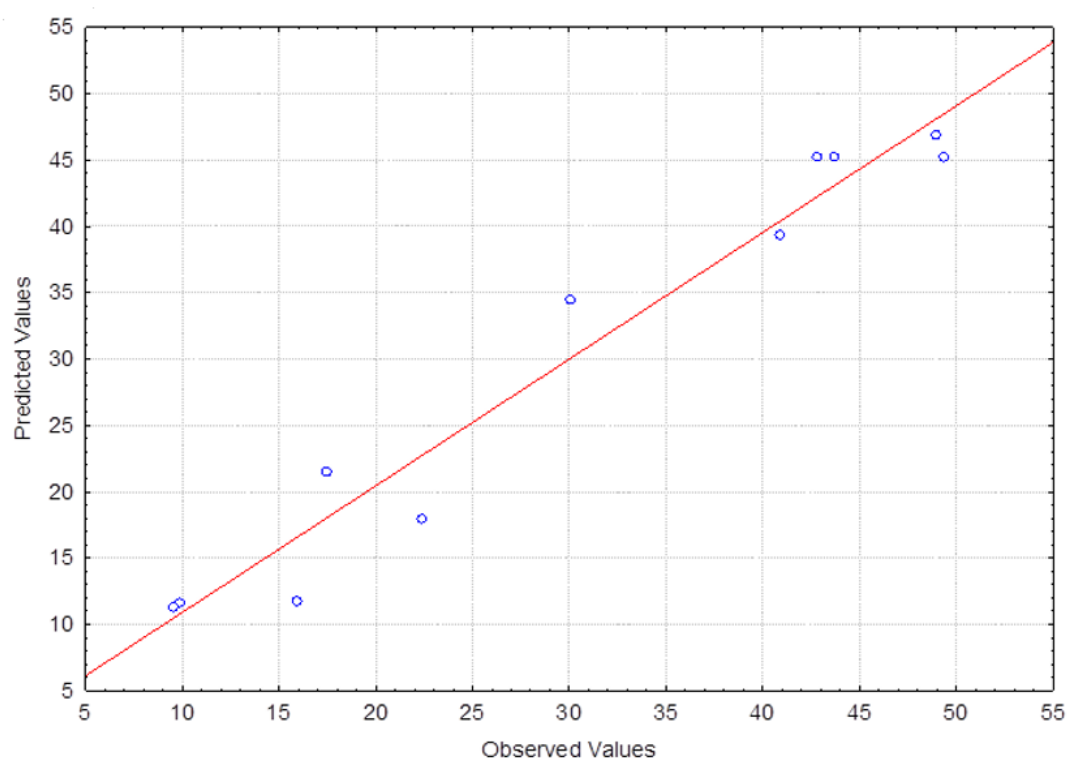
**Figure S2.2 –** Results of yield of extraction of phycocyanin extracted experimentally, and mathematical equation fit of predicted values.

# 6. BIBLIOGRAPHY

1. P. Mengal, J. Bell DC. 2016 Call for proposals. *Bio Based Industries Joint Undertaking*; 2016.

2. Ciubota-Rosie C, Gavrilescu M, Macoveanu M. Biomass - An important renewable source of energy in Romania. *Environ Eng Manag J*. 2008;7(5):559-568.

3. Evans JR. Photosynthesis and nitrogen relationship in leaves of C3 plants. *Oecologia*. 1989;78(1):9-19.

4. Singh J, Gu S. Commercialization potential of microalgae for biofuels production. *Renew Sustain Energy Rev*. 2010;14(9):2596-2610.

5. Enzing C, Ploeg M, Barbosa M, Sijtsma L. *Microalgae-Based Products for the Food and Feed Sector: An Outlook for Europe*.; 2014.

6. Ge Y, Liu J, Tian G. Growth characteristics of Botryococcus braunii 765 under high CO2 concentration in photobioreactor. *Bioresour Technol*. 2011;102(1):130-134.

7. Amaro HM, Macedo ÂC, Malcata FX. Microalgae: An alternative as sustainable source of biofuels? *Energy*. 2012;44(1):58-166.

8. Wolkers H, Barbosa M, Kleinegris D, Bosma R, Wijffels RH. Microalgae: the green gold of the future. *Green raw Mater*. 2011, 2016:9-31.

9. Beetul, K., Gopeechund, A., Kaullysing, D., Mattan-Moorgawa, S., Puchooa, D., Bhagooli R. Challenges and Opportunities in the Present Era of Marine Algal Applications. *Algae-Org for I Biotech*. 2016.

10. Hemaiswarya S, Raja R, Kumar RR, Ganesan V, Anbazhagan C. Microalgae: a sustainable feed source for aquaculture. *World J Microbiol Biotechnol*. 2011;27(8):1737-1746.

11. John RP, Anisha GS, Nampoothiri KM, Pandey A. Micro and macroalgal biomass: A renewable source for bioethanol. *Bioresour Technol*. 2011;102(1):186-193.

12. Draaisma RB, Wijffels RH, Slegers PM, Brentner LB, Roy A, Barbosa MJ. Food commodities from microalgae. *Curr Opin Biotechnol*. 2013;24(2):169-177.

13. Benvenuti G, Lamers PP, Breuer G, et al. Microalgal TAG production strategies: why batch beats repeated-batch. *Biotechnol Biofuels*. 2016;9(1):64.

14. Saha SK, McHugh E, Hayes J, Moane S, Walsh D, Murray P. Effect of various stress-regulatory factors on biomass and lipid production in microalga Haematococcus pluvialis. *Bioresour Technol*. 2013;128:118-124.

15. Vanthoor-Koopmans M, Wijffels RH, Barbosa MJ, Eppink MHM. Biorefinery of microalgae for food and fuel. *Bioresour Technol*. 2013;135:142-149.

16. Janssen, Marcel and Lamers P. Microalgae Biotechnology – Bioprocess Engeneering, Wageningen University, 2014, 32803..

17. Liu L, Pohnert G, Wei D. Extracellular metabolites from industrial microalgae and their biotechnological potential. *Mar Drugs*. 2016;14(10):1-19.

18. Griehl C, Kleinert C, Griehl C, Bieler S. Design of a continuous milking bioreactor for non-destructive hydrocarbon extraction from Botryococcus braunii. *J Appl Phycol*. 2015;27(5):1833-1843.

19. Singh P, Guldhe A, Kumari S, Rawat I, Bux F. Investigation of combined effect of nitrogen, phosphorus and iron on lipid productivity of microalgae Ankistrodesmus falcatus KJ671624 using response surface methodology. *Biochem Eng J*. 2015;94:22-29.

20. Li D, Wang L, Zhao Q, Wei W, Sun Y. Improving high carbon dioxide tolerance and carbon dioxide fixation capability of Chlorella sp. by adaptive laboratory evolution. *Bioresour Technol*. 2015;185:269-275.

21. Jin J, Dupré C, Yoneda K, Watanabe MM, Legrand J, Grizeau D. Characteristics of extracellular hydrocarbon-rich microalga Botryococcus braunii for biofuels production: Recent advances and opportunities. *Process Biochem*. 2016;51(11):1866-1875.

22. Eriksen NT. The technology of microalgal culturing. *Biotechnol Lett*. 2008;30(9):1525-1536.

23. Lavens, Patrick and Sorgerloos P. Manual on the Production and Use of Live Food

for Aquaculture. No. 361. *Food and agriculture Organization (FAO)*; 1996.

24. Bux, Faizal and Chisti Y, Algae Biotechnology. *Cham Springer International Publishing*; 2016.

25. Zenobi S. Continuous Culture of Botryococcus braunii For Hydrocarbons Production. *MSc Thesis. Exeter University* 2013.

26. Liu S. Bioprocess Engineering: Kinetics, Biosystems, Sustainability, and Reactor Design .*Elsevier*; 2012. 1-984.

27. Frisch HL, Gotham IJ. A simple model for periodic cyclostat growth of algae. *J Math Biol*. 1979;7(2):149-169.

28. Andersen RA. Algal Culturing Techniques. *Acad Press*. 2005.

29. Zhao, Y. and Skogestad S. A comparison of various control schemes for continous bioreactor. *IFAC Proceedings Volumes* 27.2 (1994): 309-314.

30. Wardley-Smith B, White DC, Lowe AE. The Continuous Culture of Luminous Bacteria: a Luminostat. *J Appl Bacteriol*. 1975;39(3):337-343.

31. Cuaresma M, Janssen M, van den End EJ, Velchez C, Wijffels RH. Luminostat operation: A tool to maximize microalgae photosynthetic efficiency in photobioreactors during the daily light cycle? *Bioresour Technol*. 2011;102(17):7871-7878.

32. Richmond A. Handbook of Microalgal Culture: Biotechnology and Applied Phycology. *Blackwell Science Ltd*; 2004.

33. Keller R, Dunn IJ. Computer simulation of the biomass production rate of cyclic fed batch continuous culture. *J Chem Technol Biotechnol*. 1978;28(11):784-790.

34. Pirt SJ. Principles of Microbe and Cell Cultivation. *Blackwell Scientific Publications*, 1975.

35. Araujo, P.W. and Bereton RG. Experimental design II. Optimization. *Trends in Analytical Chemistry*. 1996;15(2):5-6.

36. Bezerra MA, Santelli RE, Oliveira EP, Villar LS, Escaleira LA. Response surface

methodology (RSM) as a tool for optimization in analytical chemistry. *Talanta*. 2008;76(5):965-977.

37. Aslan N, Cebeci Y. Application of Box-Behnken design and response surface methodology for modeling of some Turkish coals. *Fuel*. 2007;86(1-2):90-97.

38. Draper NR, John JA. Response-surface designs for quantitative and qualitative variables. *Technometrics*. 1988;30(4):423-428.

39. Myers RH, Montgomery DC, Vining GG, Borror CM, Kowalski SM. Response surface methodology: a retrospective and literature survey. *J Qual Technol*. 2004;36(1):53.

40. Draper NR, Lin DKJ. Small response-surface designs. *Technometrics*. 1990;32(2):187-194.

41. Kirrolia A, Bishnoi NR, Singh R. Response surface methodology as a decision-making tool for optimization of culture conditions of green microalgae Chlorella spp. for biodiesel production. *Ann Microbiol*. 2014;64(3):1133-1147.

42. Weiss TL, Roth R, Goodson C, et al. Colony organization in the green alga Botryococcus braunii (Race B) is specified by a complex extracellular matrix. *Eukaryot Cell*. 2012;11(12):1424-1440.

43. Tasic MB, Pinto LFR, Klein BC, Veljkovic VB, Filho RM. Botryococcus braunii for biodiesel production. *Renew Sustain Energy Rev*. 2016;64:260-270.

44. Kavitha G, Kurinjimalar C, Sivakumar K, Palani P, Rengasamy R. Biosynthesis, purification and characterization of polyhydroxybutyrate from Botryococcus braunii krutz. *Int J Biol Macromol*. 2016;89:700-706.

45. Metzger P, Largeau C. Botryococcus braunii: A rich source for hydrocarbons and related ether lipids. *Appl Microbiol Biotechnol*. 2005;66(5):486-496.

46. Moutel B, Gonçalves O, Le Grand F, et al. Development of a screening procedure for the characterization of Botryococcus braunii strains for biofuel application. *Process Biochem*. 2016;51(11):1855-1865.

47. Gendy TS, El-Temtamy S a. Commercialization potential aspects of microalgae for

biofuel production: An overview. *Egypt J Pet*. 2013;22(1):43-51.

48.   Metzger P, Berkaloff C, Casadevall E, Coute A. Alkadiene- and botryococcene-producing races of wild strains of Botryococcus braunii. *Phytochemistry*. 1985;24(10):2305-2312.

49.   Kawachi M, Tanoi T, Demura M, Kaya K, Watanabe MM. Relationship between hydrocarbons and molecular phylogeny of Botryococcus braunii. *Algal Res*. 2012;1(2):114-119.

50.   Banerjee A, Sharma R, Chisti Y, Banerjee UC. Botryococcus braunii: A renewable source of hydrocarbons and other chemicals. *Crit Rev Biotechnol*. 2002;22(3):245-279.

51.   Khatri W, Hendrix R, Niehaus T, Chappell J, Curtis WR. Hydrocarbon production in high density Botryococcus braunii race B continuous culture. *Biotechnol Bioeng*. 2014;111(3):493-503.

52.   Largeau C, Casadevall E, Berkaloff C, Dhamelincourt P. Sites of accumulation and composition of hydrocarbons in Botryococcus braunii. *Phytochemistry*. 1980;19(6):1043-1051.

53.   Metzger P, Largeau C, Casadevall E. Lipids and Macromolecular Lipids of the Hydrocarbon-rich Microalga Botryococcus braunii. Chemical Structure and Biosynthesis. Geochemical and Biotechnological Importance. *Progress in the Chemistry of Organic Natural Products*. Springer, Vienna; 1991:1-70.

54.   Dayananda C, Sarada R, Usha Rani M, Shamala TR, Ravishankar GA. Autotrophic cultivation of Botryococcus braunii for the production of hydrocarbons and exopolysaccharides in various media. *Biomass and Bioenergy*. 2007;31(1):87-93.

55.   Yoshimura T, Okada S, Honda M. Culture of the hydrocarbon producing microalga Botryococcus braunii strain Showa: Optimal CO2, salinity, temperature, and irradiance conditions. *Bioresour Technol*. 2013;133:232-239.

56.   Wolf FR, Nonomura AM, Bassham JA. Growth and branched hydrocarbon production in a strain of Botryococcus braunii (chlorophyta) 1. *J Phycol*. 1985;21(3):388-396.

57. Ruangsomboon S. Effect of light, nutrient, cultivation time and salinity on lipid production of newly isolated strain of the green microalga, Botryococcus braunii KMITL 2. *Bioresour Technol*. 2012;109:261-265.

58. Okumura C, Saffreena N, Rahman MA, Hasegawa H, Miki O, Takimoto A. Economic efficiency of different light wavelengths and intensities using LEDs for the cultivation of green microalga Botryococcus braunii (NIES-836) for biofuel production. *Environ Prog Sustain Energy*. 2015;34(1):269-275.

59. Croft MT, Lawrence AD, Raux-Deery E, Warren MJ, Smith AG. Algae acquire vitamin B12 through a symbiotic relationship with bacteria. *Nature*. 2005;438(7064):90-93.

60. Rivas MO, Vargas P, Riquelme CE. Interactions of Botryococcus braunii Cultures with Bacterial Biofilms. *Microb Ecol*. 2010;60(3):628-635.

61. Tanabe Y, Kato S, Matsuura H, Watanabe MM. A Botryococcus Strain with Bacterial Ectosymbionts Grows Fast and Produces High Amount of Hydrocarbons. *Procedia Environ Sci*. 2012;15:22-26.

62. Chirac C, Casadevall E, Largeau C, Metzger P. Bacterial influence upon growth and hydrocarbon production of the green alga Botryococcus braunii1. *J Phycol*. 1985;21(3):380-387.

63. Jones KJ, Moore K, Sambles C, Love J, Studholme DJ, Aves SJ. Draft Genome Sequences of Achromobacter piechaudii GCS2, Agrobacterium sp. Strain SUL3, Microbacterium sp. Strain GCS4, Shinella sp. Strain GWS1, and Shinella sp. Strain SUS2 Isolated from Consortium with the Hydrocarbon-Producing Alga Botryococcus brauni. *Genome Announc*. 2016;4(1):01527-15.

64. McNaught AD, Wilkinson A. Compendium of chemical terminology. IUPAC recommendations. 1997. *Online corrected version* 2006.

65. Rinzema A. Bioreactor Design - Bioprocess Engeneering, *Wageningen and Research University*. 2014.

66. Rawat I, Ranjith Kumar R, Mutanda T, Bux F. Biodiesel from microalgae: A critical evaluation from laboratory to large scale production. *Appl Energy*. 2013;103:444-467.

67. Carvalho AP, Meireles LA, Malcata FX. Microalgal reactors: A review of enclosed system designs and performances. *Biotechnol Prog*. 2006;22(6):1490-1506.

68. Ugwu CU, Aoyagi H, Uchiyama H. Photobioreactors for mass cultivation of algae. *Bioresour Technol*. 2008;99(10):4021-4028.

69. Singh RN, Sharma S. Development of suitable photobioreactor for algae production - A review. *Renew Sustain Energy Rev*. 2012;16(4):2347-2353.

70. Mooij T De. Algaemist manual. *Wageningen and Research University.* 2012. 2-24.

71. Tredici MR. Photobiology of microalgae mass cultures: understanding the tools for the next green revolution. *Biofuels*. 2010;1(1):143-162.

72. Csőgör Z, Herrenbauer M, Schmidt K, Posten C. Light distribution in a novel photobioreactor–modelling for optimization. *J Appl Phycol*. 2001;13(4):325-333.

73. Barbosa M. Microalgal Photobioreactors :Scale-up and Optimisation. *PhD Thesis Wageningen and Research University*. 2003.

74. Bernard, O., Mairet, F., Chachuat B. Modelling of Microalgae Culture Systems with Applications to Control and Optimization. *Adv Biochem Eng Biotechnol*. 2016;153, 2015. 59-87.

75. Box GEP, Behnken DW. Some New Three Level Designs for the Study of Quantitative Variables. *Technometrics*. 1960;2(4):455-475.

76. Ferreira SLC, Bruns RE, Ferreira HS, et al. Box-Behnken design: An alternative for the optimization of analytical methods. *Anal Chim Acta*. 2007;597(2):179-186.

77. Yang F, Long L, Sun X, Wu H, Li T, Xiang W. Optimization of medium using response surface methodology for lipid production by Scenedesmus sp. *Mar Drugs*. 2014;12(3):1245-1257.

78. Skorupskaite V, Makareviciene V, Levisauskas D. Optimization of mixotrophic cultivation of microalgae Chlorella sp. for biofuel production using response surface methodology. *Algal Res*. 2015;7:45-50.

79. Kliphuis AMJ, Klok AJ, Martens DE, Lamers PP, Janssen M, Wijffels RH. Metabolic modeling of Chlamydomonas reinhardtii: energy requirements for photoautotrophic

growth and maintenance. *J Appl Phycol*. 2012;24(2):253-266.

80. Khajeh M. Response surface modelling of lead pre-concentration from food samples by miniaturised homogenous liquid–liquid solvent extraction: Box–Behnken design. *Food Chem*. 2011;129(4):1832-1838.

81. Casadevall E, Dif D, Largeau C, Gudin C, Chaumont D, Desanti O. Studies on batch and continuous cultures of Botryococcus braunii: Hydrocarbon production in relation to physiological state, cell ultrastructure, and phosphate nutrition. *Biotechnol Bioeng*. 1985;27(3):286-295.

82. Sawayama S, Inoue S, Yokoyama S. Continuous culture of hydrocarbon-rich microalga Botryococcus braunii in secondarily treated sewage. *Appl Microbiol Biotechnol*. 1994;41(6):729-731.

83. García-Cubero R, Moreno-Fernández J, García-González M. Modelling growth and CO 2 fixation by Scenedesmus vacuolatus in continuous culture. *Algal Res*. 2017;24:333-339.

84. Cuaresma M, Janssen M, Vílchez C, Wijffels RH. Productivity of *Chlorella sorokiniana* in a short light-path (SLP) panel photobioreactor under high irradiance. *Biotechnol Bioeng*. 2009;104(2):352-359.

85. Weetal HH. Studies on the Nutritional Requirements of the Oil-Producing Alga *Botryococcus braunii*. *Proc Fla State Hort Soc*. 1985.

86. Banse K. Rates of growth, respiration and photosynthesis of unicellular algae as related to cell size—a review. *J Phycol*. 1976;12(2):135-140.

87. Lupi F.M., Fernandes H.M.L., Tome M.M., Sá-Correia, I. Novais, J.M. Influence of nitrogen source and photoperiod on exopolysaccharidesynthesis by the microalga Botryococcus braunii UC 58. *Enzym Microb Technol*. 1994;16(7):546-550.

88. Zhang J. Culture of Botryococcus Brauni. *MSc Theis. Murdoch University*. 2013.

89. Al-Hothaly KA, Taha M, May BH, Stylianou S, Ball AS, Adetutu EM. The effect of nutrients and environmental conditions on biomass and oil production in Botryococcus braunii Race B strains. *Eur J Phycol*. 2016;51(1):1-10.

90. Kojima E, Zhang K. Growth and hydrocarbon production of microalga Botryococcus braunii in bubble column photobioreactors. *J Biosci Bioeng*. 1999;87(6):811-815.

91. Li Y, Qin JG. Comparison of growth and lipid content in three Botryococcus braunii strains. *J Appl Phycol*. 2005;17(6):551-556.

92. Yeesang C, Cheirsilp B. Effect of nitrogen, salt, and iron content in the growth medium and light intensity on lipid production by microalgae isolated from freshwater sources in Thailand. *Bioresour Technol*. 2011;102(3):3034-3040.

93. Talukdar J, Kalita MC, Goswami BC. Characterization of the biofuel potential of a newly isolated strain of the microalga Botryococcus braunii Kützing from Assam, India. *Bioresour Technol*. 2013;149:268-275.

94. Kalacheva GS, Zhila NO, Volova TG, Gladyshev MI. The effect of temperature on the lipid composition of the green alga Botryococcus. *Microbiology*. 2002;71(3):286-293.

95. Teles ID. The fatter the better: selecting microalgae cells for outdoor lipid production. *Diss. Wageningen University and Research.* 2016.

96. Geitler L. Cyanophyceae. *In: Cyanophyceae*. Johnson; 1932.

97. Van Geel B, Mur LR, Ralska-Jasiewiczowa M, Goslar T. Fossil akinetes of Aphanizomenon and Anabaena as indicators for medieval phosphate-eutrophication of Lake Gosciaz (Central Poland). *Rev Palaeobot Palynol*. 1994;83(1-3):97-105.

98. Granéli E, Turner JT. *Ecology of Harmful Algae*. Vol 189. Springer; 2006.

99. Frich FE. The structure and reproduction of Algae. *At the University Press; Cambridge.* 1945.

100. Benemann JR, Weare NM. Hydrogen evolution by nitrogen-fixing Anabaena cylindrica cultures. *Science (80- )*. 1974;184(4133):174-175.

101. Weissman JC, Benemann JR. Hydrogen production by nitrogen-starved cultures of Anabaena cylindrica. *Appl Environ Microbiol*. 1977;33(1):123-131.

102. Hallenbeck PC, Benemann JR. Biological hydrogen production; fundamentals and limiting processes. *Int J Hydrogen Energy*. 2002;27(11):1185-1193.

103. Dunn JH, Wolk CP. Composition of the cellular envelopes of Anabaena cylindrica. *J Bacteriol*. 1970;103(1):153-158.

104. Prasanna R, Kumar R, Sood A, Prasanna BM, Singh PK. Morphological, physiochemical and molecular characterization of Anabaena strains. *Microbiol Res*. 2006;161(3):187-202.

105. Heng R-L, Lee E, Pilon L. Radiation characteristics and optical properties of filamentous cyanobacterium Anabaena cylindrica. *JOSA A*. 2014;31(4):836-845.

106. Sarada R, Pillai MG, Ravishankar GA. Phycocyanin from Spirulina sp: influence of processing of biomass on phycocyanin yield, analysis of efficacy of extraction methods and stability studies on phycocyanin. *Process Biochem*. 1999;34(8):795-801.

107. Bermejo R, Fernández E, Alvarez-Pez JM, Talavera EM. Labeling of cytosine residues with biliproteins for use as fluorescent DNA probes. *J Lumin*. 2002;99(2):113-124.

108. Porter G, Tredwell CJ, Searle GFW, Barber J. Picosecond time-resolved energy transfer in Porphyridium cruentum. Part I. In the intact alga. *Biochim Biophys Acta (BBA)-Bioenergetics*. 1978;501(2):232-245.

109. Kim S-K. *Springer Handbook of Marine Biotechnology*. Springer; 2015.

110. Viskari PJ, Colyer CL. Separation and quantitation of phycobiliproteins using phytic acid in capillary electrophoresis with laser-induced fluorescence detection. *J Chromatogr A*. 2002;972(2):269-276.

111. Santiago-Santos MC, Ponce-Noyola T, Olvera-Ramírez R, Ortega-López J, Cañizares-Villanueva RO. Extraction and purification of phycocyanin from Calothrix sp. *Process Biochem*. 2004;39(12):2047-2052.

112. Abalde J, Betancourt L, Torres E, Cid A, Barwell C. Purification and characterization of phycocyanin from the marine cyanobacterium Synechococcus sp. IO9201. *Plant Sci*. 1998;136(1):109-120.

113. Bhat VB, Madyastha KM. C-phycocyanin: a potent peroxyl radical scavenger in vivo and in vitro. *Biochem Biophys Res Commun*. 2000;275(1):20-25.

114. Romay C, Gonzalez R. Phycocyanin is an antioxidant protector of human erythrocytes against lysis by peroxyl radicals. *J Pharm Pharmacol*. 2000;52(4):367-368.

115. El-Baky HHA, El-Baroty GS. Characterization and bioactivity of phycocyanin isolated from Spirulina maxima grown under salt stress. *Food Funct*. 2012;3(4):381-388.

116. da Silva Figueira F, Garcia Gettens J, Vieira Costa JA, de Morais MG, Moraes CC, Juliano Kalil S. Production of Nanofibers Containing the Bioactive Compound C-Phycocyanin. *J Nanosci Nanotechnol*. 2016;16(1):944-949.

117. Manirafasha E, Murwanashyaka T, Ndikubwimana T, et al. Ammonium chloride: a novel effective and inexpensive salt solution for phycocyanin extraction from Arthrospira (Spirulina) platensis. *J Appl Phycol*. 2017:1-10.

118. Chaiklahan R, Chirasuwan N, Bunnag B. Stability of phycocyanin extracted from Spirulina sp.: Influence of temperature, pH and preservatives. *Process Biochem*. 2012;47(4):659-664.

119. Patil G, Chethana S, Sridevi AS, Raghavarao K. Method to obtain C-phycocyanin of high purity. *J Chromatogr A*. 2006;1127(1):76-81.

120. Doke JM. An improved and efficient method for the extraction of phycocyanin from Spirulina sp. *Int J Food Eng*. 2005;1(5).

121. Kuddus M, Singh P, Thomas G, Al-Hazimi A. Recent developments in production and biotechnological applications of C-phycocyanin. *Biomed Res Int*. 2013;2013.

122. Silveira ST, Burkert JF de M, Costa JAV, Burkert CAV, Kalil SJ. Optimization of phycocyanin extraction from Spirulina platensis using factorial design. *Bioresour Technol*. 2007;98(8):1629-1634.

123. Zhang X-F, Wang X, Luo G-H. Ultrasound-assisted three phase partitioning of phycocyanin from spirulina platensis. *Eur J Pure Appl Chem Vol*. 2017;4(1).

124. Ventura SPM, e Silva FA, Quental M V, Mondal D, Freire MG, Coutinho JAP. Ionic-Liquid-Mediated Extraction and Separation Processes for Bioactive Compounds: Past, Present, and Future Trends. *Chem Rev*. 2017.

125. Freire MG, Claudio AFM, Araujo JMM, et al. Aqueous biphasic systems: a boost brought about by using ionic liquids. *Chem Soc Rev*. 2012;41(14):4966-4995.

126. Schröder C. Proteins in Ionic Liquids: Current Status of Experiments and Simulations. *Top Curr Chem*. 2017;375(2):25.

127. Coleman D, Gathergood N. Biodegradation studies of ionic liquids. *Chem Soc Rev*. 2010;39(2):600-637.

128. Passos H, Freire MG, Coutinho JAP. Ionic liquid solutions as extractive solvents for value-added compounds from biomass. *Green Chem*. 2014;16(12):4786-4815.

129. Martins M, Vieira FA, Correia I, et al. Recovery of phycobiliproteins from the red macroalga Gracilaria sp. using ionic liquid aqueous solutions. *Green Chem*. 2016;18(15):4287-4296.

130. Cláudio AFM, Neves MC, Shimizu K, Lopes JNC, Freire MG, Coutinho JAP. The magic of aqueous solutions of ionic liquids: ionic liquids as a powerful class of catanionic hydrotropes. *Green Chem*. 2015;17(7):3948-3963.

131. Janet R, Stein E, Stein JR. *Handbook of Phycological Methods: Culture Methods and Growth Measurements*. Cambridge University Press; 1973.

132. Simon D, Helliwell S. Extraction and quantification of chlorophyll a from freshwater green algae. *Water Res*. 1998;32(7):2220-2223.

133. Rodrigues MI, Iemma AF. *Planejamento de Experimentos E Otimização de Processos: Uma Estratégia Sequencial de Planejamentos*. Campinas; 2005.

134. McIlvaine TC. A buffer solution for colorimetric comparison. *J Biol Chem*. 1921;49(1):183-186.

135. Huddleston JG, Visser AE, Reichert WM, Willauer HD, Broker GA, Rogers RD. Characterization and comparison of hydrophilic and hydrophobic room temperature ionic liquids incorporating the imidazolium cation. *Green Chem*. 2001;3(4):156-164.

136. Lungwitz R, Friedrich M, Linert W, Spange S. New aspects on the hydrogen bond donor (HBD) strength of 1-butyl-3-methylimidazolium room temperature ionic liquids. *New J Chem*. 2008;32(9):1493-1499.

137.  Jessop PG, Jessop DA, Fu D, Phan L. Solvatochromic parameters for solvents of interest in green chemistry. *Green Chem*. 2012;14(5):1245-1259.

138.  Cláudio AFM, Swift L, Hallett JP, Welton T, Coutinho JAP, Freire MG. Extended scale for the hydrogen-bond basicity of ionic liquids. *Phys Chem Chem Phys*. 2014;16(14):6593-6601.

139.  Vieira FA, Guilherme RJR, Neves MC, et al. Single-step extraction of carotenoids from brown macroalgae using non-ionic surfactants. *Sep Purif Technol*. 2017;172:268-276.

140.  Hosikian A, Lim S, Halim R, Danquah MK. Chlorophyll extraction from microalgae: a review on the process engineering aspects. *Int J Chem Eng*. 2010.

141.  Liu L-N, Chen X-L, Zhang X-Y, Zhang Y-Z, Zhou B-C. One-step chromatography method for efficient separation and purification of R-phycoerythrin from Polysiphonia urceolata. *J Biotechnol*. 2005;116(1):91-100.

142.  Soni B, Trivedi U, Madamwar D. A novel method of single step hydrophobic interaction chromatography for the purification of phycocyanin from Phormidium fragile and its characterization for antioxidant property. *Bioresour Technol*. 2008;99(1):188-194.